U. S. ARMY
TRANSPORTATION RESEARCH COMMAND
FORT EUSTIS, VIRGINIA

TRECOM TECHNICAL REPORT 64-61

HIGH-PERFORMANCE HELICOPTER PROGRAM

SUMMARY REPORT, PHASE II

Task 1D121401A14301
Contract DA 44-177-TC-711

October 1964

prepared by:

BELL HELICOPTER COMPANY
Fort Worth, Texas

5984-64

DISCLAIMER NOTICE

When Government drawings, specifications, or other data are used for any purpose other than in connection with a definitely related Government procurement operation, the United States Government thereby incurs no responsibility nor any obligation whatsoever; and the fact that the Government may have formulated, furnished, or in any way supplied the said drawings, specifications, or other data is not to be regarded by implication or otherwise as in any manner licensing the holder or any other person or corporation, or conveying any rights or permission, to manufacture, use, or sell any patented invention that may in any way be related thereto.

* * *

DDC AVAILABILITY NOTICE

Qualified requesters may obtain copies of this report from

Defense Documentation Center
Cameron Station
Alexandria, Virginia 22314

* * *

This report has been released to the Office of Technical Services, U. S. Department of Commerce, Washington 25, D. C., for sale to the general public.

* * *

The findings and recommendations contained in this report are those of the contractor and do not necessarily reflect the views of the U. S. Army Mobility Command, the U. S. Army Materiel Command, or the Department of the Army.

HEADQUARTERS
U S ARMY TRANSPORTATION RESEARCH COMMAND
FORT EUSTIS, VIRGINIA

This report has been reviewed by the U. S. Army Transportation Research Command and is considered to be technically sound. The program was basically an extension of previous work performed under Contract DA 44-177-TC-711 and reported in TRECOM Technical Report 63-42, September 1963. The results presented further substantiate the higher performance potential of rotary-wing aircraft and are published for the exchange of information and stimulation of ideas.

The Army is currently continuing to sponsor several high-speed programs of similar nature to provide basic technology for the future design of high-performance rotary-wing aircraft.

GARY N. SMITH
Project Engineer

PAUL J. CARPENTER
Group Leader
Applied Aeronautical
Engineering Group

APPROVED.

FOR THE COMMANDER:

for LARRY M. HEWIN
Technical Director

Task 1D121401A14301
Contract DA 44-177-TC-711
TRECOM Technical Report 64-61
October 1964

HIGH-PERFORMANCE HELICOPTER PROGRAM

Summary Report, Phase II

Prepared By

BELL HELICOPTER COMPANY
POST OFFICE BOX 482 · FORT WORTH 1, TEXAS
A DIVISION OF BELL AEROSPACE CORPORATION
A textron COMPANY

for

U. S. ARMY TRANSPORTATION RESEARCH COMMAND
Fort Eustis, Virginia

BELL HELICOPTER COMPANY
TECHNICAL DATA REPORT
533-099-010

Prepared by:

J. F. Van Wyckhouse
Assistant Project Engineer

and

W. L. Cresap
Development Group Engineer

FOREWORD

This report summarizes the results of a flight research program conducted to investigate rotor operation at high speeds and under conditions of partial unloading. The program was accomplished by Bell Helicopter Company under Modification 4 to USATRECOM Contract DA44-177-TC-711 (Reference 1). Under Modification 4 (Reference 2), wings and auxiliary jet engines were installed on the research helicopter provided by the basic contract.

The original program results have been reported in USATRECOM TR 63-42 (Reference 3). Design of the wing and auxiliary engine installations commenced in September 1962. The initial flight with the wing installed was conducted in March 1963. The first flight with the auxiliary engines installed was in October 1963. Demonstration and evaluation flights were completed in April 1964.

This program was conducted under the technical cognizance of the Applied Aeronautical Engineering Group of the USATRECOM. Principal Bell Helicopter Company personnel associated with the program were Messrs. W. Cresap, J. Van Wyckhouse, W. Jennings, J. Drees, L. Hartwig, W. Quinlan, K. Edenborough, and R. Lynn.

HIGH-PERFORMANCE HELICOPTER WITH WINGS AND AUXILIARY ENGINES

TABLE OF CONTENTS

ILLUSTRATIONS

SUMMARY

This report describes and presents the results of a flight research program to investigate high-speed loaded and unloaded rotors. The work is an extension of the prior high-performance UH-1B flight research program reported in Reference 3.

The compound flight research helicopter, instrumentation, and test program are described and the test results presented and discussed. Major modifications to the basic high-performance helicopter (HPH) involved the addition of two J69-T-9 engines, a controllable incidence wing, and controls and elevator-horizontal stabilizer changes.

With the addition of the wing, a maximum true airspeed of 154 knots was obtained at a gross weight approximately 20 percent greater than the basic HPH and severe pitch, roll, and rotor speed control problems were encountered. These were eliminated by sweeping the wing aft and coupling the wing incidence with collective control.

With the initial jets-only configuration, dynamic stability problems, and an increased fuselage drag were encountered due to flow separation between the engine nacelle and fuselage, and engine-pylon-horizontal elevator interference. These were corrected by refairing the engine-pylon and adding an elevator panel on the vertical fin. Subsequent to these changes, the helicopter was flown to a level-flight true airspeed of 182 knots. With the wing and jet engines, no further problems were encountered and the machine was flown to a true airspeed of 186 knots in level flight and 189 knots in a slight dive (200 fpm). As a full compound, mild maneuvers ($\sim$1.5g) and simulated power failures were investigated up to speeds of 177 knots.

It is shown that the structural loads, vibration characteristics, and stability and control of the vehicle were satisfactory for all conditions tested. With the exception of the pitch link loads, rotor system loads and vibrations were found to be lower than those of the UH-1B at its power limit speed. The pitch stability of the machine in its final configuration was excellent; and although the lateral stability was deficient, no difficulty was encountered by Bell and Army pilots who flew the machine.

During the program, the UH-1B rotor blades were replaced by an experimental set with a tapered thickness over the outboard 20 percent of the blades. With these blades, the full compound machine was flown to a true airspeed of 193 knots at a gross weight about 40 percent greater than the basic HPH. Control loads were found to be reduced with the tapered tip blades.

It is concluded that higher speed and increased load capability can be achieved by compounding the helicopter. This can be accomplished with good stability and control, with no increase in vibration and structural loads, and without compromising the autorotation safety characteristics of the helicopter.

CONCLUSIONS

Flight tests have shown the benefits to be derived from the addition of wings and auxiliary propulsion to the helicopter. Higher speeds and increased load capability can be obtained with no increase in rotor loads or cabin vibrations. Level flight speeds of 186 knots were obtained with a 9000-pound machine using less than 2000 horsepower. The production UH-1B rotor system proved entirely satisfactory for these flight conditions although originally designed for only 6600 pounds at 130 knots. The only structural limitations encountered were due to the rapid rise in control system loads at the higher speeds. These were accommodated by the installation of special higher strength components.

Stability and control were satisfactory at all speeds without recourse to stabilizing devices, although some form of roll stabilization at higher speeds is desirable.

Problems with rotor speed and roll control in autorotation, caused by high wing loadings, can be resolved by coupling the wing incidence to the collective control to maintain a more constant rotor-wing loading ratio; or by limiting the wing angle or size.

Rapid increases in rotor system power requirements and control system loads above advancing blade tip Mach number of .87 show the significance of compressibility and indicate that they will be a major factor limiting high-speed rotary-wing flight.

RECOMMENDATIONS

For missions where helicopter hovering capabilities are desired in combination with moderately high (200 to 250 knots) speeds, the compound helicopter configuration should be considered.

Efforts to establish a more ideal rotor blade configuration for high speed flight should include modifications of the inboard section to minimize reverse flow effects and modifications of the outboard section to minimize compressibility effects.

Additional tests should be conducted to evaluate methods of reducing wing lift during autorotation and to determine the limits of the research vehicle flight envelope at high speeds.

The research program should be continued to investigate other auxiliary propulsion systems such as propellers and compound engines, which will improve fuel consumption, helicopter range, and productivity.

INTRODUCTION

In recent years a considerable portion of the research activity in the rotary-wing field has been directed toward development of the full-speed and performance potential of the helicopter. Studies have shown that the basic helicopter configuration is capable of much higher performance than generally assumed or exhibited by contemporary machines. It was shown that although a considerable research effort is required, the speed and performance potential of rotary-wing aircraft, with various degrees of compounding, offers a great deal of promise up to speeds of about 250 knots.

In 1961 a high-performance research program was initiated (Reference 1) with the UH-1B helicopter, and test results proved that the predicted trends with respect to the increased performance, speed, and productivity were valid. The maximum speed of the basic UH-1B was increased from about 130 knots to 157 knots, with rotor and control loads and fuselage vibrations maintained within acceptable limits. It was shown that stability deteriorates with speed as predicted. Although the helicopter was easily flyable without recourse to stabilizing devices, some form of roll stabilization would be desirable.

In late 1962 a Phase II of this program was initiated (Reference 2). The original contract was modified to include flight test of the high-performance helicopter with a wing and auxiliary jet engines installed. The purpose of these tests was to determine rotor behavior at reduced lift and at higher speeds than were possible with the basic machine. This report summarizes the results of the Phase II program.

DESCRIPTION OF THE TEST VEHICLE

BASIC CONFIGURATION

The basic test vehicle is a YH-40 with UH-1B dynamic components modified into a high-performance configuration. These modifications include changes to the pylon mounting, the fixed and rotating controls, and the external fuselage lines. A detailed description of the test vehicle is given in USATRECOM Technical Report 63-42 (Reference 3). Figure 3 shows the basic high-performance helicopter configuration.

The rotor system is a standard two-bladed UH-1B rotor. This rotor is a semirigid, "see-saw", underslung, feathering axis design with the following characteristics:

Number of Blades	2
Airfoil Designation	NACA 0012
Chord	21 inches
Diameter	44 feet
Blade Twist	-10 degrees
Blade Area (total)	77 square feet
Disc Area	1521 square feet
Solidity	.0507
Rotor RPM @ 6600 Engine RPM	324
Tip Speed	746 ft/sec
Disc Loading @ 6500 lbs GW	4.3 lb/sq ft

In the latter portion of the flight test program, the UH-1B rotor blades were replaced by an experimental set with a thickness ratio tapering from 12 percent to 6 percent over the outboard 20 percent of the blades.

WING INSTALLATION

The wing installation consists of removable wing panels, incidence controls, and the airframe-mounted support structure. Figure 4 shows the HPH with wing installed.

Wing Support Structure

The wing panels were attached to the helicopter by means of a built-up sheet metal beam that was installed in the cabin and attached to, and forward of, the Station 123 bulkhead. This beam supported attachment fittings for each wing panel, the incidence control actuator, and a bellcrank and hydraulic cylinder assembly that coupled the wing panels to the lateral cyclic and collective control system.

The attachment fittings for each wing panel were located under the support structure and mated with fittings that were located on top and along the leading edge of the wing spar. The fittings on the support structure had self-aligning bearings to provide pivoting for the variable wing incidence. The inboard fitting for each wing panel was adjustable in the fore and aft direction to permit ground adjustment of the sweep from 13° aft to 23° aft.

Wing Controls

Wing incidence could be adjusted in-flight by the pilot through an angle change of 20°. Initially this control was accomplished by an electrical actuator that was mounted on top of the wing support structure and connected to a compound bellcrank assembly. A control tube was connected between the bellcrank and a fitting on the trailing edge of each wing panel spar. Movement of the actuator, controlled by a switch on the pilot collective stick, caused the wing to pivot about the hinge fittings on the leading edge of the spar. Later in the test program the electric actuator was replaced by a hydraulic boost cylinder that was actuated by the collective control system. This change was made to increase the rate of incidence change and to couple the wing incidence control with collective for the purpose of improving controllability and rotor rpm control during autorotation entry and descent. An increase in the collective setting resulted in an increase in the wing incidence. A slip clutch and a manual override control were provided in the wing incidence control system so the pilot could select any desired wing incidence at any collective control setting. The wing setting, in degrees, was indicated on an instrument in the pilot instrument panel.

The differential wing incidence control was accomplished with a hydraulic cylinder assembly connected to the compound bellcrank used to vary the wing incidence. Actuating the cylinder, by means of controls coupled with the lateral cyclic control system, resulted in differential movement of the wings. The amount of differential movement, with the lateral cyclic stick moved from stop to stop, could be set at $5\frac{1}{2}$° or $7\frac{1}{2}$° (one wing relative to the other) by changing the control ratio in a bellcrank in the wing control system. Also, provisions were made so the differential incidence control could be decoupled and the wings locked in the neutral position.

Wing

The wing has an NACA 64, 3-218 airfoil, a 26.8-foot span, a constant 2.2-foot chord length, and a -3° twist from the root to the tip. Wing area, including carryover, is 64 square feet.

AUXILIARY PROPULSION INSTALLATION

Auxiliary propulsion was provided by two J69-T-9 turbojet engines with a 5-minute static thrust rating of 920 pounds each. They were mounted on

the side of the fuselage above the wings and near the vertical and longitudinal center of gravity locations. The line of thrust was parallel to the centerline of the helicopter but was set at a +7° angle to the waterline so the jet wake would pass under the elevators mounted on the tail boom. Figure 5 shows the HPH with auxiliary engines installed.

Support structure for the engines was attached to the Station 123 bulkhead and the engine and transmission compartment work deck. All of the exposed engine support structure, fuel and oil lines, electrical wires, and throttle linkages between the fuselage and engine cowling were enclosed in an airfoil-shaped fairing set at +3° with respect to the centerline of the helicopter. Figure 6 shows the nacelle and engine pylon fairing, including the final fairing installation. The change resulted from flight test data which showed that the drag of the initial installation was considerably higher than expected.

Each engine had an independent lubrication system, but the fuel for both engines was taken from the same tanks that supplied the T-53-9A main propulsion engine. Fuel boost pressure for both auxiliary engines was supplied by one electrically driven pump.

Controls and instruments for both engines were mounted on a panel that was located in the pedestal between the pilot and copilot. The panel had a throttle, an oil temperature indicator, an exhaust gas temperature indicator, a low oil pressure warning light, a turbine speed indicator for each J69 engine, and a fuel boost pressure indicator for both engines. The location of the panel made the engine throttles and instruments accessible to both pilots.

Elevator

One UH-1D elevator was mounted on the top right-hand side of the dorsal fin to improve the controllability and stability of the helicopter with the auxiliary propulsion engines installed. This elevator was used in addition to the tail-boom-mounted elevators. The fin-mounted elevator was not coupled to the main rotor control system, but the incidence of the elevator was ground adjustable.

Wing-Jet Configuration

An in-flight photograph of the wing jet configuration of the HPH is shown as the frontispiece of this report. A general arrangement three-view drawing of the machine is given by Figure 7.

INSTRUMENTATION

Instrumentation was installed to record and/or monitor the test helicopter's performance, stability, controllability, rotor and control loads, fuselage vibrations, and other information as desired during the ground and flight test programs. The information was recorded on two oscillographs installed on the wing support structure in the cabin area.

INSTRUMENTED ITEMS

Specific channels of instrumentation were provided for recording the following information:

- Airspeed
- Rotor azimuth
- Gas producer speed
- Engine and rotor rpm
- Differential torque pressure
- Outside air temperature
- Pressure altitude
- Mast conversion angle
- CG acceleration
- Pilot and copilot location acceleration
- Pitch and roll attitude
- Cyclic, directional, and collective control positions
- Main-rotor flapping and feathering position
- Main-rotor mast moments
- Main-rotor hub assembly beam and chord moments
- Main-rotor blade beam and chord moments at three stations
- Main-rotor drag brace loads
- Main-rotor pitch link loads
- Cyclic and collective control tube loads
- Pylon lift link load
- Pylon motion (3 pickups)
- Tail-rotor hub flapping position
- Tail-rotor hub beam and chord moments
- Tail-rotor blade beam and chord moments
- Horizontal stabilizer moments
- Horizontal stabilizer position
- Pylon actuator cylinder loads
- Wing beam and chord bending
- Wing position (angle of incidence)
- Auxiliary engine rpm
- Wing angle of attack

Wiring and connectors for all channels were routed to the oscillographs. To reduce the possibility of reading errors in data reduction, only the specific channels necessary for a particular test were connected into the oscillographs. If postflight inspection of data indicated an area of particular concern, additional channels were connected to provide a more comprehensive evaluation of the area in question. In general, vibration, fuselage attitude, power, rotor flapping, yoke loads, cyclic and collective control positions, and pylon elevator positions were recorded for each flight. Additional information was recorded as necessary throughout the test program.

CALIBRATION AND REPEATABILITY

All instrumented items were calibrated either in the laboratory, on the ship, or in-flight. Pre- and postflight calibrations were made for all oscillograph recorded items. The ship's airspeed system was calibrated against a trailing bomb airspeed sensor at speeds up to approximately 160 knots. For the higher airspeeds the helicopter airspeed system was calibrated using a Cessna 310 as a pace ship. The airspeed system of the Cessna 310 was calibrated to 174 knots by flying a measured course. Calibrations were made with and without the wing installed. It was found that the wing influenced the airspeed system slightly.

Throughout the program, the repeatability of all flight data was good. In most instances power data were repeatable within 25 to 50 main rotor horsepower. The accuracy of the jet thrust values shown is not known; however, based on the repeatability of the main rotor speed power data, it appears acceptable. Strain gauge, position, and vibration level data were found to be repeatable within 5 to 10 percent.

GROUND TESTS

Upon completion of the modification for installation of the wings and auxiliary engines, the wings were proof tested and the auxiliary engine installation was functionally checked. Ground runs were conducted with the helicopter tied down to establish satisfactory operation of the vehicle.

WING PROOF LOAD

The wing installation and associated controls were proof loaded to 80 percent of the design limit load to demonstrate the structural integrity of the components. Loads were applied to produce chord, beam, and torsional moments.

Chord loading was accomplished by applying shear loads to the wings perpendicular to the leading edge and along the chord plane at wing Station 94.65. The loads were applied in the forward direction in 100-pound increments to 500 pounds, which produced a maximum bending moment of 27,325 inch-pounds at the wing root.

The beam proof loading was accomplished by placing form blocks under each wing at wing Station 103 and applying vertical-lift loads perpendicular to the chord plane. The loads were applied in increments to 2900 pounds on each wing, which resulted in a maximum bending moment of 182,700 inch-pounds at the wing root.

A torsional moment of 4050 inch-pounds was applied to each wing in 450 inch-pound increments at wing Station 94.65. In addition to loading the wing, the torsional moment also loaded the control system from the wings to the actuators. The control system from the differential wing incidence actuator to the cyclic control system was not proof loaded because of the low magnitude of loads in those controls. A spring-loaded telescopic tube in this system would not let the load in the tube exceed 15 to 20 pounds. This provision was made to eliminate the possibility of high cyclic stick forces in the event of a malfunction of the differential wing incidence actuator.

There was no evidence of buckling, excessive deflection, or yielding in the wing support structure, wing, or controls during the proof load test. The wing installation was considered to be structurally sound and satisfactory for flight.

AUXILIARY ENGINE FUNCTION TEST

The auxiliary engine installation was functionally tested in accordance with the ground and flight test agenda (Reference 4). The engines were operated up to maximum available thrust, and no major problems were

encountered; however, engine cooling was found to be deficient. The temperatures in the area of the aft firewall were found to be excessive. An additional air inlet was installed on the nacelle, and the tail pipe fairing was extended aft of the tail pipe to act as an ejector. These changes were successful, and no further cooling problems were encountered.

TIEDOWN (GROUND) RUNS

The helicopter was operated on tiedown with normal rated power to both rotor and auxiliary thrust engines to establish satisfactory operation of the controls and systems. No significant problems were encountered, and the helicopter was considered ready for flight.

FLIGHT TESTS

The helicopter with the wing installed was first flown on 19 April 1963. The initial flights were limited to low speeds and were for the purpose of pilot familiarization and helicopter shakedown. These flights were conducted with the wing swept at 13° (maximum forward). Nose-up pitching was experienced during low-power letdowns at speeds above 80 knots, and the wing sweep angle was increased to 23° (maximum aft). The nose-up pitching was greatly reduced. The remainder of the flight program was conducted with the wings at 23° sweep.

Evaluation flights were conducted with the wings installed, and performance, stability and control, vibration, and structural load data were obtained at speeds up to 154 knots. At the higher speeds, nose-up pitching, lateral control, and rotor rpm control problems were experienced during autorotation entry. Various combinations of spoilers were evaluated in an effort to improve these adverse characteristics. There was no change with the spoilers installed. During the course of these investigations, it was found that satisfactory characteristics were obtained at negative wing angles of 5° to 10°. To provide positive wing angles for level flight and negative wing angles for autorotation, it was necessary to couple the rotor collective and wing incidence control systems. Tests of the HPH configured with the wing were interrupted to allow design and fabrication of a wing-collective coupling system.

During the period that the wing-collective coupling system was being designed and fabricated, the auxiliary engines were installed. The first flight with the auxiliary engines installed was on 21 October 1963. Again, initial flights were conducted at low speeds for the purpose of pilot familiarization and helicopter shakedown. During these flights, stability and control were explored and found to be unacceptable. Also, it was found that the drag of the jet engine installation was significantly higher than anticipated. From an in-flight tuft survey, the high drag was found to result from fully developed stall in the area between the jet engine nacelles and the fuselage. An increased area pylon fairing (see Figure 6) was installed; this reduced the drag of the installation to the previously expected value.

To improve the dynamic stability characteristics of the machine, various elevator configurations were evaluated. An elevator configuration, consisting of the standard elevator plus an additional elevator panel located on the vertical fin, was found to provide satisfactory stability. Evaluation flights with the auxiliary propulsion configuration were then conducted. During these tests, a true airspeed of 182 knots was attained using maximum (98 percent engine rpm) auxiliary thrust.

Following these flights, the wing with new wing controls was installed and the test program continued. The HPH with a wing and auxiliary jets was first flown on 2 March 1964. Evaluation flights were begun on 5 March 1964. Performance, stability and control, vibration, and structural load data were obtained at level flight speeds up to 186 knots, and a true airspeed of 189 knots was attained during a 200 ft/min descent. Maneuver data including throttle chops were obtained up to speeds of 177 knots.

Testing was completed in April 1964 after 49 hours of ground and flight time, and 17.8 hours of auxiliary engine time. At the conclusion of the flight test evaluation, the test vehicle with wing and jets installed was demonstrated to pilots from USATRECOM.

Immediately following the demonstration flights, special tapered-tip main rotor blades were installed on the test vehicle as part of the Bell Helicopter Company independent research program. Tests with these blades resulted in a significant reduction in power required, and a level-flight true airspeed of 193 knots was attained using maximum auxiliary thrust.

FLIGHT TEST RESULTS

Presented in this section are the test results. Additionally, standard UH-1B and basic HPH data are given for purposes of comparison. Measured performance, stability and control, rotor and control loads, and fuselage vibrations are presented and discussed.

The configurations tested, test flight numbers, and primary flight parameters which form the basis of this report are given in Table 1.

PERFORMANCE

Hovering Performance

Hovering data for the HPH with the wing and auxiliary propulsion are shown in Figure 8. Also shown are hovering data for the basic HPH. From the figure it is seen that the addition of the wing and jets on the HPH does not significantly affect the hovering power requirements.

Level Flight Performance

Maximum Speed - Configuration Comparisons - The maximum speed attained by the basic HPH in level flight was 155 knots. With a wing added, the maximum test speed was 154 knots; higher speeds were not attempted due to poor autorotation characteristics at high speeds (see page 27). The HPH with jets operating at full thrust reached an airspeed of 183 knots. With the wing and jet engines operating at full thrust, the highest speeds attained were 186 knots in level flight and 189 knots in a slight dive using the standard UH-1B main rotor, and 193 knots in level flight using a main rotor with tapered-tip blades.

The maximum-speed flight test data points given above are for values of gross weight/density ratio (GW/σ') varying from 6420 pounds to 10,058 pounds, and for various values of T53 power and J-69 thrust. As wing, jets, and combined wing and jets were added during the test program, the test gross weights (GW/σ') of the configurations progressively increased. A comparison of the speeds attained with the various configurations at approximately the same values of GW/σ', T53 SHP, and total power is shown in Table 2. Additional comparisons are made with the standard UH-1B where applicable, and of power required for the several configurations at the same airspeed.

It can be seen from the comparisons that the wing, in general, results in a speed increase of several knots and a greatly increased lift capability. The cold jets cause a slight speed penalty. The effect of auxiliary jet propulsion is to greatly increase the maximum speed capability of a rotor originally designed for much lower speeds. A speed increase of 43 knots was realized at 98 percent jet engine rpm (N_I). The addition of the highly efficient wing of the HPH in combination

with the jets resulted in a slight speed increase and lower rotor loads. The tapered tips show a considerable advantage in terms of power required at the maximum airspeeds tested. Also, with the tapered tips, rotor control loads were reduced.

Over-All L/D - Additional indications of the relative merits of the various flight test configurations are given by their L/D ratios (see Figure 9). These L/D ratios are for the entire aircraft with the main rotor operating at a tip speed of 746 fps (except as noted). Lift (L) in the expression for L/D is the gross weight/density ratio (GW/σ') for the flight. Drag (D) is the equivalent drag/density ratio (D/σ') obtained from

$$D/\sigma' = \frac{(SHP/\sigma')(550)}{V_{Fwd\ Flt'\ fps}} + \text{Net Jet Thrust, Lbs}/\sigma'$$

Some interesting effects can be seen from Figure 9. The drag cleanup of the basic HPH, for example, results in a 26 percent increase in L/D at 100 knots and 37 percent at 130 knots in comparison with the UH-1B. Adding wings to the HPH increases L/D another 8 percent at 150 knots. Above 150 knots L/D of the basic HPH and the HPH with wings decreases. At high speeds, the wing plus auxiliary propulsion combination appears to result in the best L/D. The large increase in L/D of the full compound configuration with the jet engines operating at 80 percent N_I as compared to the case with those engines operating at 98 percent N_I (about 40 percent of maximum thrust at 150 knots) has not been explained at this writing. It is possible that this difference simply illustrates the need to match rotor parameters such as blade twist, tip speed, and blade area with rotor lift and auxiliary propulsion.

L/D of Lifting System - Figure 10 shows the L/D ratio of the lifting system only. For the UH-1B and basic HPH, this is the approximate L/D of the main rotor. For the compound, the lifting system includes the rotor, the wing, and auxiliary jets installation. The lift value (L) is, as for Figure 9, obtained from the gross weight over density ratio. Drag (D), however, is found by subtracting from the total, that drag attributed to the fuselage (see page 18). The values of equivalent flat-plate drag area used where 19.2 square feet for the UH-1B, 10 square feet for the basic HPH, and 11 square feet for the HPH with jet installation. The wing drag is considered as part of the lifting system and is included in the L/D value shown. Rotor power was reduced by a factor of .9 to account for transmission and tail rotor losses.

The results indicate that good L/D values are maintained even at the higher speeds. The L/D values of Figure 10 are comparable to those of an airplane wing of a moderate to low aspect ratio. The dashed curve on Figure 10 indicates the trend of maximum L/D with airspeed for the UH-1B rotor. With the proper selection of unloading and auxiliary

propulsion, any point on the trend curve should be attainable. As noted in the preceding section, the high L/D values for the 80 percent N_I case (curve d) have not been explained.

For future rotorcraft, the efficiency of the various lifting systems can be substantially improved by such means as increasing the aspect ratio of the wing or improving the rotor performance by the use of reduced blade area, lower tip speed, optimized blade twist, or tapered tip blades. Curve h on Figure 10 shows the effect of the latter. The measured effect of reducing the rotor rpm is also indicated on the figure.

Basic High-Performance Helicopter - The shaft horsepower savings due to drag reduction accomplished on the basic HPH are seen on Figure 11. Measured power-required data versus true airspeed are given for both the standard UH-1B and for the HPH with the stabilizer bar on, at the same GW/σ'. The HPH data, with the bar on, have been corrected to illustrate the effect of removing the bar. This is shown on the figure. The correction is based on the flight test data of Reference 3.

In addition to the measured data, calculated power-required points are shown for the standard UH-1B and the HPH. These data were obtained using the method discussed on page 21. The "f" used for the UH-1B calculations was 19.2 square feet; for the HPH, 10.0 square feet. These values give good correlation and are in close agreement with those shown in Reference 5. A drag cleanup of about 9.2 square feet is indicated versus the 9.4 to 11.0 square feet determined previously (Reference 3).

Wing Installation - Figure 12 shows the measured shaft horsepower required data points for the HPH with wing installed and, for comparison, the basic HPH data. In addition, a curve through the calculated power-required points is shown for the HPH with wing. Good agreement between calculated and measured data is indicated. The following gives wing lift and drag increments which were used in the calculations.

V (knots)	f_{wing} (sq ft)	L_w (lbs)
120	2.0	2160
140	1.6	2580
160	1.2	2640
$\sigma' = .897$ $GW/\sigma' = 7870$ $i_{wing} = 8^\circ$ $i_{mast} = 9^\circ$		

Wing incidence sweeps were made to determine the effect of wing angle of attack (defined as the angle between the zero lift line and the flight path) on power required at constant GW/σ' and airspeed. These data are shown on Figure 13. The angle of attack data were obtained by adding the measured airframe attitudes to the wing incidence settings (with respect to fuselage). These wing angle data were checked against pitch vane data and found to be in substantial agreement. Wing angle of attack for minimum power was found to be approximately 8°.

Additional wing lift data from other flight conditions are given below.

Condition	True Airspeed (knots)	Wing Incidence (deg)	Wing Lift (lbs)
Jets on, T53 at near idle power	107	5	2000
2700 ft/min climb	70	8.5	-150
High-speed turn	163	10	2800

These data show that the wing produces a slight amount of negative lift during a climb and that it provides a load factor increment of 0.3g in the turn. Added wing incidence is needed for these conditions.

Problems Encountered with Wing Installation - A number of problems were encountered during the first phase of the wing-on tests. These are discussed and the various solutions attempted are noted below.

- Nose-up pitching. Initially, with the wing swept 13°, there was an excessive amount of nose-up pitching following a throttle chop. This situation was corrected by moving the wing aft to a sweep angle of 23°, thereby moving the center of wing lift nearer to the center of gravity.

- Roll oscillation in autorotational descent. Another difficulty was a roll oscillation in autorotational descents above about 60 knots. This problem was caused by the alternate stalling of the right and left wing panels. This condition reversed the effectiveness of the aileron control. Also, the unloading of the main rotor reduced the roll control power which it could provide. The solution to this problem is the same as for the next one and will be discussed in the paragraphs following.

- Inability to maintain rotor rpm. Above 100 knots during low-power letdown, and during autorotation, the wing lift unloaded the main rotor to the extent that rpm could not be maintained at the desired level with the minimum collective pitch setting used.

Several methods were evaluated for alleviating the rpm and roll-oscillation problem discussed above. One was a leading-edge spoiler over the inboard portion of the wing. This helped reduce lift but also resulted in severe buffeting. Another fix was to remove the fairing, leaving a gap at the wing-fuselage junction. The purpose of this was to separate the wing-fuselage combination into three low-aspect-ratio lifting surfaces. This change did produce the desired effect. For the test vehicle, the mechanical complexity involved in opening a gap when collective pitch is reduced made this approach undesirable. The solution finally adopted was to couple the wing incidence control to collective pitch. When collective pitch is lowered to the power-off setting, the wing incidence reduces to -10°. With this incidence setting the wing does not stall and the lift is low so that rotor rpm can be maintained.

Jet Engine Installation - Net jet thrust/ σ' of the J69-T-9 turbojet engine is given on Figure 14 as a function of airspeed and percent maximum engine rpm (%N_I). The equivalent drag/ σ' or SHP/ σ' ratio due to the jet engines was derived from these curves.

Power required from the T-53-9A engine is given on Figure 15 as a function of airspeed for several values of J69 N_I. The configuration is jet engines only, i.e., no wing.

Data with the J69 jets cold (data points on Figure 15) indicate that the drag increase due to the auxiliary jet engine installation on the basic HPH is about 1 to 4 square feet, depending on angle of attack of the nacelle. Estimated drag of a similar installation (unpublished data) indicated a drag increase of .15 square foot per engine with the engine operating, and .75 square foot per engine with the jet engine shut down (at zero angle of attack).

With the J69 auxiliary jet engines operating at 80 percent and 98 percent N_I speeds, power required from the T53 engine was reduced sharply, resulting in an increase in maximum speed to 182 knots for the standard-rotor, no-wing configuration. At 140 knots, T53 power required was reduced such that an equivalent of 10.9 square feet flat-plate drag area was realized at 80 percent N_I. At 98 percent N_I, the equivalent flat-plate drag area reduction is of the order of 18.8 square feet.

Total power-required data for all flights with the auxiliary jet engine installation are given on Figure 16. All data appear consistent in the total power required, which is the sum of the T53 shaft horsepower and the J69 thrust horsepower, with the exception of the 80 percent N_I J69 data points and those of the tapered-tip blades.

Aerodynamic problem areas encountered during the initial flight tests of the HPH with the jet engine installation involved interference drag and the longitudinal stability and control characteristics of the helicopter. To correct these items, the pylon fairings between the airframe and engine nacelles were increased in chord, and a fixed horizontal stabilizer was added opposite the tail rotor. The first of these two changes reduced the drag and improved the airflow characteristics over the elevator. The increased tail surface area further improved the longitudinal stability and control characteristics by making up for the remaining loss of effectiveness of the original stabilizer caused by the pylon-nacelle installation.

Wing and Jet Engine Installation - Power required for the jet engine installation in combination with the wing is shown on Figure 15. The curves are for "cold" jets, 80 percent N_I and 98 percent N_I. Estimated lift and drag increments are shown in Table 3. Estimated drag versus lift data for the jet and wing installations are also given by Figure 16. Wing lift and drag increments were calculated by the same method as for the wing-only case. The jet-nacelle lift and drag increments were computed in a similar manner except that the downwash angle at the nacelle due to the lift of the wing was taken into consideration. This angle was obtained from simple lifting-line theory.

An important effect of the jet thrust was measured on the pitch attitude of the helicopter. Figure 19 shows that with the wings at 10°, a level fuselage attitude is obtained at 170 to 180 knots with full jet thrust. For the test vehicle, the fuselage attitude decreases as the speed increases. This drag effect reduces the wing and fuselage angle of attack and in most instances the lift. This can be seen from Table 3.

No serious problem areas were encountered with the combined wing and jet installations. The wing incidence coupled with the collective pitch eliminated the autorotation problems previously encountered during the flights with wing only.

Drag Value Summary - Drag values for the various configurations of the flight research vehicle are summarized below:

UH-1B including the effect on download (100 knots)	19.2 sq ft
HPH (Basic) with blade cuffs	10.0 sq ft
without blade cuffs	11.0 sq ft
with bar	11.5 sq ft
HPH with jets in original fairing	17-19 sq ft depending on the nacelle lift
HPH with jets in modified fairing	11-15 sq ft depending on the nacelle lift
HPH with wing	11-15 sq ft depending upon wing lift

Lift Carryover and Distribution

Lift carryover describes the additional lift produced by the fuselage due to the addition of lifting surfaces such as wings and elevators. The amount of carryover is expressed as a percentage which relates the sum of the fuselage and wing panel lift to the lift that would be produced by a continuous wing. In normal subsonic airplane configurations, the wing span is large compared to fuselage width. Winged helicopters, however, generally have wing span to width ratios considerably smaller. Hence, test data on carryover are scarce for helicopter applications. The limited test data that are available and the studies conducted during this program indicate that the assumption of 100 percent carryover is reasonable.

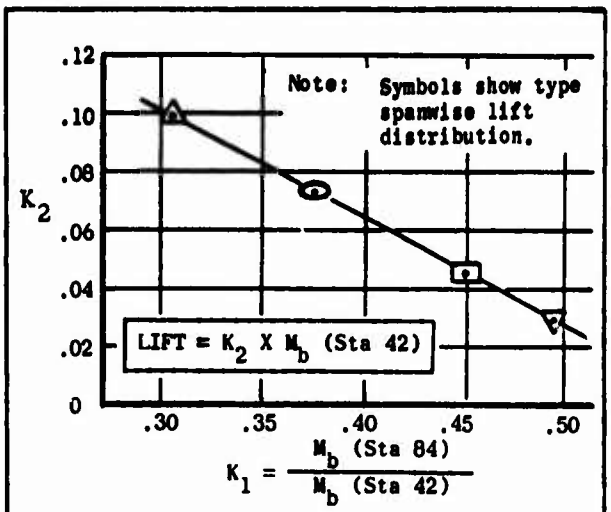

FIGURE 1. DETERMINATION OF WING LIFT FROM BENDING MOMENT DATA.

Strain gauge data on the wing structure were taken to assist in determining the wing lift. The adjacent Figure 1 shows the factors used to determine the wing lift from the bending moment data. The factor K_1 is a measure of the wing lift distribution; and from this, the factor K_2 for determining the wing lift (including 100 percent carryover) is obtained. The symbols, as shown on the figure, represent the type of spanwise distribution for that particular point. Rotor lift was determined from the steady bending moments in the hub according to Figure 20. The sum of the wing lift and rotor thrust thus obtained should appropriate the gross weight for any given flight condition.

Figure 21 gives an example, showing that good agreement is obtained using the 100 percent carryover factor for the estimation of wing lift from bending moment data. From Figure 21 it is seen that a 30 percent unloading of the rotor was achieved for the test conditions shown. The wing lift attained a maximum value near 150 knots and remained nearly constant thereafter. At higher speeds the angle of attack of the wing is less because of the nose-down pitching of the fuselage. At low speeds little wing lift is produced due to the low q and the downwash from the rotor. The maximum rotor unloading tested during the flight program was of the order of 70 percent.

The lift carryover calculated for the engine pylon and nacelles, which are set at a mean angle of 5° incidence relative to the airframe, also shows good agreement using 100 percent carryover. This is shown on Figure 22. The lift on the nacelles was not measured but was estimated based on a projected area of 76 square feet, a lift curve slope of .047 per degree (aspect ratio of 2.24), an angle of attack based on a mean pylon-nacelle incidence with respect to the fuselage, and the measured fuselage attitude.

Lift distribution data are not shown for the HPH with wing and jets. As shown earlier, both the wing and nacelles provide a considerable amount of lift. With the wing-nacelle combination, the spanwise lift distributions are altered due to mutual interference effects, and the lift of the combination is less than the sum of the wing and nacelle lifts when they are installed separately. The wing spanwise lift distribution with the wing-nacelle combination does not conform to the theoretical distributions used to determine the wing lift from bending moment data as shown in Figure 1. At low speeds (100 to 140 knots) and with the nacelles installed, the wing lift coefficients, as determined from bending moment data, were found to be considerably higher than the theoretical maximum lift coefficient for the wing.

An estimate of the lift distribution, based on calculated wing lift and an arbitrary assignment of lift carryover values for the wing and nacelles at an airspeed of 140 knots, shows 28 percent of the lift to be carried by the rotor, 59 percent carried by the wing, and 13 percent carried on the nacelle. A concise determination of lift distribution would entail extensive instrumentation beyond the scope of the program.

Correlation

Bell Helicopter Company has a digital computer performance program for the calculation of rotor aerodynamic force and moment characteristics, which includes the effects of stall and compressibility. With this program and synthesized 0012 airfoil data tables based on both wind tunnel section tests and flight tests, an acceptable correlation has been obtained for several different rotors and helicopters throughout their operating range. This program was used to calculate the shaft horsepower required for the various HPH configurations and the correlation work discussed below.

Figures 23 and 24 give typical plots of the calculated data at 170 knots. T53 SHP is calculated and plotted as a function of thrust and equivalent flat-plate drag area ("f"). For a given T53 shaft horsepower and rotor thrust, a value of "f" can be found from Figure 23. Figure 24 also gives a value for "f" if the collective pitch and rotor lift are known. With only the T53 SHP and the collective pitch known, the rotor thrust and the flat-plate drag area can be found.

Compressibility Tip Speed Effects

The effects of compressibility assume considerable importance with the high speeds attained with the HPH. The influence of rotor speed on power requirements is shown on Figure 25. An indication of the magnitude of power required due to compressibility is shown on Figure 2. It is seen that above an advancing tip Mach number of .90, the rotor blade profile drag coefficient (C_{D_o}) increases rapidly. The shaded area in the sketch represents the power requirements due to the increase in blade drag coefficient.

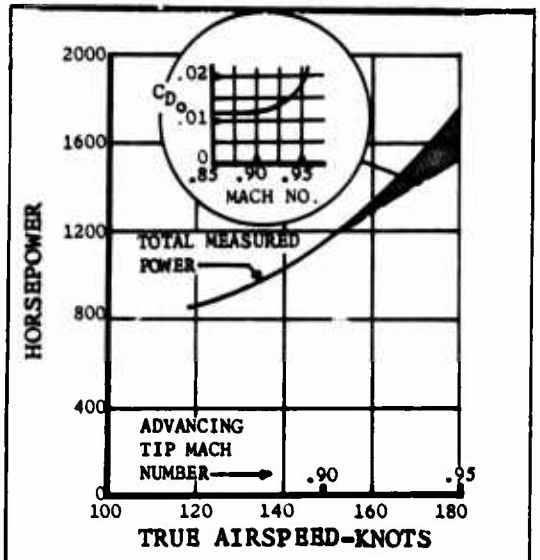

FIGURE 2. POWER REQUIRED DUE TO COMPRESSIBILITY.

To alleviate these compressibility effects, a set of tapered rotor blade tips was constructed and tested under another program. These tips tapered in thickness ratio over the outboard 53 inches of the rotor blade from the standard 12 percent to 6 percent at the blade tip. Figure 26 shows the power savings resulting from this modification and indicates a significant reduction of compressibility losses. Figure 27 combines the data given in Figures 25 and 26 and shows that the power reduction with the tapered-tip blades is approximately equivalent to the power reduction obtained by decreasing rotor rpm from 324 to 304 at 170 knots.

STABILITY AND CONTROL

Flight tests of the HPH with wing and jets have pointed out numerous areas of interest with respect to compound helicopter stability and control. Such problems as pitch, roll, and rotor rpm control during autorotation -- wing and auxiliary engine installation induced aerodynamic effects on the elevator -- and aircraft response following various combinations of power failure are outstanding examples. In the following section, the important effects on stability and control of compounding the HPH with a wing and auxiliary propulsion are discussed.

Effect of Fin-Mounted Elevator

During the initial flights with the HPH in the jets-only configuration, it became apparent to the pilot that above 80 to 100 knots, the pitch oscillation (phugoid) was unstable. The instability was great enough

that constant attention was required by the pilot to fly the aircraft. The reduction in stability was caused by loss in elevator effectiveness through the induced downwash effect of the auxiliary engine-pylon installation acting as a wing and the lowered aerodynamic pressure at the elevator resulting from the stalled area between the engine and fuselage.

Action taken to improve the stability was as follows. A flight was conducted with the engine pylon fairings removed; this resulted in much better stability than with them in place. Plans were drawn for an improved fairing. Flight testing was continued to check the effect of increased download on the elevator and aft c.g. shift, both of which tend to retrim the main rotor and cause its contribution to angle-of-attack stability to be more favorable. Each of these changes improved the pitch stability but had undesirable side effects. The increase in elevator download raised the bending moment level in the elevator main spar such that elevator lift at high speed would be limited. The c.g. movement sharply increased the vibration level (response) in the cabin area.

In view of the above developments, it was considered most expedient to add an additional elevator panel to the helicopter. The top of the dorsal fin was chosen for the mounting location since it is farther removed from the auxiliary engine installation wake and is at a greater arm from the c.g. than the standard elevator location.

Flights with the dual elevator installation demonstrated its ability to provide satisfactory pitch phugoid stability. The undesirable side effects that were anticipated were also demonstrated and included an abrupt change in fore-and-aft trim when the main rotor wake moved over the additional tail surface and an increase in the fore-and-aft trim change from level flight to autorotation. The "bump" in the fore-and-aft stick plot required some 30 percent of available control to trim as the helicopter went through the 20- to 40-knot speed range. The fixed dorsal-fin elevator effect on the change in trim from level flight to autorotation is illustrated on Figure 28 and is a result of the increase in angle-of-attack stability and lack of collective/cyclic synchronization of this elevator panel. It can be concluded that an improved installation would result if an increased area synchronized elevator were placed slightly aft and higher than the standard location.

Effect of Auxiliary Thrust on Roll Stability

The operation of a rotor at the high inflow ratios associated with high speed and drag causes the rotor to destabilize the helicopter. This is because of its unstable contribution to pitch and roll damping. The phenomenon, which is termed the "Amer Effect", is a direct function of inflow; therefore, when inflow is decreased by the application of auxiliary thrust, a more stable situation exists. The change in

stability is much more pronounced in roll than it is in pitch, since the rotor is the major source of damping in roll (for the no-wing configuration) and does not include damping surfaces such as the elevator.

The flight data shown on Figure 29 illustrate the beneficial effect of auxiliary propulsion on roll stability. The configuration is jets-only (no wing). A lateral pulse was used to disturb the helicopter, and the controls were held fixed until recovery was necessary. Although a full cycle of the roll motion was not obtained for either the low or the high jet thrust condition, it is obvious that the latter is considerably more stable. The reduced damping with the low jet thrust condition allowed roll rate to buildup rapidly and caused roll control to require constant attention. The stabilizer bar, which was removed for the Phase II program to reduce drag, normally provides damping augmentation. The electronic roll rate feedback that was tested under the Bell Helicopter Company independent research program was also effective in providing roll damping.

Effect of Auxiliary Thrust, Wing and Wing Lift, "Aileron", and Speed on Roll Control Response

Directly related to the roll damping is the roll "response" (roll rate per inch of lateral cyclic stick input). Since the Phase II program involved rotor operation through a wide range of inflow and damping conditions, the roll response also varied widely. A discussion of the effect of flight variables and configuration on response follows.

Auxiliary Thrust - With increases in auxiliary thrust, a definite and pronounced decrease in roll response was apparent. Accounting for the lowered rates is the increased rotor damping with auxiliary thrust discussed earlier in conjunction with roll stability. Step inputs in control were made to evaluate the roll response. On Figure 30 the roll rate generated by some of these inputs is shown. Comparing the high and low jet thrust curves with no "aileron" control provided, it can be seen that increased thrust cuts the response in half. For non-maneuvering flight this is not considered objectionable, but when tactical maneuvering is required, higher values than the 6 to 8 deg/sec/inch of stick shown for the high jet without aileron control are desirable.

Wing and Wing Lift - The wing's contribution to roll damping was such that at the upper speed range of the wing-only configuration, the roll response was kept to the order of 12 deg/sec/inch, whereas the Phase I no-stabilizer-bar configuration demonstrated nearly 30 deg/sec/inch (see Figure 30). The wing's contribution to roll damping is obviously very helpful for this configuration. The effect of wing lift was only evaluated qualitatively, but the expected trend of increased response (roll rate) with increased wing lift was noted by the pilots.

"Ailerons" - The aileron function of the wing was provided by synchronizing wing differential incidence with the lateral cyclic. Two ratios were provided: ±1.5 deg/panel with left-to-right stick and ±3 deg/panel. Flights with the fixed-wing installation and the higher of the two ratios indicated that when wing stall was imminent, such as during autorotation, the synchronization was undesirable as it would cause the wing to contribute an opposite moment to that desired because of stall. Later flights with the collectively synchronized wing proved the aileron function to be beneficial. Data shown on Figure 30 point out that with the high jet thrust, the response was increased by over 75 percent at 160 knots with the ±1.5 deg/side synchronization. This synchronization value is near optimum because of the strong effect of speed on response.

Speed - All configurations exhibited an increase in response with speed. This is a result of the previously mentioned "Amer Effect" and is directly related to rotor inflow. At no speed, however, was the high level of response a limiting factor on the pilot's ability to control the aircraft.

Effect of Auxiliary Thrust, Wing and Wing Lift, "Ailerons", and Speed on Roll Control Sensitivity

The roll "sensitivity" (roll acceleration per inch of lateral cyclic stick input) is a function of the input moment and the roll inertia. The input moment from the rotor varied over a wide range since the rotor was unloaded to various amounts by the wing. Further changes in the input moment were created by the aileron function of the wing. In addition, the roll inertia was increased by the wing and jets. The following summarizes the results.

Auxiliary Thrust - The roll inertia from the jet installation accounts for a 35 percent increase in roll inertia over the basic HPH -- or a 26 percent thrust installation on the HPH and is constant throughout the aircraft's operating range. The only direct effect of auxiliary thrust is to reduce the rotor's net thrust slightly because of the reduced propulsive force required from the rotor. In the jets-only configuration, this was not reported by the pilots to be great. The major associated consequence of adding auxiliary thrust comes through its action on pitch attitude -- leading to higher wing lift values and thereby reducing the roll sensitivity. No detailed separation of the effects has been attempted; however, since the wing lift effect on sensitivity is known to predominate, the net effect is discussed next with regard to wing lift.

Wing and Wing Lift - The addition of the wing to the HPH increased the roll inertia by some 25 percent over the basic HPH. This accounts for a 20 percent decrease in sensitivity. In combination with the jet installation, the total inertia increase drops the sensitivity to 62 percent of the basic HPH. The data point shown on Figure 31 for the wing with idle jet falls in this region. With wing lift increase, the rotor lift decreases -- as does sensitivity. This is the main cause for the change

from high to low jets (and the resulting high to low wing lift) as has been discussed previously. From Figure 31, the wing lift effect can be seen to reduce the sensitivity with high lift to less than half that with low lift.

"Ailerons" - The differential lift function of the wing (aileron control) was very effective. It increased the roll sensitivity of the HPH at high speeds to a more desirable level than that demonstrated by the no-"aileron" configuration. For example, at 160 knots, the "ailerons" increased the sensitivity by nearly 60 percent. The increased aileron gearing ($\pm 3^{\circ}$) was not tested after the difficulty with wing stall in autorotation with the fixed wing. It is possible that the additional sensitivity it would provide would be desirable during maneuvering flight.

Speed - The basic HPH roll sensitivity increased with speed because of the increase in rotor thrust required to overcome drag. The wing and jets configuration shows the same trend. However, with increased lift on the wing, the tendency toward increased sensitivity is reduced (with no "aileron"). The effectiveness of the ailerons increases with aerodynamic pressure; as a result, there is a strong increase in sensitivity with speed for this configuration.

Effect of Wing on Roll Stability

The increased roll damping from the wing markedly increased the level-flight roll stability of the winged HPH over that of the basic HPH. Figure 32 compares a roll time history following a lateral pulse input for the basic and winged (with idle jets) HPH. The improvement in stability is obvious. When jet thrust is increased to overcome the drag of the wing and jet installation (thereby simulating the wing-off case except for wing damping), a further improvement takes place. The roll stability at high speeds for the first configuration of the HPH was not, however, as good as was desired. There still remained a tendency for the roll to drift slowly away from trim. It is expected that some form of roll rate feedback system such as that tested under the Bell Helicopter independent research program will be required for optimum roll characteristics. The additional aerodynamic damping from the wing gave a noticeable increase in roll gust sensitivity (even during hover), but under no flight conditions did this reach an undesirable level. The effect of the wing on roll during autorotation entry is discussed under the next heading.

Speed Effect on Roll Stability

The HPH with wing and jets did not exhibit a strong tendency toward roll stability deterioration with speed as did the basic HPH. The response of the helicopter at 160+ knots with full jets did not differ materially from the 80 percent NI jet condition at 142 knots as shown in Figure 32. The tendency to drift slowly from trim is also present

at higher speeds. The beneficial effect of the wing (which increases with speed as has been discussed) and the reduction in main rotor inflow caused by the jet thrust are responsible for the more favorable stability at increased speeds with this configuration.

Effect of a Wing on Pitch-up, Rotor RPM and Roll Control During Autorotation Entry

Initial flights with the HPH in the wing-only configuration demonstrated that a wing has a major effect on pitching, roll control (during wing stall), and main rotor rpm decay during autorotation entry. These effects are discussed below.

Pitching - During initial flights of the HPH with wing only, autorotation entry was attempted. The result was a strong nose-up pitching tendency. This can be attributed to two effects. The first is the direct effect of the wing's lift on pitching moments. With the wing swept to 13°, and with the c.g. location being flown, the aerodynamic center of the wing was forward of the c.g. This contributed a nose-up moment as wing lift increased. Also, as the wing approached stall, it is believed that the stall progressed from the wing tips to the roots, thereby moving the aerodynamic center forward since the wing was swept.

The second effect was that of the induced angle change at the elevator from the wing's downwash. This loss in angle-of-attack stability, together with the wing's direct effect, resulted in unstable static pitching moments for the fuselage-wing-elevator combination. In anticipation of such effects, the wing sweep had been made adjustable. With full aft sweep (23°), the pitch-up tendency was greatly reduced. Wing incidence was also found to contribute to pitch-up through its effect on the main rotor equilibrium condition. Since the pilot must watch rotor rpm and since wing lift has an important effect on rpm (next topic of discussion), he is required to flare more with the lower rotor lift associated with higher wing angles. The aft motion of the cyclic stick in the flare then causes the helicopter to nose-up. This effect is illustrated by the time history on Figure 33. It can be seen that the aft motion of the cyclic stick to keep rotor rpm decay to a safe level caused the 5° incidence wing configuration to pitch-up nearly 6°. With 0° wing, the ship nosed over a maximum of some 7°.

Rotor RPM - In addition to the pitching effect, a rapid decay of the main rotor rpm was evident with the winged HPH. This effect was so severe that with all but the very low angles of wing incidence, the rotor decay equaled or exceeded that of the main engine so that no "needle-split" was possible at higher speeds. For example, with the -5° incidence wing, no needle-split was possible above about 135 knots. The problem is simply a matter of the change of rotor equilibrium rpm with various combinations of rotor lift and rotor attitude -- and the collective and cyclic required for these combinations. When the rotor

starts being unloaded by the wing during autorotation entry, the collective must be reduced rapidly and the rotor tilted back in order to hold rpm. If the wing is allowed to generate an increasing amount of lift by being set at a higher incidence, a more rapid and greater application of control is required to maintain rpm. This effect is illustrated on Figure 33, where it can be seen that more collective and more aft cyclic are required to hold a similar level of rotor rpm. (Note: As the decay problem was more severe with the 5° incidence wing, minimum rpm was not allowed to decay as far as with the 0° wing). Inboard spoilers were in place on the wing when the records of Figure 33 were taken. Their primary effect was to cause buffeting rather than to aid in correcting the rpm problem. The pilot technique of reducing wing incidence upon autorotation entry demonstrated that this was a satisfactory solution to the rpm problem (and the roll control problem to be discussed next). Calculations that have been correlated with the HPH flight test data indicate that when the ratios of minimum wing (or lifting surface) lift to the gross weight of the helicopter exceeded 0.3, the problem of rpm control occurred. Wing incidence to collective stick synchronization hardware was installed (see description of test vehicle). The simulated power-failure time histories shown in this section demonstrate that the synchronization system was successful. The system can be further improved, however, since the $\pm 10°$ incidence range is not adequate for a wide range of c.g. locations. Also, the synchronization tested does not give a specific wing incidence for each collective setting because it is not a true proportional control.

Roll Control - Alternate stalling of the wing panels during autorotation with the wing fixed at high incidence caused the helicopter to roll. Corrective control then caused an increase in angle-of-attack through the aileron function of the wing and further aggravated the stall. Although not explained, the roll normally occurred to the left first (the basic aircraft also had a left rolling tendency). Synchronization of the wing with collective corrected the roll control problem by avoiding the stalled condition. Wing stall characteristics remain important even with synchronization provisions: wing sections with abrupt stall characteristics should be avoided.

Helicopter Response Following Simulated Power Failure

High-Speed Power Loss - Figure 34 illustrates a simulated power failure of both the primary and the auxiliary engines simultaneously at a speed of 177 knots. The reaction of the helicopter and the control motions required to trim were found to be surprisingly moderate. The initial pitching was not severe, and only slight fore-and-aft cyclic motion was required. Lateral cyclic was moved to the right as the anti-torque couple was reduced. The left roll tendency and the roll oscillation were apparent in the roll attitude trace. Although not shown, the rotor rpm did not drop to an unsafe level.

Effect of Delay in Auxiliary Thrust Reduction - To simulate loss of the primary engine with no loss in auxiliary engine thrust, various amounts of time delay in cutting the J-69 power were investigated. It was immediately obvious that a strong nose-up pitching tendency was associated with delay in auxiliary thrust reduction. Figure 35 compares the reaction of the HPH to a T-53 power chop with no delay on J-69 chop and with a 2- to 3-second delay before reducing the J-69 power. The pitching increased from a maximum of about 5° nose-up to approximately 9° with the delay. The mechanism by which this effect takes place is as follows: With the jets operating, the main rotor requires less forward cyclic for trim than with the jets inoperative. Following autorotation entry, the stick is trimmed farther aft than normal. Until the jet thrust is reduced, this trim of the rotor noses the ship up. Only a small amount of moment change comes from the jet, since its line of action passes within a few inches of the vertical c.g.

Right-Hand J-69 Simulated Power Failure - Figure 36 illustrates the fact that asymmetric loss of jet thrust creates no control problem. This fact is a result of the strong directional stability of the aircraft and its high directional control power. Unless the thrust of moment arm of the jet installation is greatly increased, asymmetric loss of thrust will not be a problem.

Normal Acceleration Response and Range Attained

The normal acceleration response to a fore-and-aft cyclic input for the full compound HPH is shown on Figure 37. Although there was a definite increase with speed in "g" sensitivity to cyclic inputs, at no time was it considered objectionably high. Good pitch stability helped in this regard. Although it was not the purpose of this program to explore maneuvering flight, a number of steady turns and fore-and-aft cyclic inputs were completed. Typical maximum g's are plotted on Figure 38 against the speed at which they occurred. This distribution of load during maneuvering flight indicated that the rotor increases lift more rapidly than does the wing. For example, in the pull and hold shown on Figures 37 and 38, the change in wing lift was only 10 percent as large as that of the rotor. Since at high speeds the lift capability of the wing is greater than that of the rotor, it would be desirable to modify wing incidence synchronization to allow it to lift more during maneuvers.

STRUCTURAL LOADS AND VIBRATIONS

The modification of the basic HPH to the compound configuration resulted in changes to the dynamic characteristics of the machine. During the program, both analytical and experimental investigations were conducted to assure that no overloading or resonant conditions existed. The significant changes to the fuselage dynamics involved increased cabin stiffening and improved mass distribution.

In the following paragraphs the vibration characteristics, main rotor and control loads, wing loads, and tail rotor loads are discussed. Except where noted, all data presented are for the UH-1B two-bladed rotor, no stabilizer bar and 6600 engine rpm (324 rotor rpm). One exception is that the HPH with jets-only data are for a 2-3/4° preconed yoke (the UH-1B rotor precone angle is 4°). Vibration levels and main rotor, tail rotor, and control loads for the UH-1B are taken from Reference 6. Similar data for the basic HPH are from Reference 3. The vibration levels and rotor and control loads during maneuvering flight (data shown on Figure 38) are still less than those obtained during the high-speed steady-state flight condition. Consequently, maneuver data are not presented.

Vibration Characteristics

Rotor Natural Frequencies - Calculated natural frequencies for the UH-1B/HPH two-bladed rotor are shown on Figure 39. The cyclic and collective modes are indicated on the figure. For a two-bladed, semi-rigid rotor, the collective modes can be excited by even-numbered forcing functions (2,4,6 .../rev); the cyclic modes, by all odd-numbered harmonic forcing functions (1,3,5 .../rev). Use of this terminology for the blade natural frequencies allows the coupled response characteristics of the rotor to be considered in relation to the forcing functions to which it can respond.

As shown on Figure 39, the effect of collective pitch is to reduce the frequency of the first inplane symmetric mode about 20 percent and to increase the second vertical asymmetric mode frequency about 10 percent (for a collective pitch of 20°). The natural frequencies of the UH-1B/HPH rotor are well situated with respect to the forcing functions, resulting in low dynamic response over the normal helicopter ranges of forward speed, rotor rpm, and collective pitch.

Auxiliary Engine Response - In the flight tests following the addition of the auxiliary engines, the helicopter was flown without the engine fairings installed. During these flights, severe engine vibrations were noted. Two dampers were installed in the mounting system to suppress these vibrations. The dampers could not be located near the point of maximum amplitude and were not successful in reducing the vibration.

Shake test of the engines revealed that resonant peaks occurred near two-per-rev with the damper installed. Replacement of the dampers with a stiff support raised the frequencies slightly above two-per-rev, with another resonant peak at four-per-rev. Addition of the fairings between the fuselage and engine cowling did not significantly change the resonant frequencies but reduced the amplitude associated with each peak. The skin apparently carried sufficient torsional shear load to serve as a torque-box. All subsequent flight tests were conducted with the stiff brace and the fairings installed. The engine vibrations were acceptable with this configuration.

Wing Response - The basic wing resonant frequencies were measured at 8.8 and 11.1 cps beamwise and 13.0 cps chordwise. Flight tests showed that the beamwise response at two-per-rev was unacceptable. Tip weights were added to the wing in increments up to 44 pounds. A tip weight of 15 pounds was found to give the best compromise between beamwise and chordwise response. For this condition, the wing resonant frequencies were 8 cps beamwise and 11.8 cps chordwise.

Although the measured oscillatory loads were not high enough to cause structural damage, the oscillatory motion of the left wing was objectionable at high forward speed and fuselage vibrations were increased. Frahm dampers, consisting of a steel rod and 5-pound weight, were added inside each wing tip in place of the tip weight. The dampers were tuned to give minimum wing response in the 1.5- to 11.0- cps range. Plots of static wing displacement versus frequency for both the basic wing with 15-pound tip weight and the wing with dampers are shown in Figure 38. With the dampers, the resonant peaks were shifted to 7.8 and 13 cps beamwise and 10 and above 13 cps chordwise. At two-per-rev (10.8 cps), both the beam and the chord wing responses are reduced due to the dampers. Subsequent flights with the dampers installed showed the wing's dynamic response to be satisfactory and the fuselage vibration reduced.

Pylon Response

Throughout the program, attention had to be given to maintaining adequate pylon damping. As reported in Reference 3, friction dampers were installed between the upper transmission case and the cabin roof to increase the damping. With the jets installed, additional lateral pylon dampers were required. As a result of wear of the special damper installation, the dampers had to be replaced occasionally during the flight tests.

During the test program, a roll rate stabilization system was designed and evaluated. It was found that this system improved the roll stability characteristics of the machine; however, it contributed a negative effect with respect to pylon damping. To evaluate the effectiveness of such a device to increase the pylon damping, the rate sensor of the stabilization system was mounted on top of the transmission case of the HPH. It was found that the pylon rate control coupling markedly improved the pylon stability of the aircraft and, as expected, decreased the rigid-body dynamic stability of the airframe.

Cabin Vibration Levels

As mentioned previously, the HPH fuselage is a modified YH-40 which has a higher response to two-per-rev excitations than the production UH-1A or UH-1B aircraft. Although a direct comparison is not possible, the major effects of various configurations on the pilot and copilot vibration

levels are shown on Figures 41 and 42 respectively. Additionally, calculated data are presented on Figure 43.

Effect of Auxiliary Propulsion - Figure 41 shows that the augmentation extends the speed range approximately 40 knots above that of the basic HPH for a vibration level of ±.15. For the cold jet case, the vibration levels for the basic HPH and HPH with jets-only are the same up to about 120 knots. Above 120 knots, the vibration level is less, which is explained by the increased cabin stiffness and improved fuselage mass distribution for the jet-configured HPH. With full jet thrust, the level at 182 knots does not exceed that for the basic HPH at 142 knots. The data shown are for a favorable fuselage mass distribution. This effect is discussed in Reference 3 and illustrated by Figure 43.

Effect of Wing and Auxiliary Propulsion - The compound HPH follows the same lowering trend in vibration levels as experienced with the jets-only case. As shown in Figure 41, the pilot two-per-rev vibration level never exceeds ±.15g's for the high speed regime. In addition, a lowering trend is indicated above 70 knots. From the figure it is seen that slightly lower levels are associated with the compound configuration than for the jets-only case. This reduction is the result of the reduced rotor lift and the Frahm dampers installed in the wing tips.

Correlation - Correlation studies were conducted for the basic HPH and also for the configuration with auxiliary propulsion only. The results of these studies and corresponding flight test data are shown on Figure 43.

Good agreement is shown for the basic HPH case. For the HPH with auxiliary propulsion, the calculated values are shown to be greater than actually experienced at the higher airspeeds for the cold jet condition. With full jet thrust, the calculated data are shown to be high in relation to those obtained from flight test. The data from two flights are shown to illustrate the effect of fuselage mass distribution. Lower vibration levels are obtained with added weight in the nose of the machine.

Main Rotor Loads

Throughout the flight test phases, blade oscillatory loads were monitored to assure that safe operating limits were not exceeded and that the helicopter could safely enter a higher speed regime. These data also provided a means by which correlation could be made between calculated and measured loads.

The distribution of loads along the blades followed closely the trends found for the UH-1B. As a result, only the bending moments at the rotor

hub (yoke) are presented, since they are indicative for those of the entire rotor. Direct comparison can be made between the UH-1B and the various HPH configurations, since all use the same two-bladed rotor.

Chord - The main rotor chord loads show a significant decrease as a result of drag reduction and the addition of a wing and auxiliary propulsion. These effects are summarized on Figure 44. With the basic fuselage cleanup, a speed of 142 knots could be achieved at the same load level as that for the UH-1B at 110 knots. Since the fuselage drag and download directly influence the inplane blade loads, their reduction is the principal reason for this load decrease. The addition of a wing further reduces the chord loads and permits speeds in excess of 150 knots at inplane rotor loads lower than those for the basic HPH.

In the high speed regime, with the jets operating, chord loads are also low as a result of auxiliary propulsion and wing lift. For the jets-only configuration with full jet thrust, the inplane loads at 180 knots are shown to be about 50 percent of those of the UH-1B at 110 knots. With the wing, the inplane rotor loads are reduced to about 60 percent of those of the standard UH-1B for the same speed conditions.

The load curve for the compound HPH with full jet thrust and the wing at 10° shows a decrease in the 150 to 170-knot speed range. This unusual trend may be attributed to changes in the distribution of rotor and wing lift and the rotor and auxiliary engine propulsive force. The trim changes of the aircraft and rotor resulting from the various distributions of lift and power produce variations in the rotor efficiency and operating conditions as a function of speed. At the low speed point with full jet thrust and wing, the data indicated that the rotor was actually providing a retarding force.

The effects of rotor speed on the chord loads are also shown by Figure 44 for the wing-jets configuration. A general trend of lower inplane loads with reduced rotor speed is seen except at the upper limit of the airspeed range. This increase at higher airspeeds is the result of approaching blade stall and illustrates the importance of wing lift for high-speed rotorcraft.

Beam

The main rotor beam loads for the various HPH configurations and UH-1B are shown on Figure 45. The general trend of those loads, to increase with speed, is as expected. The important beneficial effects of auxiliary propulsion and reduced drag are seen by comparing the curves for the basic HPH and jets-only configurations with that for the UH-1B. The additional load reduction resulting from the wing for both the wing-only and full-compound configuration is also shown to be significant. The effects of rotor speed on the beam loads are also given by Figure 45 for the wing-jets configuration. It is seen that rotor speed does not influence the beam loads appreciably.

Correlation

During the course of the program, correlation studies were conducted to establish the validity of the analytical techniques used to predict high-speed-rotorcraft loads. Some results of these studies are given on Figure 46, where beam and chord yoke oscillatory bending moments are shown.

Good agreement between calculated and measured data is shown for the inplane loads for all conditions investigated. For the beamwise loads, good agreement is shown for the cold-jets case; however, the beneficial effects of auxiliary propulsion are seen to be grossly overestimated.

Control Loads

A comparison of control loads as represented by pitch link loads is presented for the various HPH configurations on Figure 47. The basic HPH and the wing-only configurations show a delay in control load rise relative to the standard UH-1B. Low fuselage drag and download for the basic HPH configuration reduce blade stall and thus the pitch link loads. For the wing-only configuration, the rotor is partially unloaded and thus has lower collective pitch, which also has a beneficial effect on the control loads.

At the higher airspeeds with full jet thrust, the control loads for both the full-compound and jets-only configurations become a limiting factor for high-speed flight. As a consequence, the standard UH-1B rotating control system had to be redesigned to accommodate these higher loads.

The effect of rotor speed is also shown on Figure 47. At the higher airspeeds (above 160 knots), it is seen that lower rpm operation resulted in lower control loads. This is believed to be the result of reduced compressibility effects on the advancing blade. This effect will be discussed further in the subsequent paragraphs.

As seen by the configuration comparison of Figure 47, flights with tapered-tip main rotor blades show that for the same control load, the maximum speed for the full-compound configuration could be extended some 15 knots. At 193 knots the control loads for the tapered-tip blades are about 20 percent less than those for the standard blades at 186 knots.

The effect of the modified blade tip on control loads may be seen by a comparison of pitch link load oscillograph traces for the standard and tapered-tip blades. These traces are shown on Figure 48 for various azimuth positions and airspeeds. The data for the standard blades show a large negative pitch link load at about $\psi = 120^\circ$, which may be attributed to advancing blade Mach number effects. The large positive load at approximately $\psi = 270^\circ$ is believed to be associated with the reversed

flow on the retreating blade. It can be seen that the negative load at near $\psi = 120^{\circ}$, which appears at an advancing blade Mach number of about .87 and increases rapidly thereafter for the standard blade, is absent for the tapered-tip section cases. This reduction, in addition to the lower power required, made possible airspeeds up to 193 knots. Figure 48 also explains the trend of lower control loads with lower rpm as noted earlier.

Tail Rotor Loads

The measured tail rotor blade beam and chord oscillatory bending moments for the wing-only and jets-only configurations are shown on Figure 49. For comparison, flight test data for the UH-1B are also presented. As shown on the figure, the beam loads are lower than those for the UH-1B up to 150 knots. At the higher airspeeds, the beam moments increase; however, they remain within the endurance limit for all flight conditions. The tail-rotor-blade steady beam bending moments are shown on Figure 50 for the UH-1B and two configurations of the HPH.

The addition of wing and auxiliary propulsion result in a substantial reduction in the tail-rotor steady load. Two factors bring about the reduction in tail-rotor loads on the HPH. First, the significant decrease in drag of the basic fuselage reduced the power required to drive the main rotor at a given airspeed, consequently reducing the anti-torque force required at the tail. Further decreases in tail-rotor loads, as reflected on Figure 49, are due to the addition of wing and auxiliary propulsion, which also reduce the main-rotor power. Second, the tail rotor is unloaded by the cambered vertical fin. Calculated data indicate that for the HPH without auxiliary propulsion, up to 90 percent of the required anti-torque load is carried by the fin at high speed. The side force developed on the cambered fin can even exceed the amount necessary to counteract main rotor torque. A negative thrust must then be produced by the tail rotor to trim the aircraft at zero sideslip angle. This negative thrust is shown on Figure 50 for the auxiliary propulsion configuration. Note that a negative bending moment does not necessarily indicate negative thrust on the tail rotor, as a large negative moment is exerted on the blades by centrifugal force due to preconing of the hub. The measured zero thrust line for 324 main rotor rpm is shown on the figure.

With the auxiliary propulsion configuration, an additional effect on load reduction is indicated. Since the airflow from the main rotor affects the tail rotor inplane loads, the higher nose-up fuselage attitude orients the tail rotor away from the main-rotor downwash.

Measured flapping angles for the UH-1B and the HPH are presented on Figure 51. It is seen that the combined effects of power reduction and the cambered fin result in reductions in tail-rotor flapping amplitudes which are consistent with the decreased tail-rotor thrust requirements.

Wing Loads

The mean and oscillatory wing loads were measured to determine the resulting lift and wing response. The measured oscillatory beam and chord loads at Station 42 for the right and left wing panels are shown on Figure 52.

It is seen that the oscillatory loads for the left panel are, in general, higher than those for the right. These oscillatory wing loads cause an increase in cabin vibrations, and, as discussed previously, Frahm dampers were designed and installed in the wing tips.

The effect of Frahm dampers on the left and right wing panel loads is also shown on Figure 52. A significant reduction in both the left and the right panel loads can be seen.

EXTERNAL NOISE

Noise measurements were conducted for the full-compound configuration, with cold jets and 90 percent jet N_I, during flyover at 120 and 155 knots, respectively. Similar measurements were made for a Model 204B (commercial version of UH-1B with 48-foot-diameter rotor) at 120 knots. Both aircraft flew over a ground-based microphone at an altitude of approximately 100 feet, and the microphone output was recorded on magnetic tape. Later, these data were reduced by an octave band analyzer to define the peak sound pressure levels for the various frequencies.

A comparison of the measured peak, over-all, and octave band sound pressure levels is shown on Figure 53. With the jets off, the HPH is seen to produce less noise than the commercial machine. This is believed to be due to the Mach number and power effects. The high-speed flyover noise of the compound HPH with jets operating is of the same over-all magnitude as that for the 204B. However, there are differences in the noise characteristics of the two machines due to the frequency distribution of each aircraft's noise.

At frequencies below 300 cps, the maximum flyover noise of the full-compound HPH peaks in the second octave (75-150 cps); whereas, for the 204B, the peak noise occurs in the first octave (20-75 cps). For the compound HPH, the higher level in the second octave is associated with the increased contribution of the tail rotor due to the higher flight speeds.

For the octave bands above 300 cps, a 5- to 9- decibel increase in the noise of the compound HPH can be seen. This increase in noise at the higher frequencies is associated with the compressors of the jet engines.

The approach noise of the compound HPH at 155 knots was observed to be less noticeable than that for the 204B at 120 knots. The noise propagated forward is associated with the pulsating or "slapping" component of the main rotor and is greater for the 204B due to the higher tip speed of the advancing blade. In addition, the high-frequency noise of the auxiliary jets, although predominant during flyover, is not heard during the approach due to atmospheric attenuation.

REFERENCES

1. High Performance Helicopter, U. S. Army TRECOM Contract DA 44-177-TC-711, July 31, 1961.

2. Modification 4, Supplemental Agreement to U. S. Army TRECOM Contract DA 44-177-TC-711, September 28, 1962.

3. Van Wyckhouse, J. F., and Cresap, W. L., Summary Report, High Performance Helicopter Program Phase I, TRECOM Technical Report 63-42, September 1963.

4. Van Wyckhouse, J. F., High Performance Helicopter Test Program Extension Agenda, Bell Helicopter Company Report 533-099-012, March 1963.

5. Brown, E. L., Summary Report, HU-1 Full-Scale Wind Tunnel Tests, Bell Helicopter Company Report 204-099-764, October 1961.

6. Wheelock, R., Preliminary Load Survey, UH-1 Helicopter, Bell Helicopter Company Report 204-099-949, July 1960.

APPENDIX

TABLES AND FIGURES

TABLE 1

FLIGHT PARAMETERS AND HELICOPTER CONFIGURATION FOR PRIMARY EVALUATION FLIGHTS

Flight No.*	Configuration	GW/σ'	Rotor RPM**	Mast Incidence i_m, deg	Wing Incidence i_w, deg
522	Wings Only	7483	324	7-1/2	8
523	Wings Only	7760	324	7-1/2	8
524A	Wings Only	7870	324	9	8
525B	Wings Only	7533	321	11	10
525B	Wings Only	7516	321	11	8
549	Jets Only [1]	8157	324	Varied	-
553	Jets Only, Cold	8285	324	7	-
555	Jets Only, Cold	8394	324	6	-
581	Jets Only, Cold	8755	324	6	-
555	Jets Only at Idle	8458	324	6	-
558	Jets Only at Idle	9264	324	7-1/2	-
581	Jets Only at 80% N_I	8843	324	6	-
558	Jets Only at 98% N_I	9264	324	9	-
580C	Jets Only at 98% N_I	9225	324	8-1/2	-
575A,B	Wings & Jets, Cold	9280	319	7-1/2	5
580B	Wings & Jets, Cold	9725	319	8-1/2	Varied
575A,B	Wings & Jets at 80% N_I [2]	9170	322	7-1/2	5
571C	Wings & Jets at 98% N_I [2]	9616	324	8-1/2	10
575A,B	Wings & Jets at 98% N_I	9300	320	7-1/2	5
575A,B	Wings & Jets at 98% N_I	9220	319	7-1/2	Varied
575B,C	Wings & Jets at 98% N_I	9270	311	7-1/2	5 & 10
575B,C	Wings & Jets at 98% N_I	9310	302	7-1/2	5 & 10
578A,B,C	Wings & Jets at 98% N_I	9600	324	7-1/2	Varied
579A	Wings & Jets at 98% N_I	9000	324	7-1/2	Varied
580A,B	Wings & Jets at 98% N_I	9725	319	8-1/2	10
590	Tapered Tip Blades, Wings & Jets at 98% N_I	10058	324	7-1/2	10

* Flight numbers with letter suffix indicate a series of flights with the same basic configuration. When flight numbers are used without a letter suffix the data shown are applicable for all flights in the series.

** 324 = Normal operating RPM

1 With stabilizer bar on
2 With cuffs off

TABLE 2

SPEED AND POWER COMPARISON OF THE HPH WING AND/OR JET CONFIGURATIONS

Comparison and Configuration	GW/σ'	Comparison of Speed at Constant SHP/σ' & GW/σ'				Comparison of Power Req'd at Constant Airspeed		
		T53 SHP/σ'	J69 % RPM	Total Power	True Airspeed knots	True Airspeed knots	T53 SHP/σ'	Total Power
Effect of Wings								
- Basic HPH	7600	1000	-	1000	146	150	1075	1075
- HPH With Wings			-		151		980	980
- UH-1B Reference			-		130		-	-
Effect of Jet Engine Installation								
- Basic HPH	8046	1000	-	1000	144	140	915	915
- HPH With Jets, Cold	8500		-		143		945	945
- UH-1B Reference	8046		-		127		-	-
Effect of Auxiliary Jet Propulsion *								
- Basic HPH	9000	1000	-	1000	144	150	1120	1120
- HPH With Jets	9200	380	98	1000	145		700	900
- HPH With Jets	9200	1000	98	1860	186		440	1160
- UH-1B Reference	9500	1000	-	1000	117			
Effect of Combined Wings and Auxiliary Propulsion								
- HPH With Jets Only	9200	800	98	1610	177	180	850	1695
- HPH With Wings and Jets	9500	800	98	1630	178		815	1660
Effect of Thin-Tip Blades								
- HPH With Jets and Wings	9500	800	98	1630	178	180	850	1695
- HPH With Jets, Wings, & Special Thin-Tip Blades	10058	800	98	1660	184		710	1555

* The engine-nacelle-pylon served as a wing. (See Text Page 21.)

TABLE 3

LIFT AND DRAG DISTRIBUTION FOR WING AND JET ENGINE CONFIGURATION

True Air-speed (knots)	N_I Jet (%)	i_{Wing} (deg)	$\Theta_{Fus.}$ (deg)	Drag (f) - Sq Ft				GW/ σ' Lb.	Lift/σ' - Lb.		
				Wing	Nacelle	Jet Engine	Total		Wing	Nacelle	Rotor
120	80	5	4.2	2.8	3.1	-13.9	2.0	9150	2850	1510	4790
140			2.0	1.6	2.2	- 9.7	4.1		2850	1630	4670
160			-0.4	1.2	1.4	- 7.1	5.5		2740	1460	4750
120	80	10	2.4	5.9	2.1	-13.9	4.1	9526	4110	1150	4226
140			0.5	2.8	1.5	- 9.7	4.6		4110	1210	4206
160			-1.5	1.8	1.0	- 7.1	5.7		4060	1090	4376
140	98	5	5.8	4.6	3.9	-23.5	-5.0	9270	5100	2350	1820
160			3.7	2.8	2.9	-17.8	-2.1		5250	2450	1480
180			1.3	1.9	1.9	-13.9	-0.1		5300	2700	1270
160	98	10	2.4	2.9	2.2	-17.8	-2.7	9270	5500	2140	1630
180			-0.4	1.7	1.3	-13.9	-0.9		5000	2070	2200

i_{Wing} = Wing incidence with respect to fuselage waterline.

$\Theta_{Fuselage}$ = Fuselage attitude with respect to horizon.

$f_{Total} = f_{Basic} + f_{Wing} + f_{Nacelle} - \frac{F_n \text{ Jets}}{q}$ where $f_{Basic} = 10.0 \text{ Ft}^2$,

q = Dynamic Pressure.

$L_{Rotor}/\sigma' = GW/\sigma' - L_{Wing}/\sigma' - L_{Nacelle}/\sigma'$.

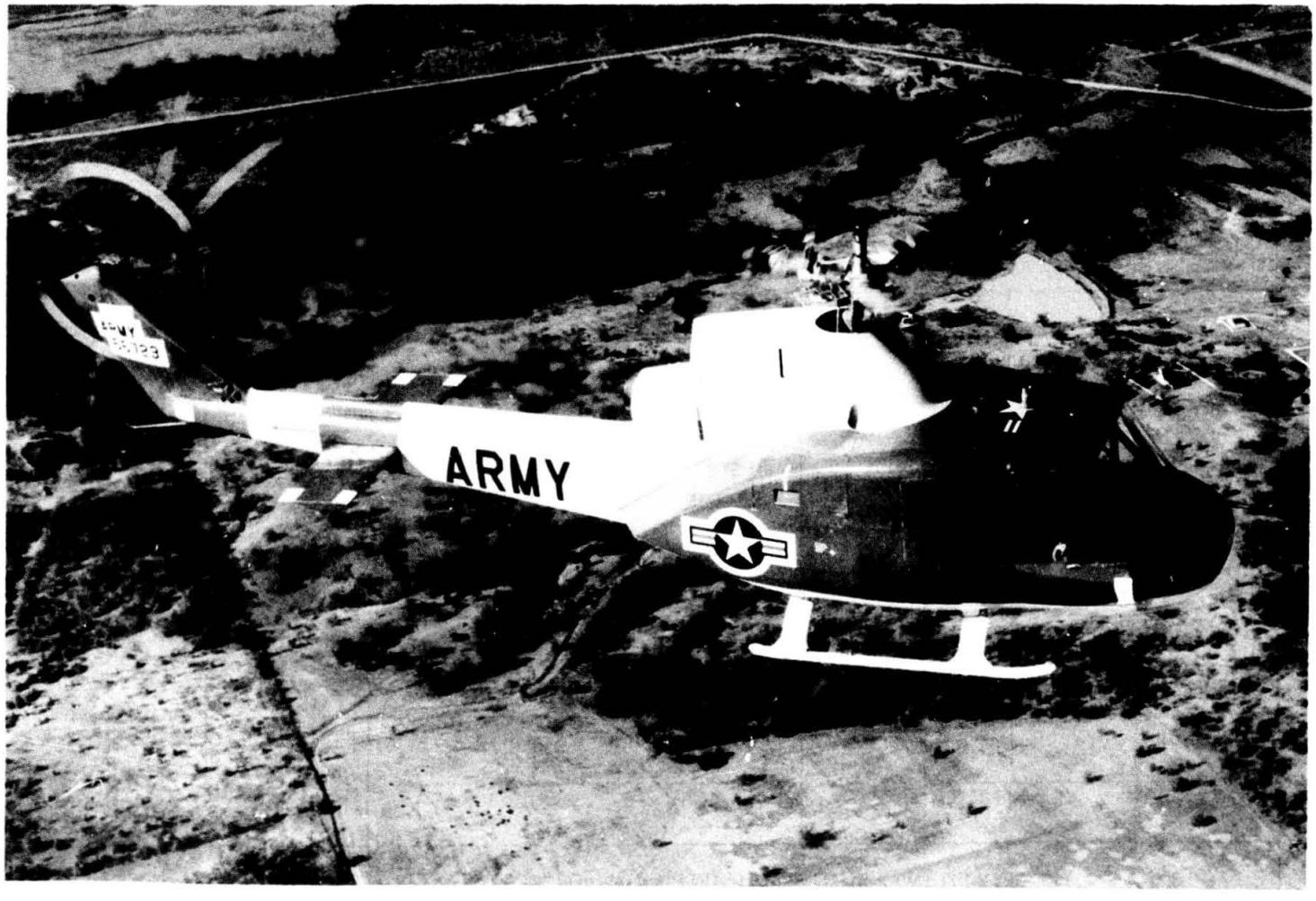

FIGURE 3. BASIC HIGH-PERFORMANCE HELICOPTER.

FIGURE 4. HIGH-PERFORMANCE HELICOPTER WITH WINGS.

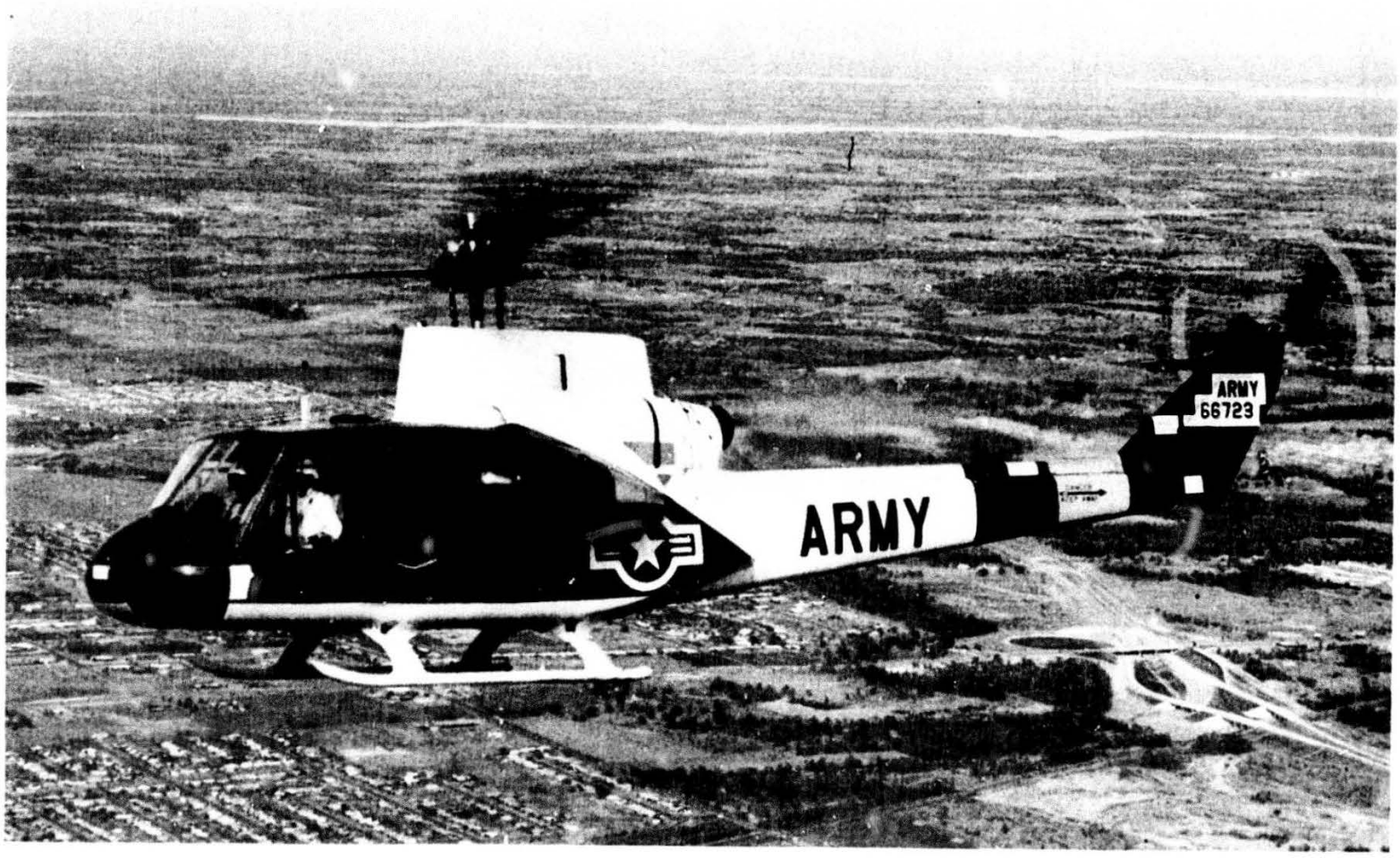

FIGURE 5. HIGH-PERFORMANCE HELICOPTER WITH AUXILIARY ENGINES.

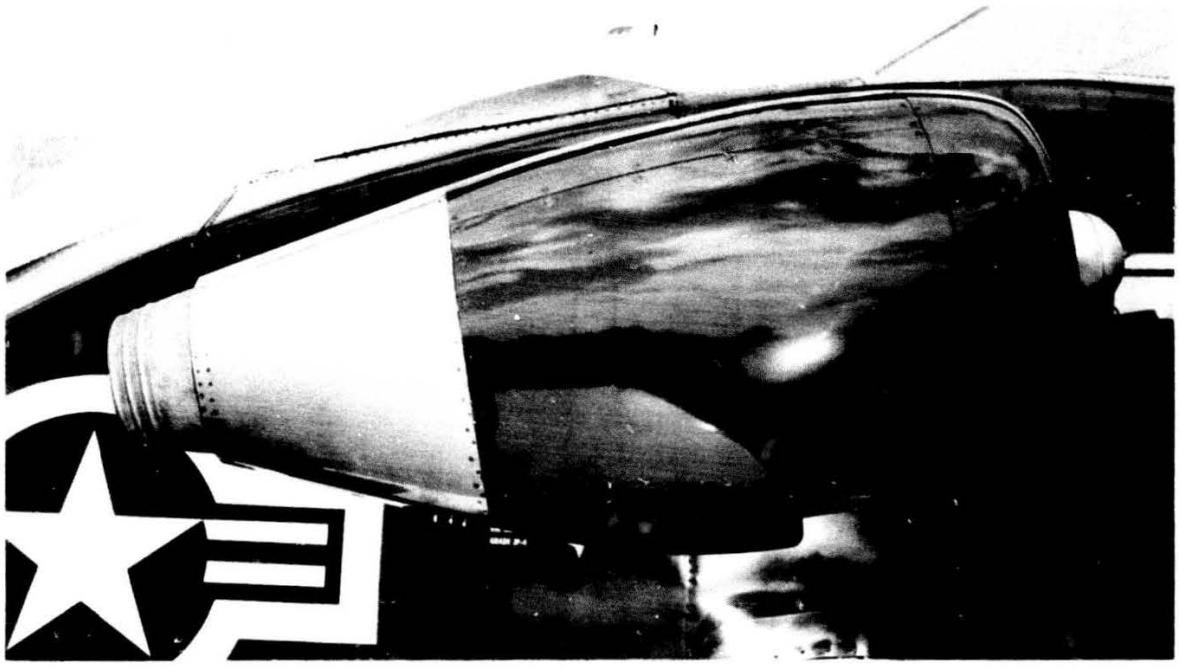

SIDE VIEW OF ORIGINAL NACELLE FAIRING

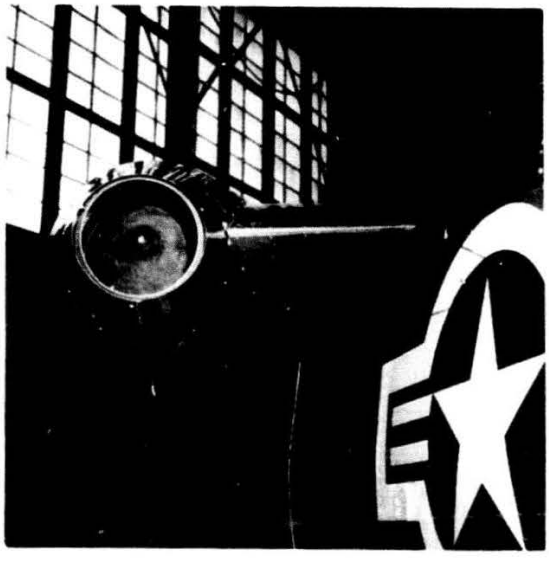

REAR VIEW OF ORIGINAL
PYLON FAIRING

REAR VIEW OF FINAL
CONFIGURATION

FIGURE 6. NACELLE AND ENGINE PYLON FAIRINGS.

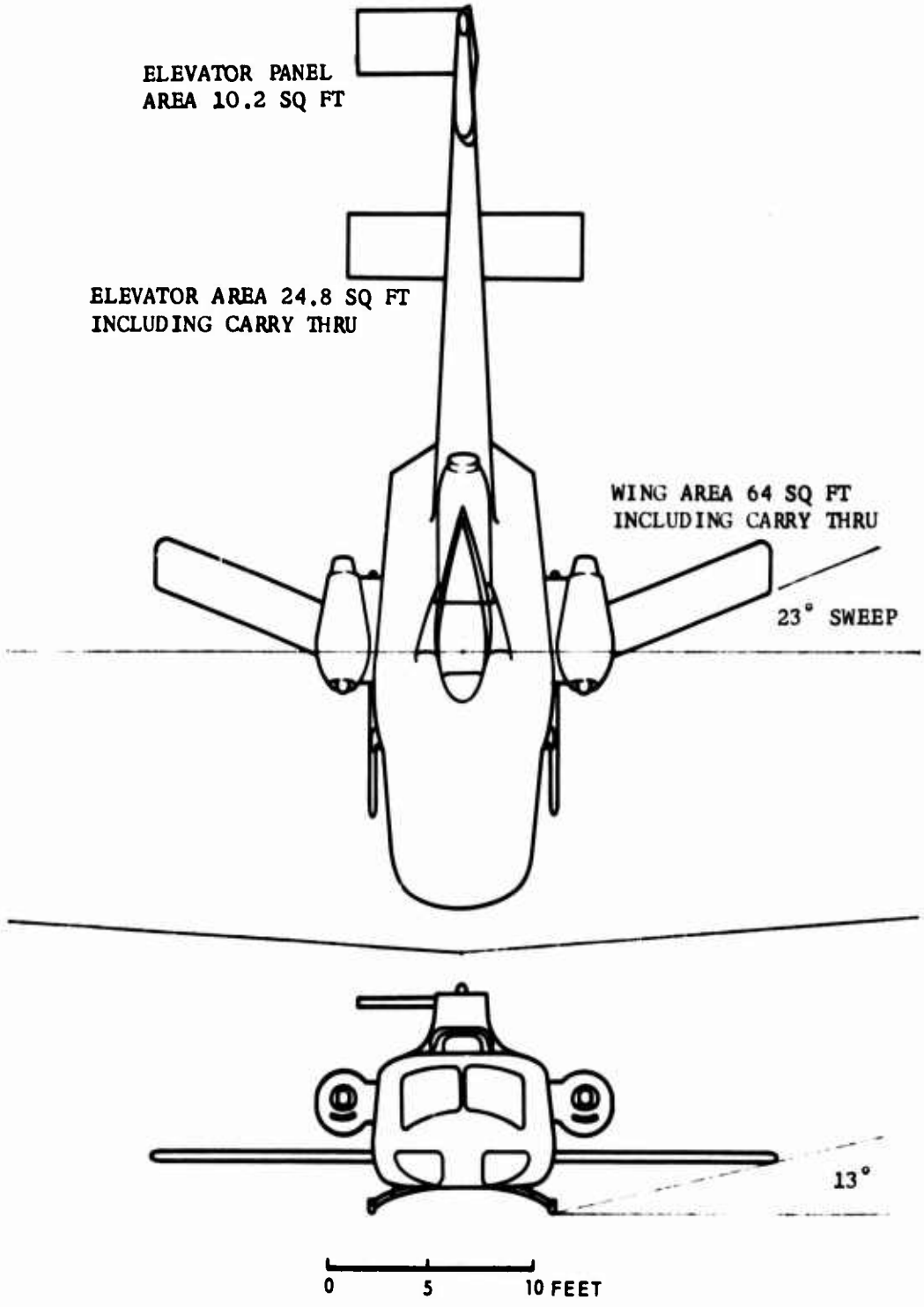

FIGURE 7. GENERAL ARRANGEMENT OF THE HPH WITH WING AND JETS.

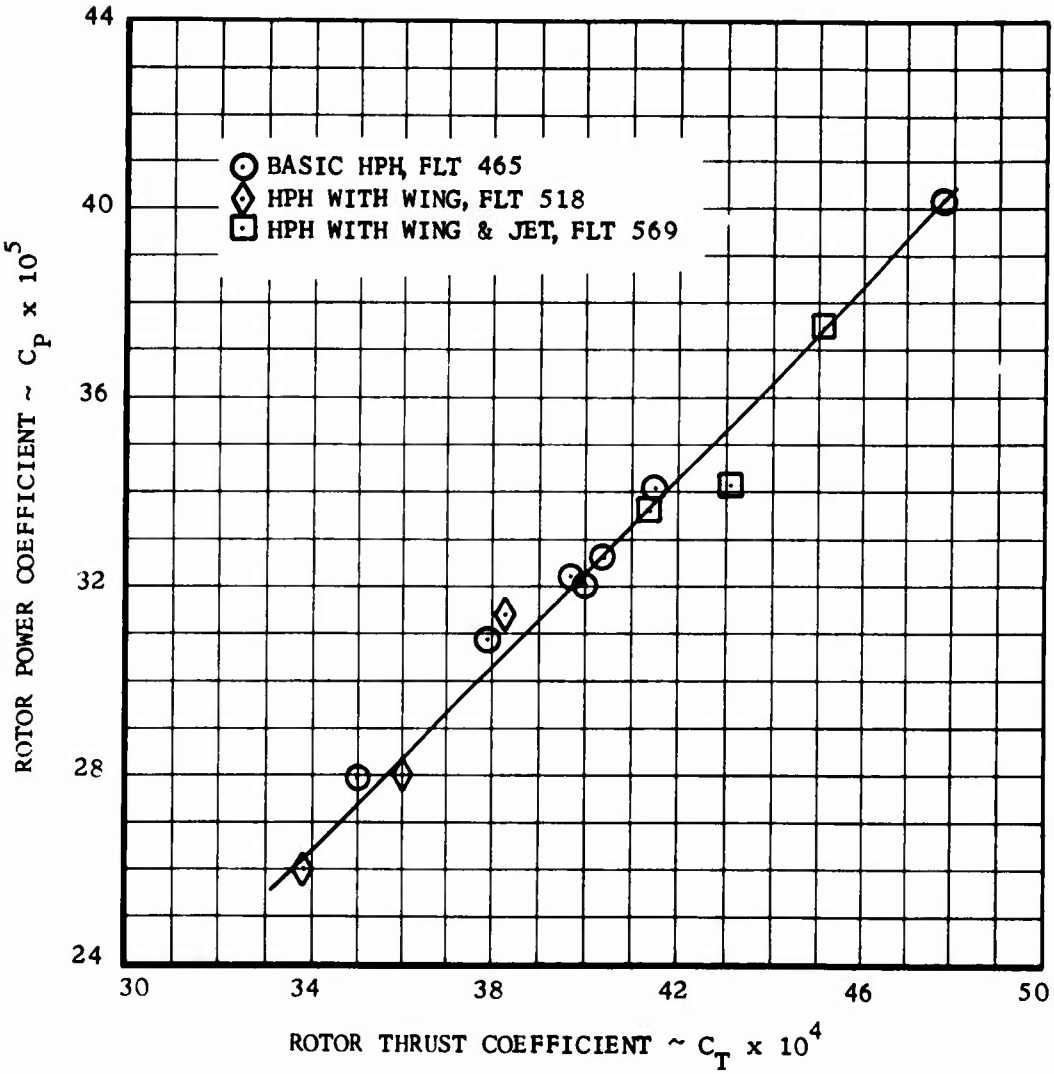

FIGURE 8. HOVERING POWER REQUIRED, O.G.E.

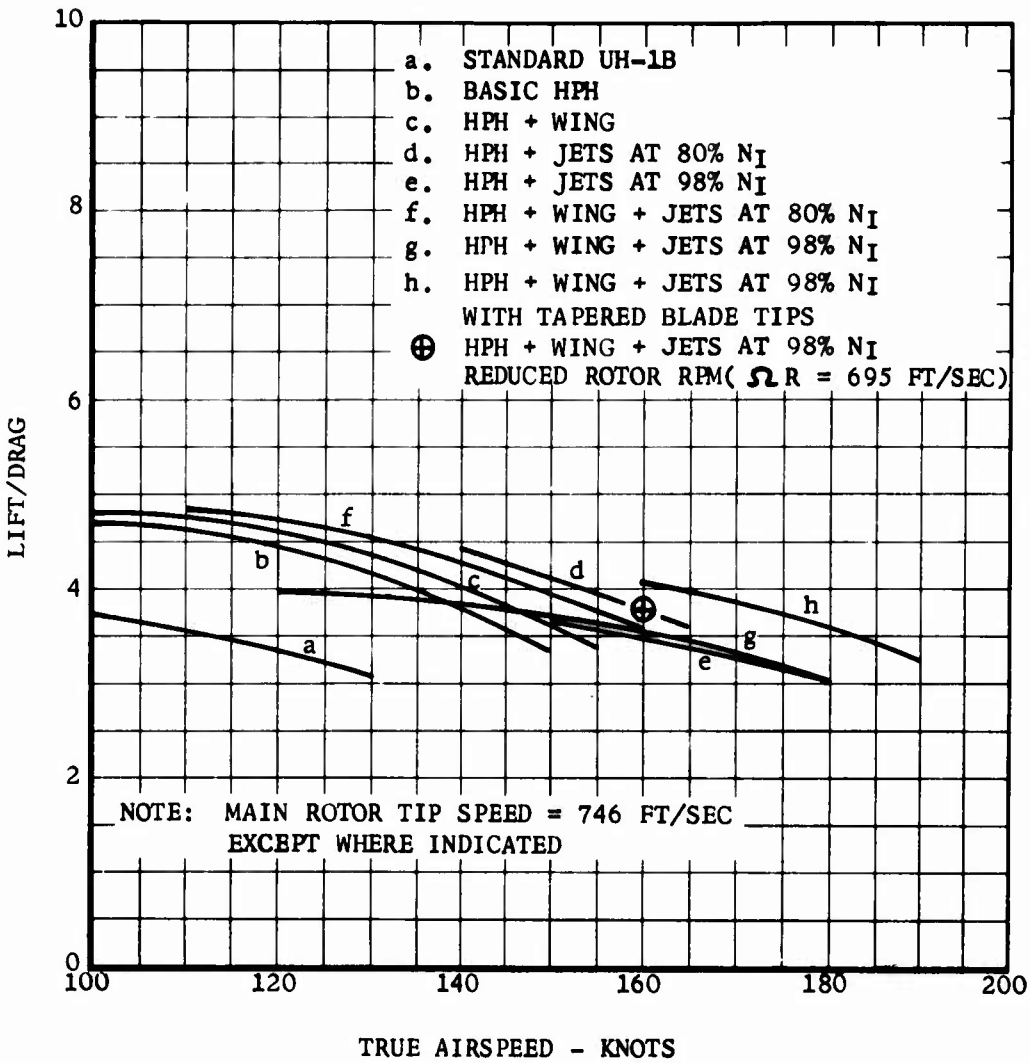

FIGURE 9. OVER-ALL L/D OF FLIGHT RESEARCH VEHICLE.

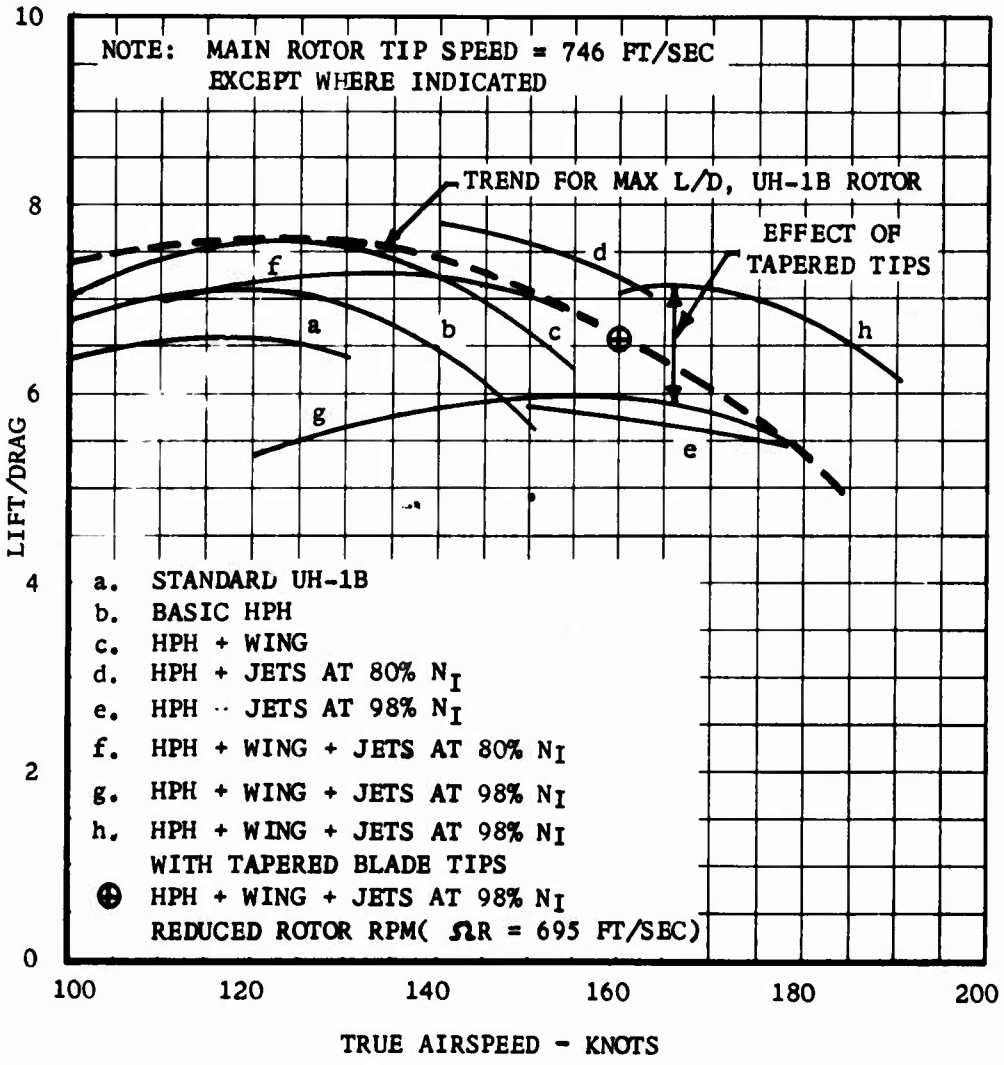

FIGURE 10. L/D OF LIFTING SYSTEMS.

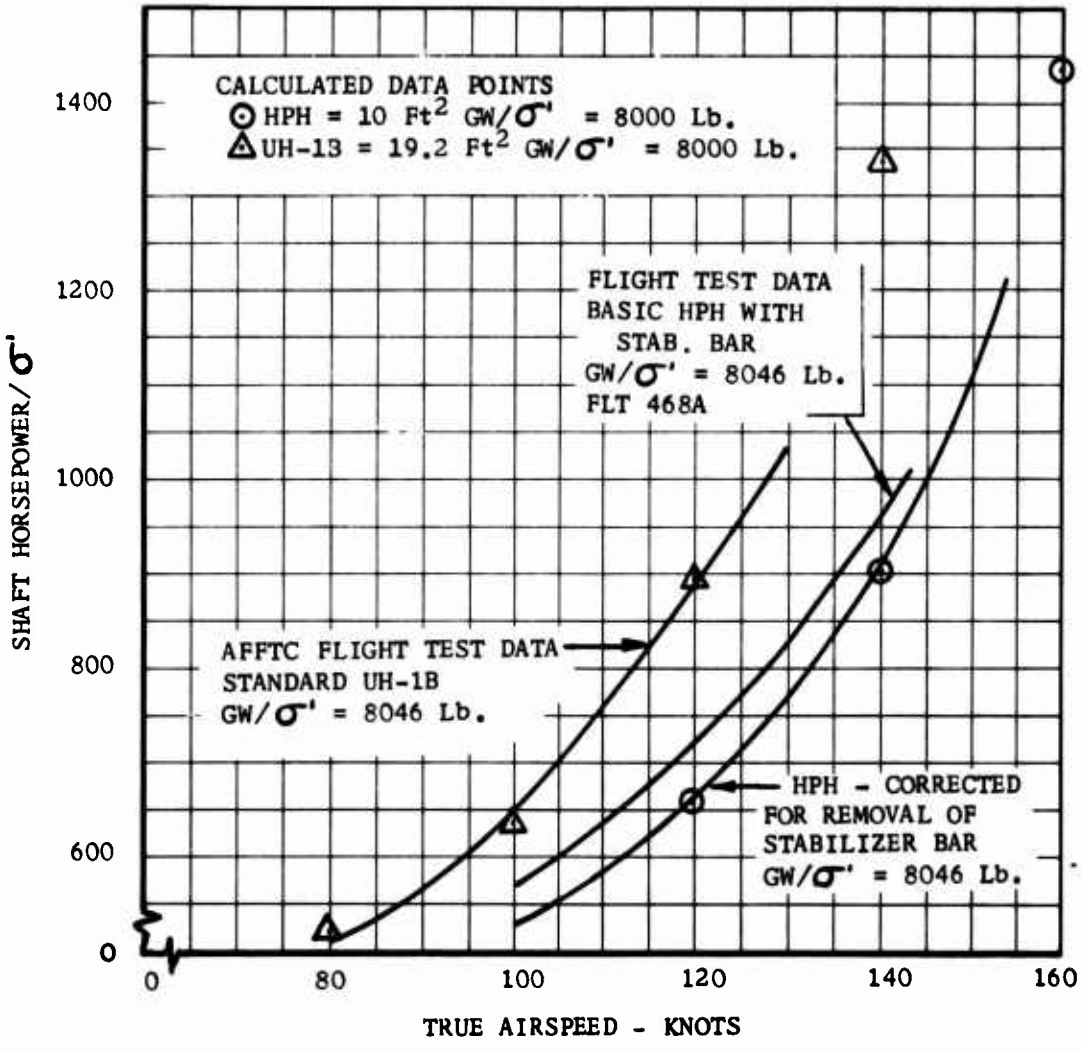

FIGURE 11. COMPARISON OF MEASURED AND CALCULATED POWER REQUIREMENTS OF THE UH-1B AND THE HPH.

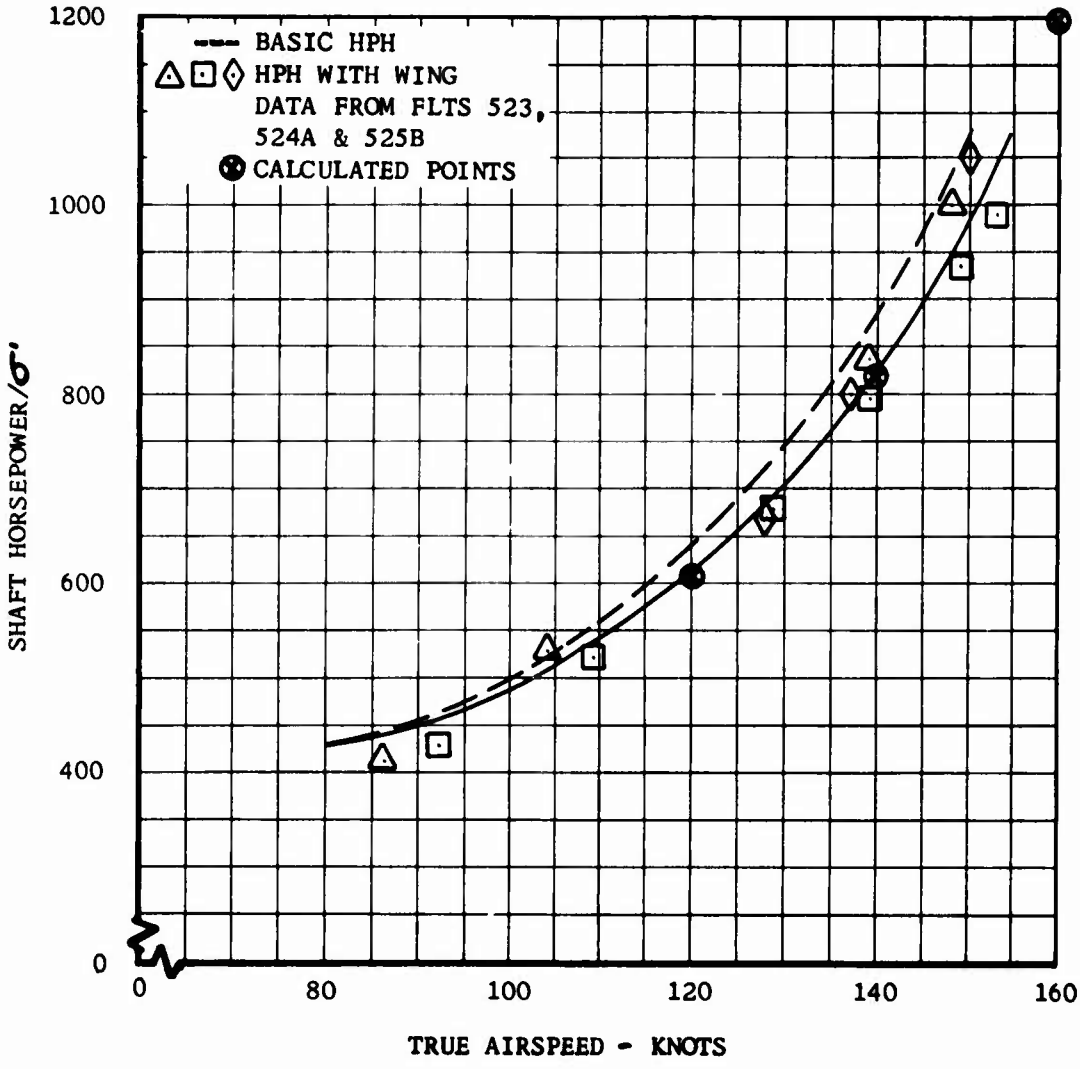

FIGURE 12. POWER REQUIRED FOR THE HPH WITH WING.

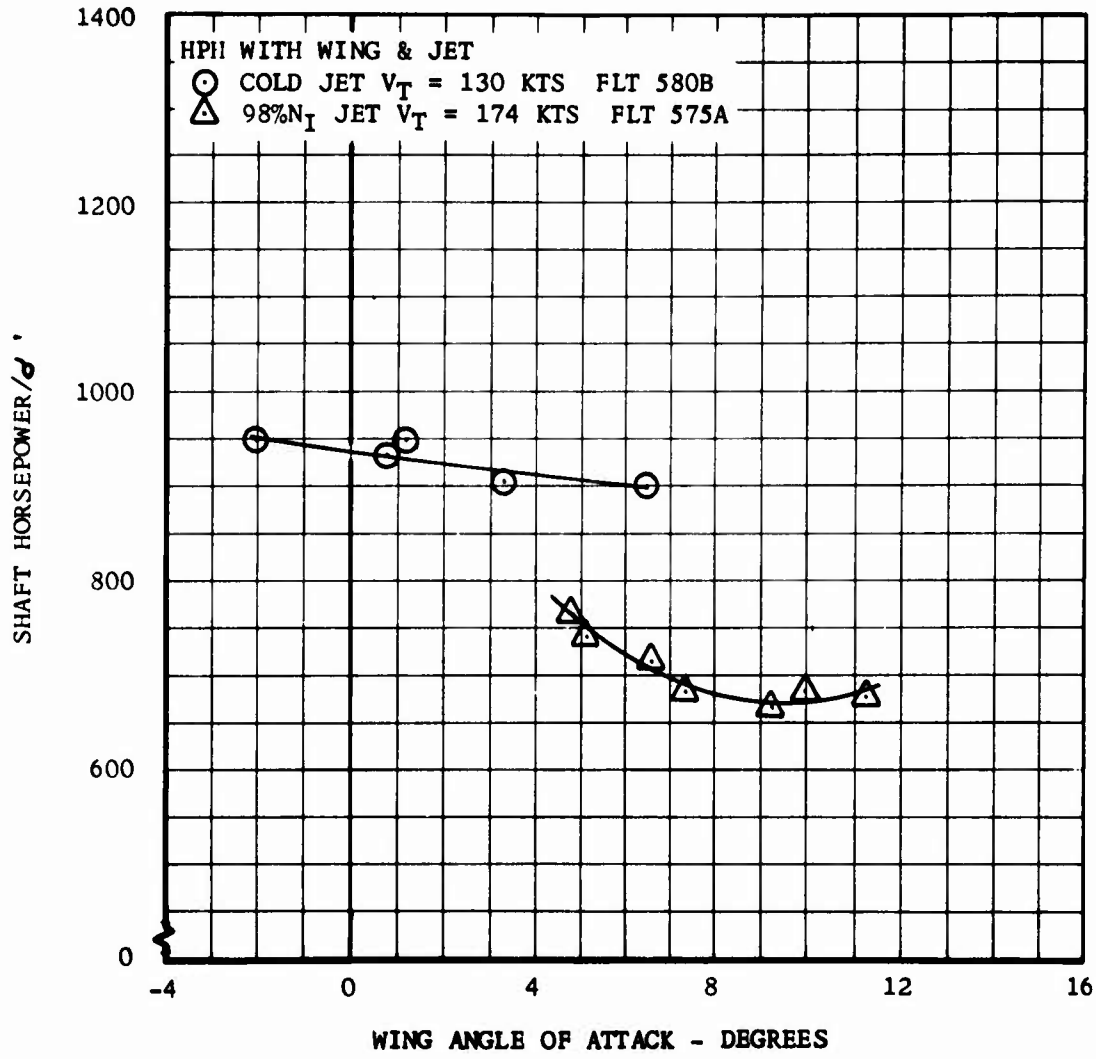

FIGURE 13. INFLUENCE OF WING ANGLE OF ATTACK ON POWER REQUIRED.

J69-T-9 Turbojet Engine
Ref.: Continental Spec. 2089-

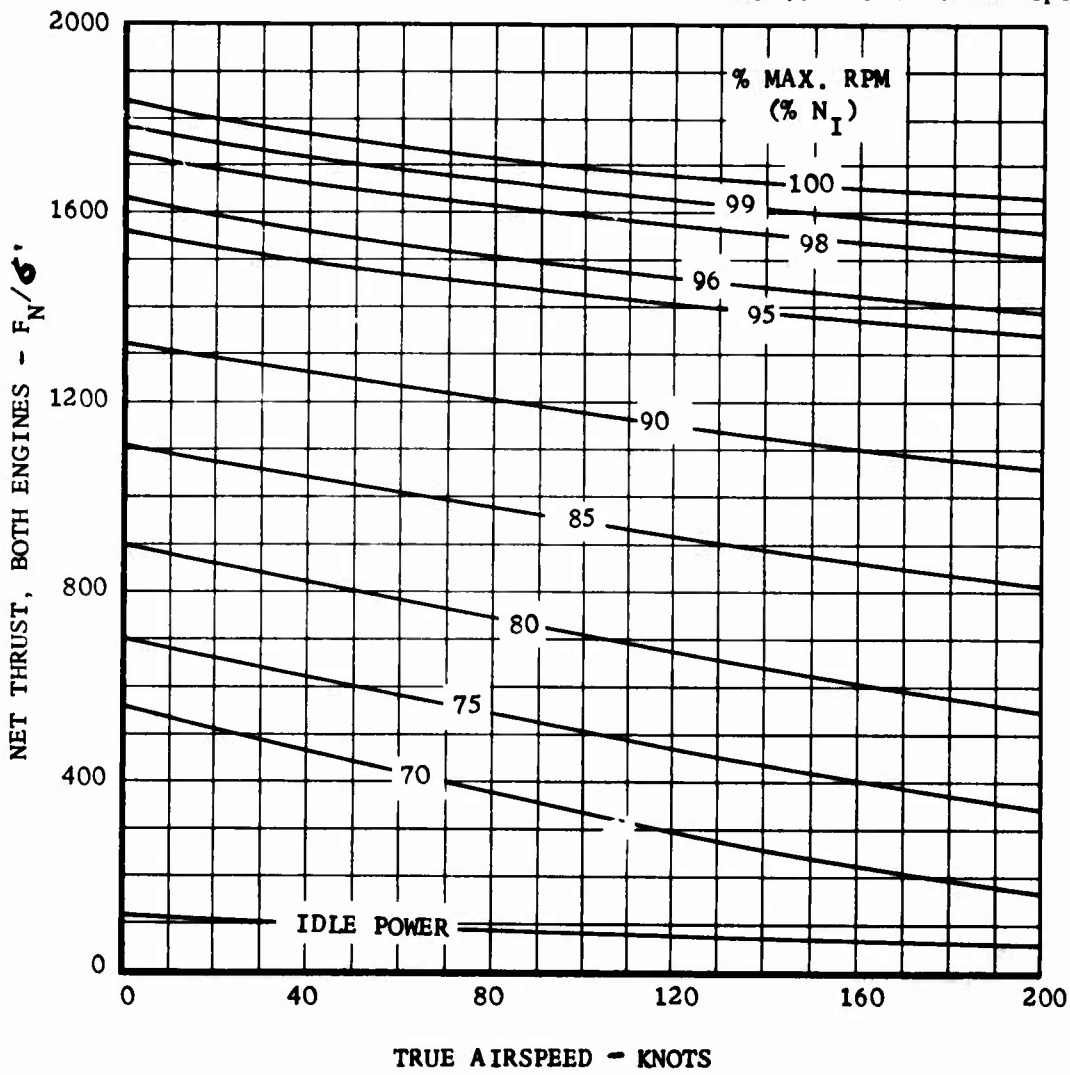

FIGURE 14. NET JET THRUST AVAILABLE.

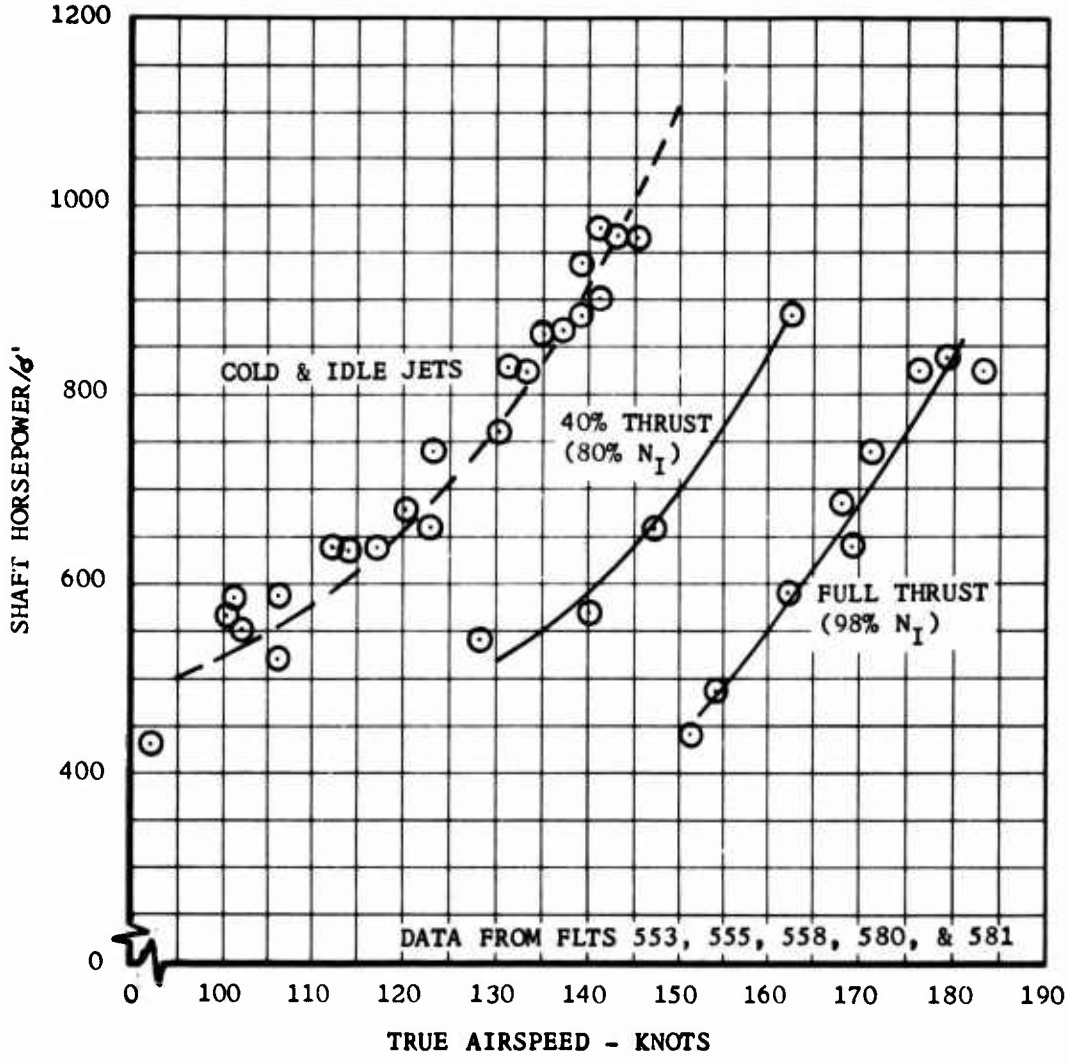

FIGURE 15. T-53 POWER REQUIRED FOR VARIOUS LEVELS OF AUXILIARY THRUST.

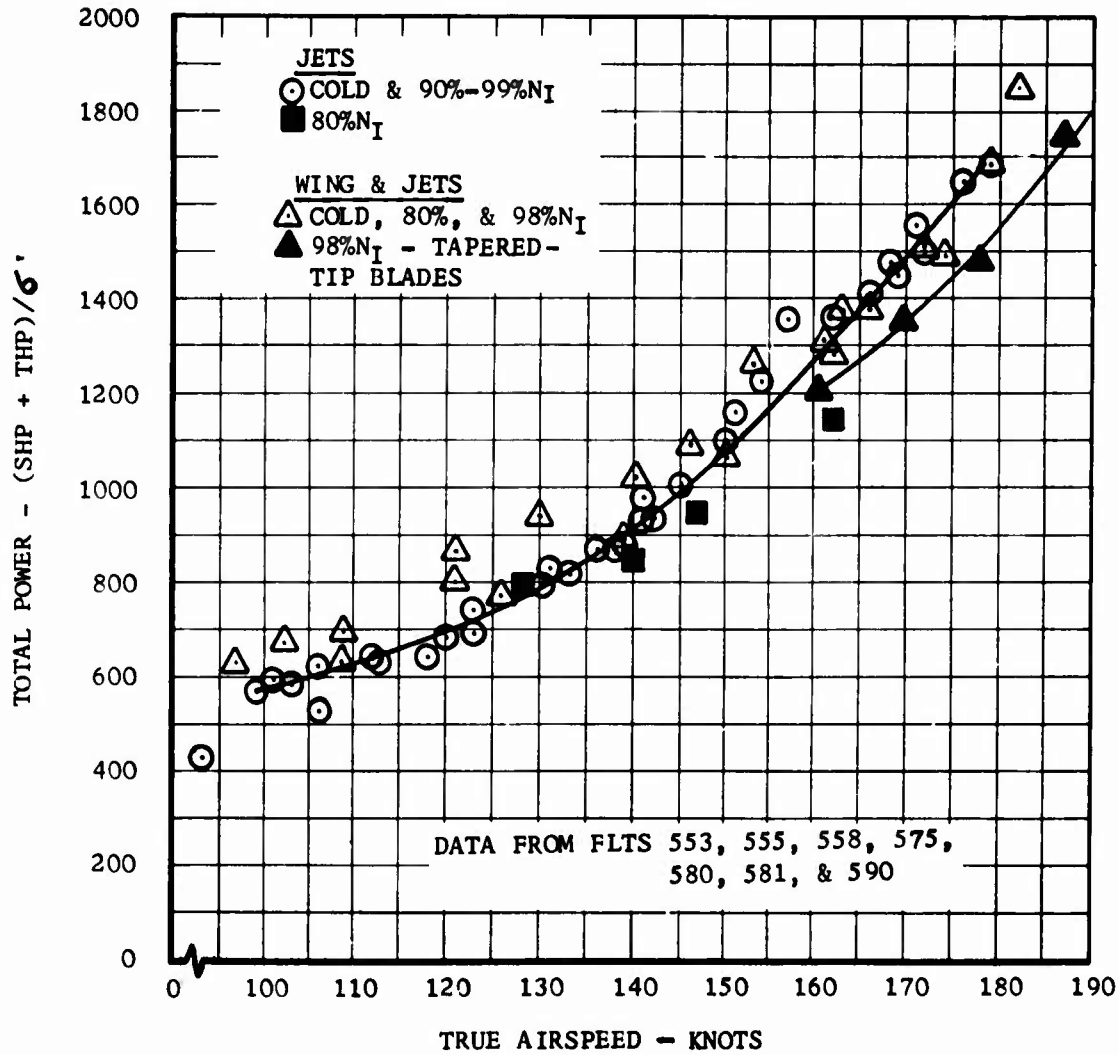

FIGURE 16. TOTAL POWER REQUIRED (T53 SHP + J69 THP).

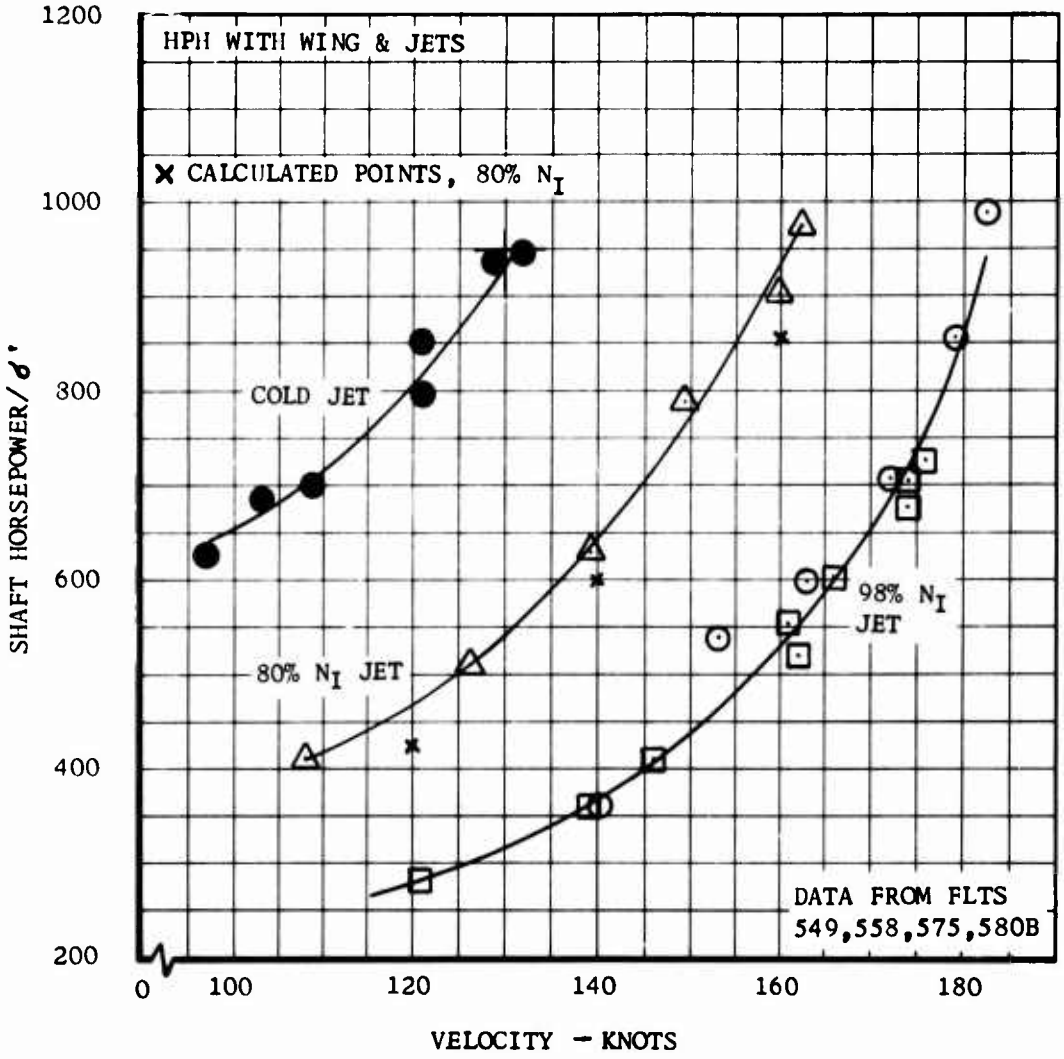

FIGURE 17. INFLUENCE OF JET THRUST ON POWER REQUIRED.

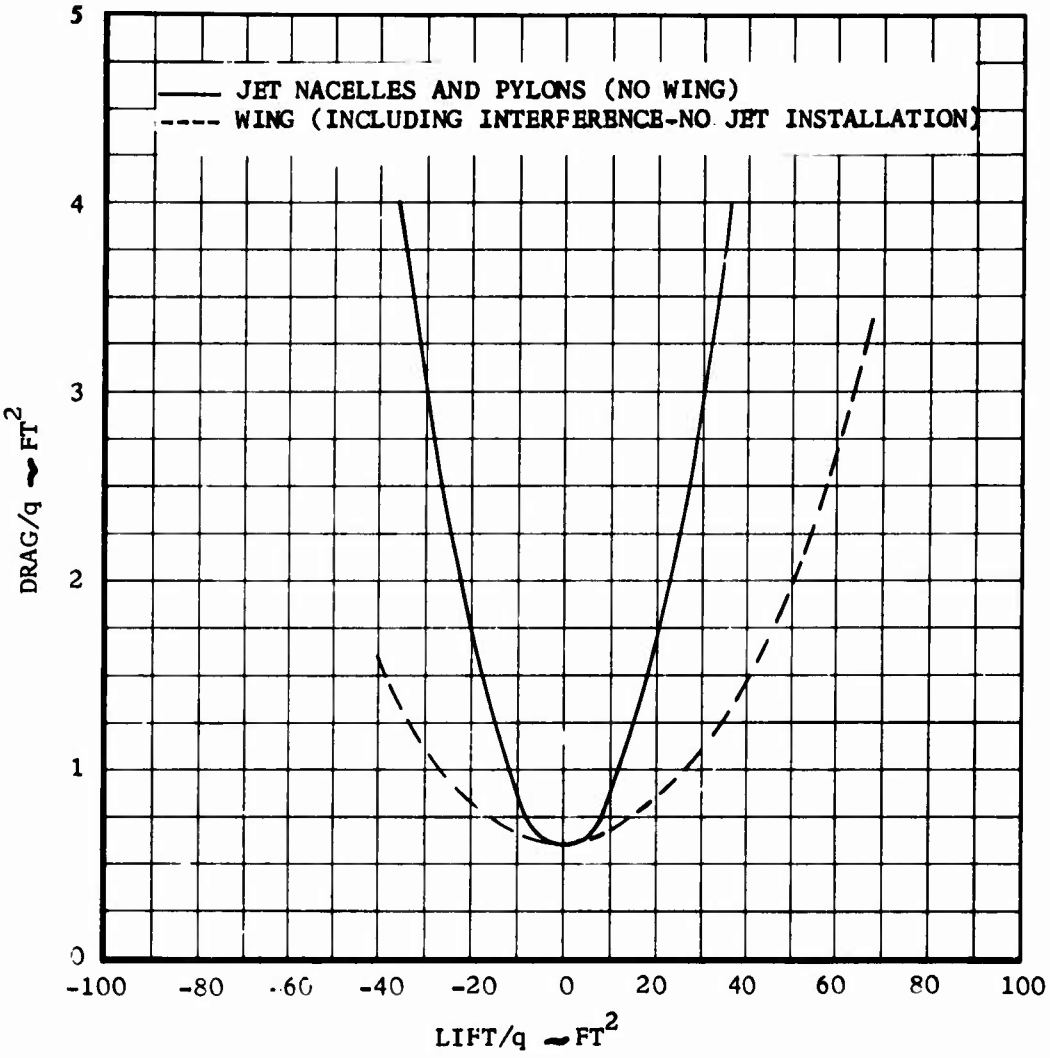

FIGURE 18. ESTIMATED WING AND NACELLE DRAG OF THE HPH.

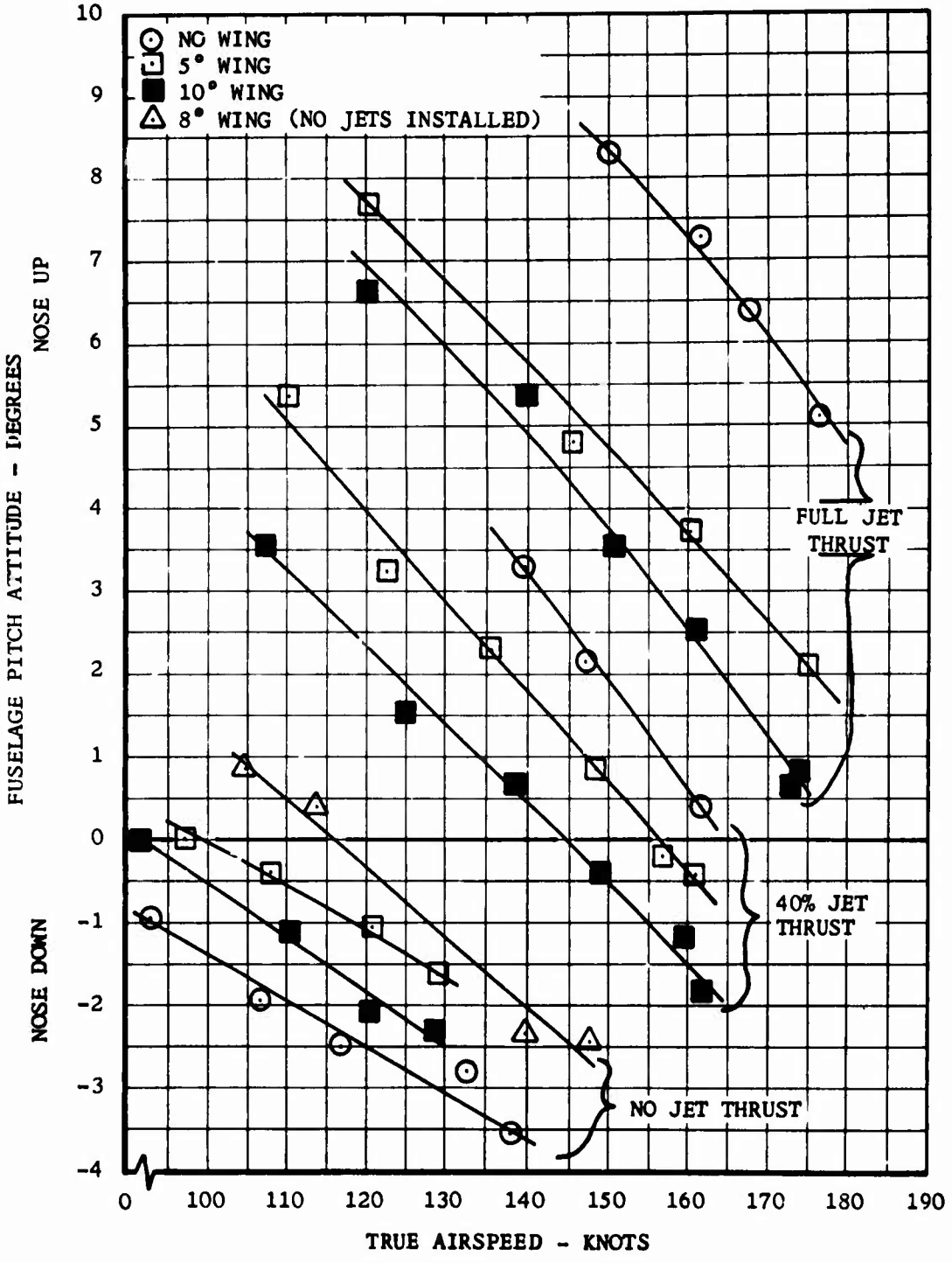

FIGURE 19. INFLUENCE OF AUXILIARY THRUST ON FUSELAGE ATTITUDE.

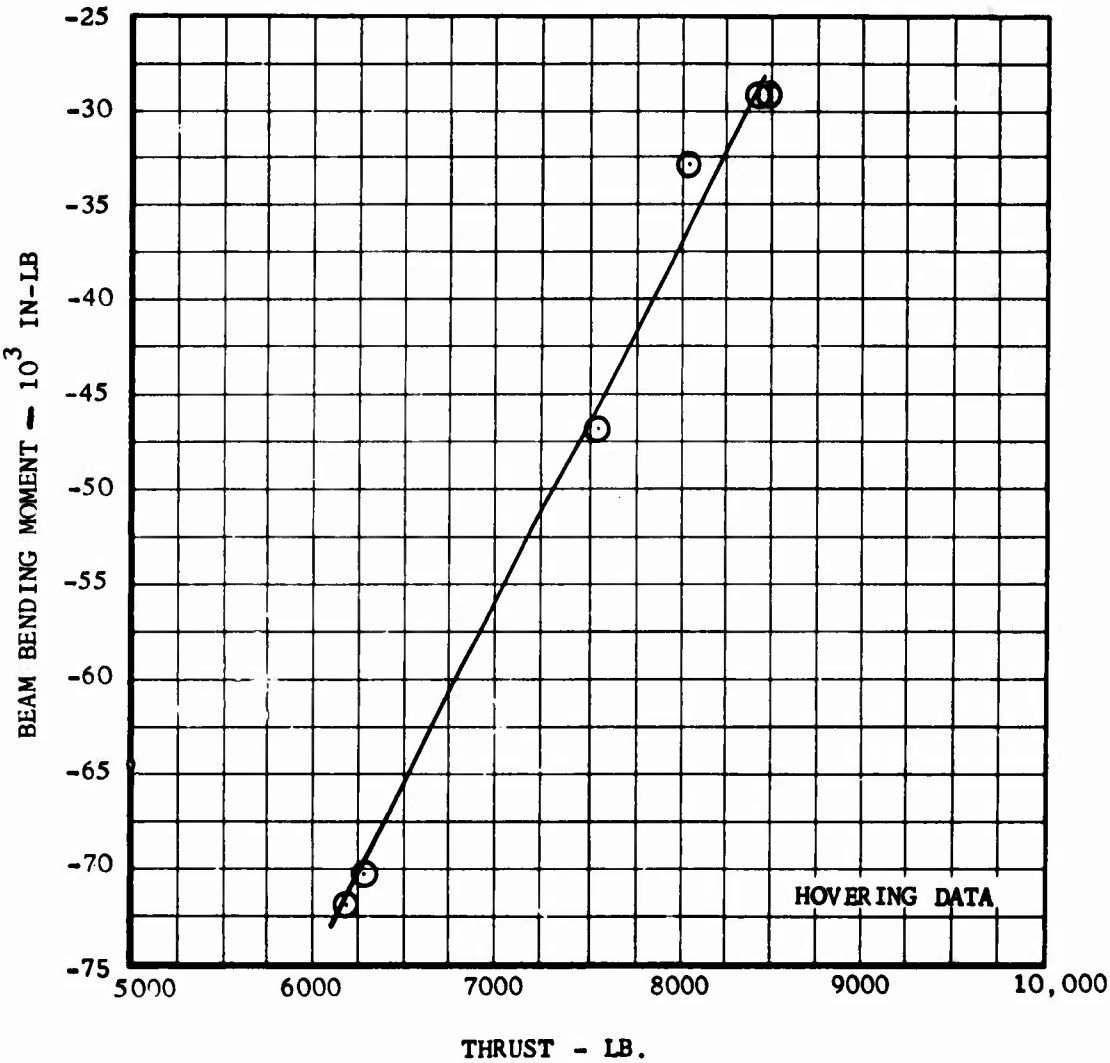

FIGURE 20. STEADY YOKE BENDING MOMENT VS. ROTOR THRUST.

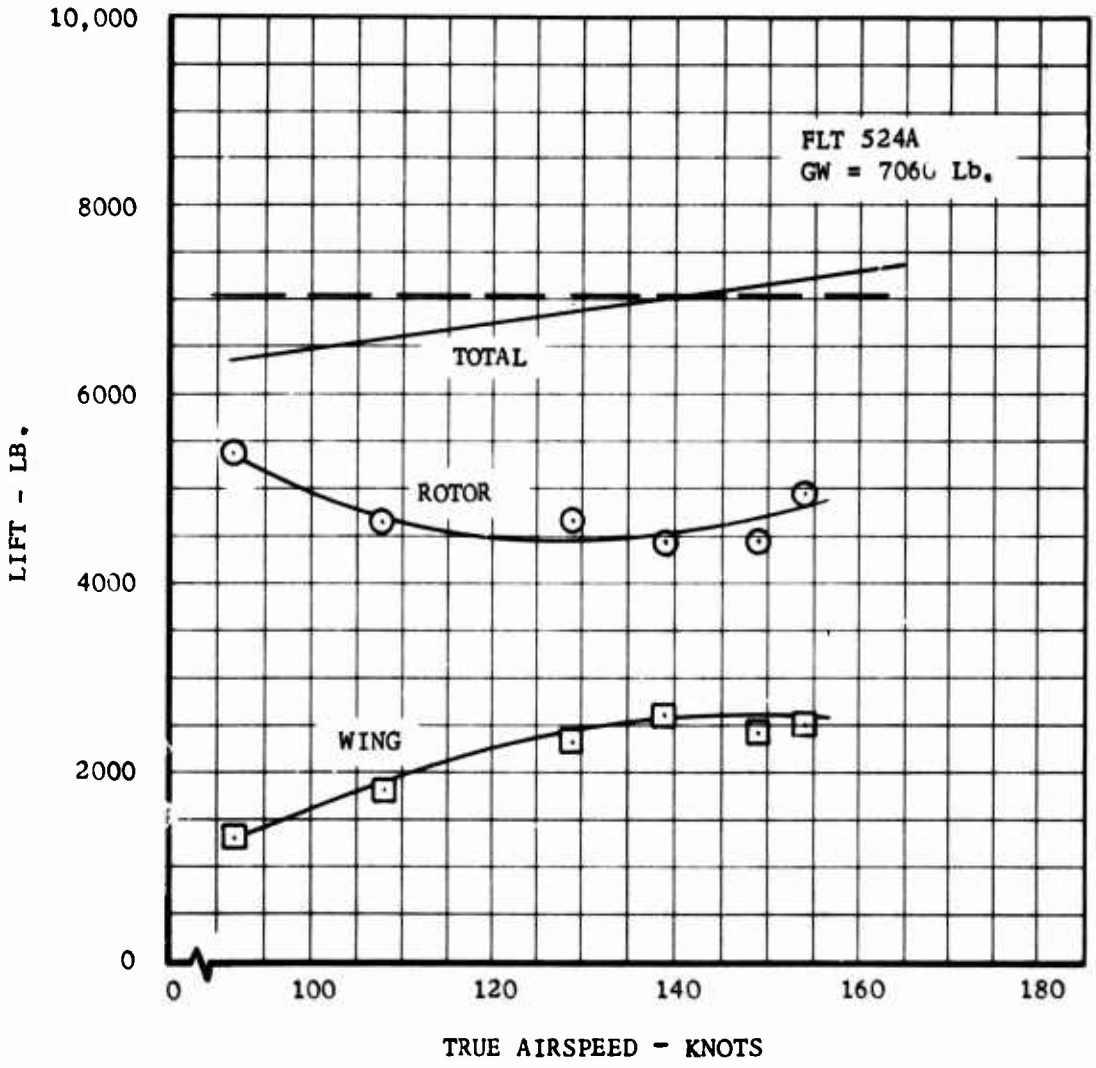

FIGURE 21. LIFT DISTRIBUTION FOR HPH WITH WING.

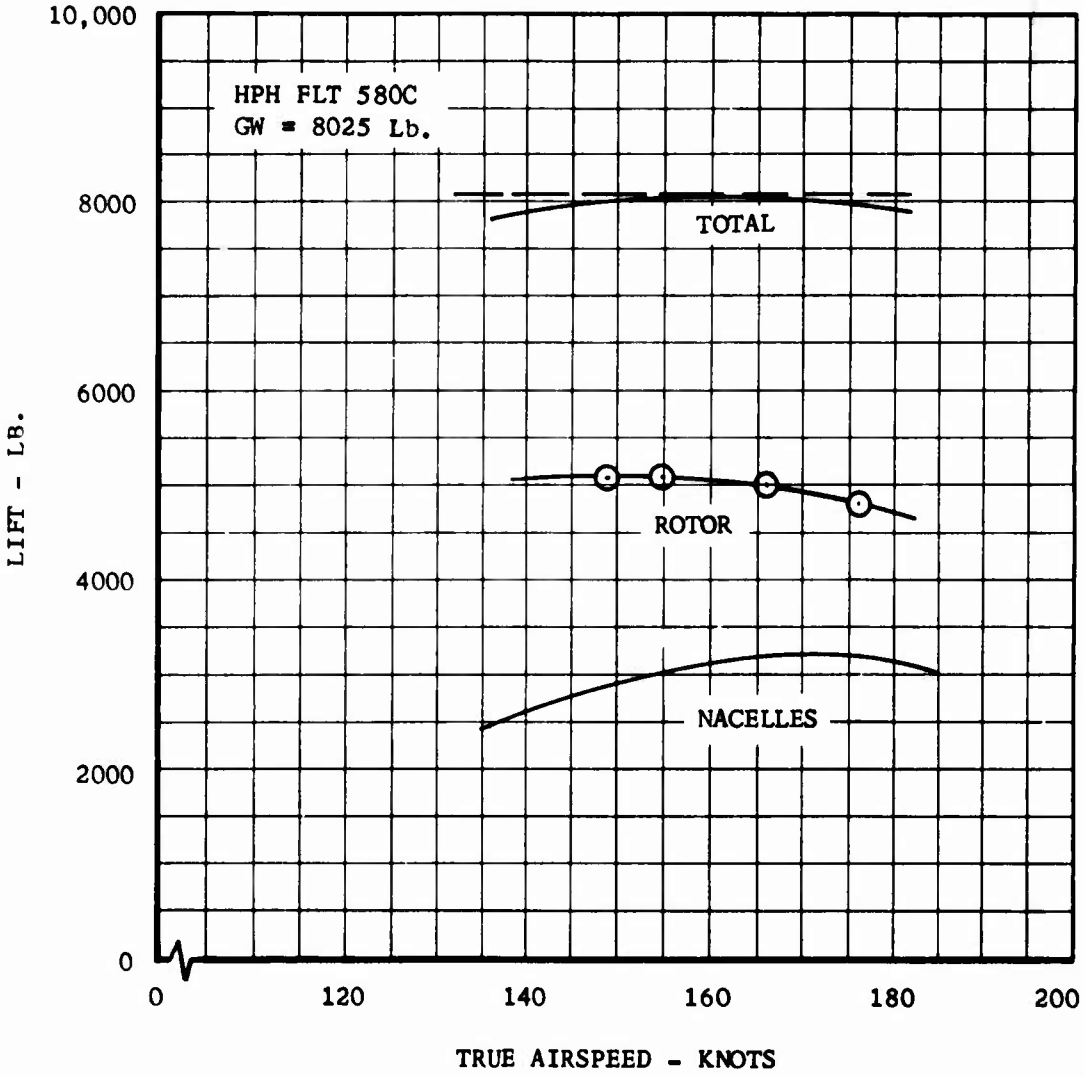

FIGURE 22. LIFT DISTRIBUTION -
AUXILIARY JET INSTALLATION.

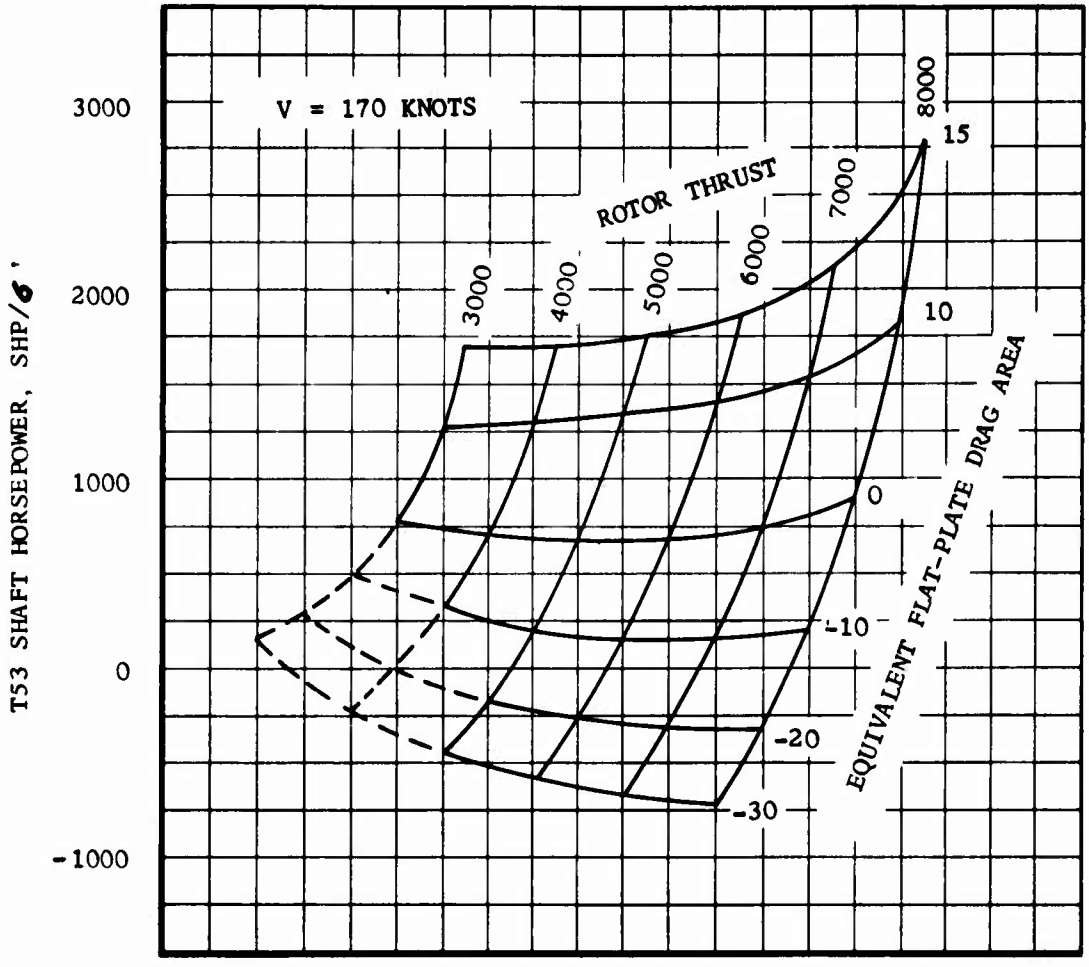

FIGURE 23. CALCULATED SHP AS A FUNCTION OF ROTOR THRUST AND EQUIVALENT FLAT PLATE DRAG AREA.

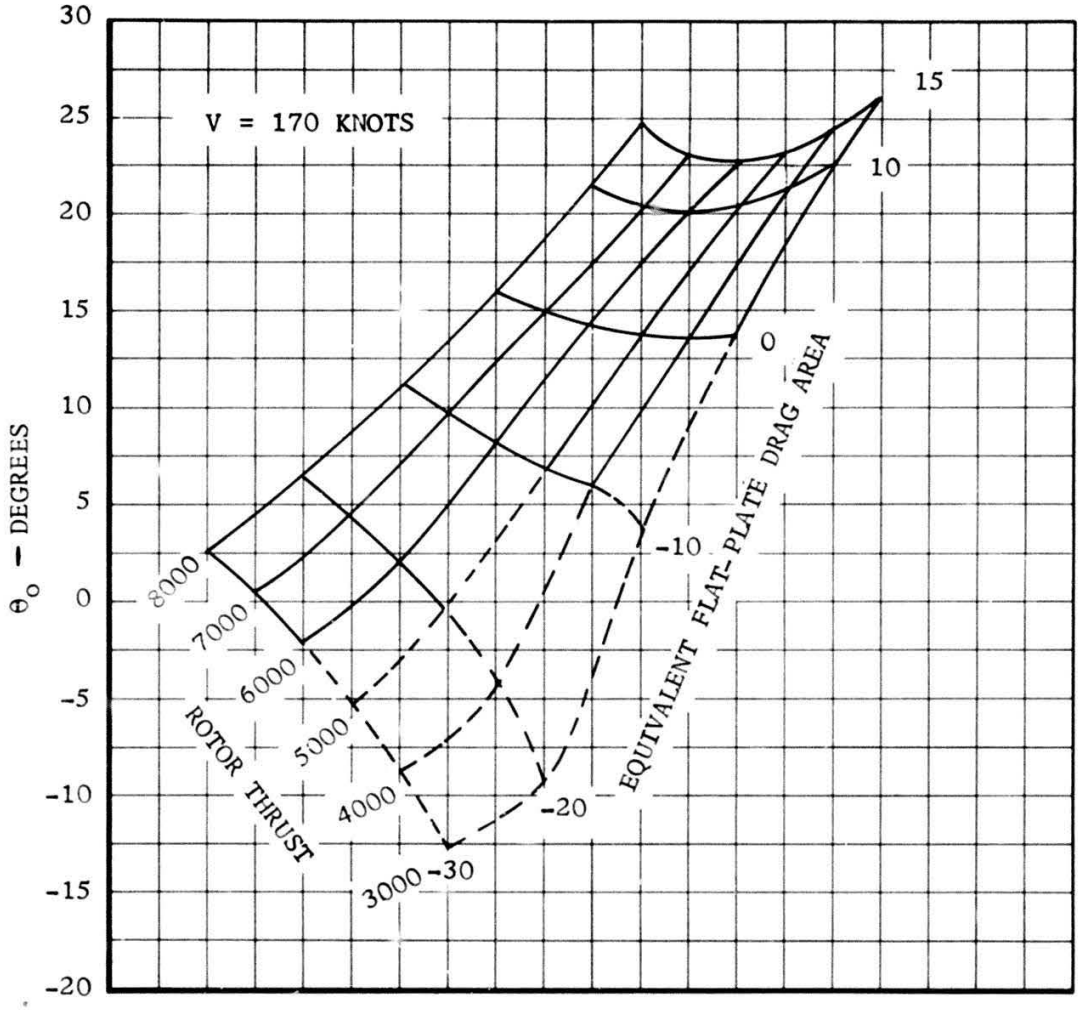

FIGURE 24. CALCULATED θ_o AS A FUNCTION OF ROTOR THRUST AND EQUIVALENT FLAT PLATE DRAG AREA.

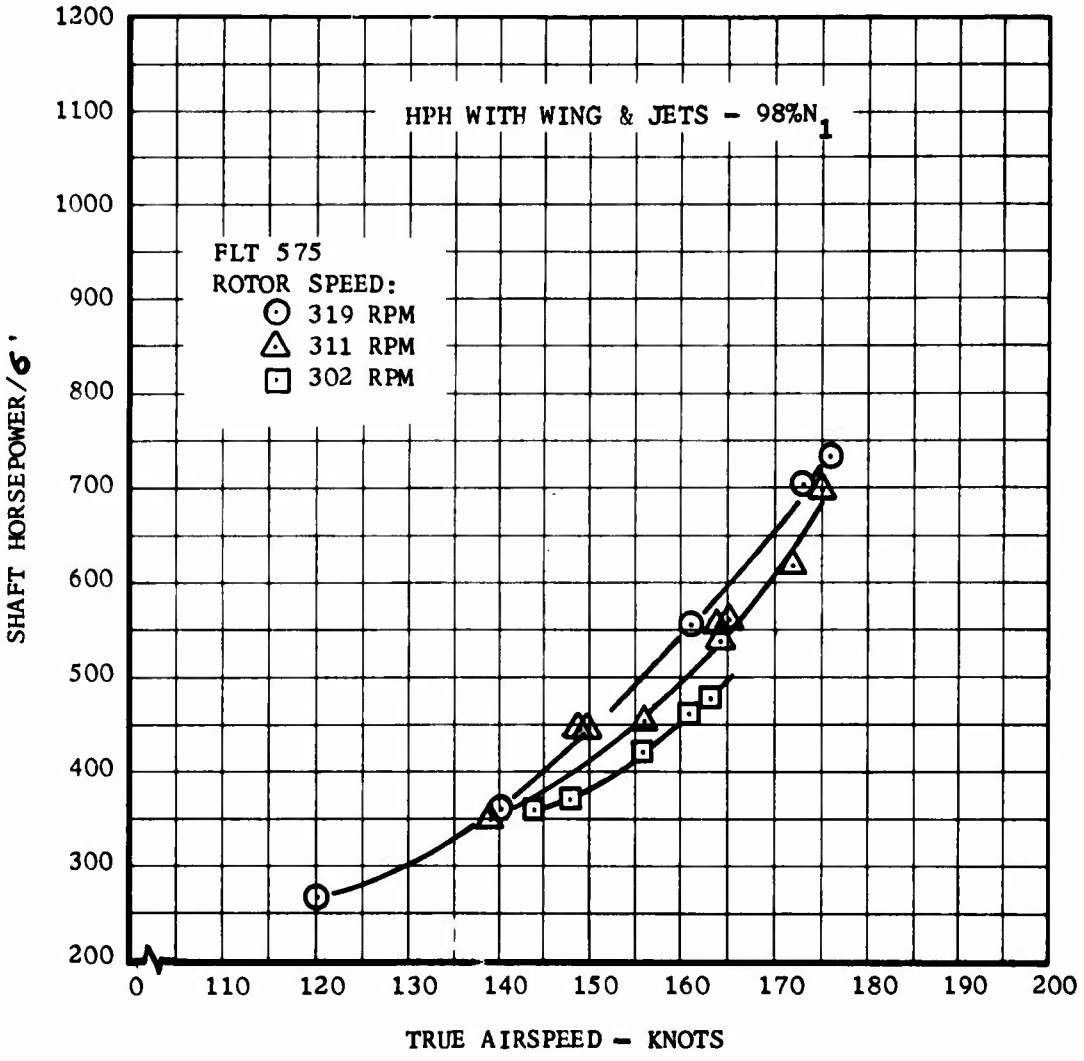

FIGURE 25. INFLUENCE OF ROTOR SPEED ON POWER REQUIREMENTS.

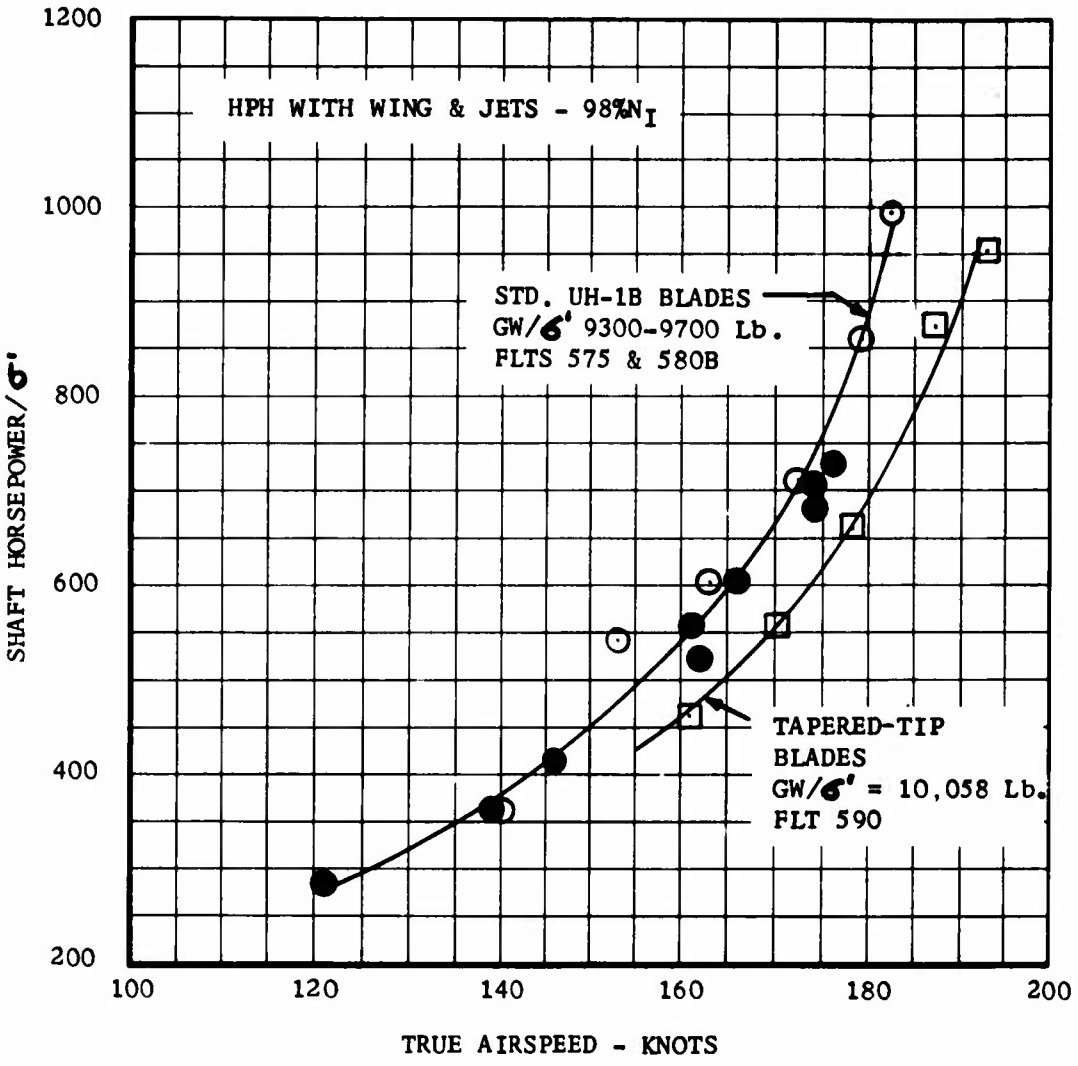

FIGURE 26. INFLUENCE OF TAPERED TIP BLADES ON POWER REQUIRED.

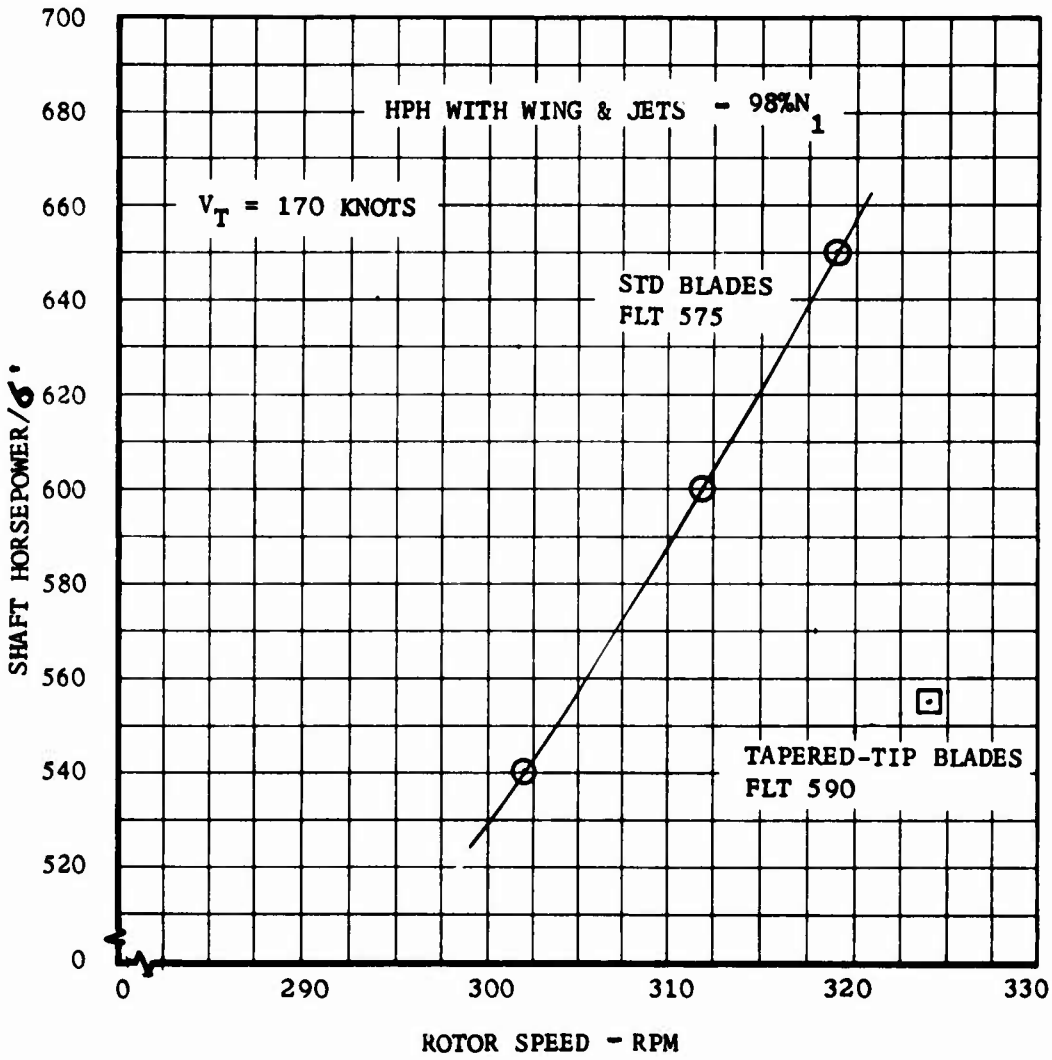

FIGURE 27. POWER REQUIREMENTS AT 170 KNOTS VS. ROTOR SPEED FOR THE STANDARD AND TAPERED-TIP BLADES.

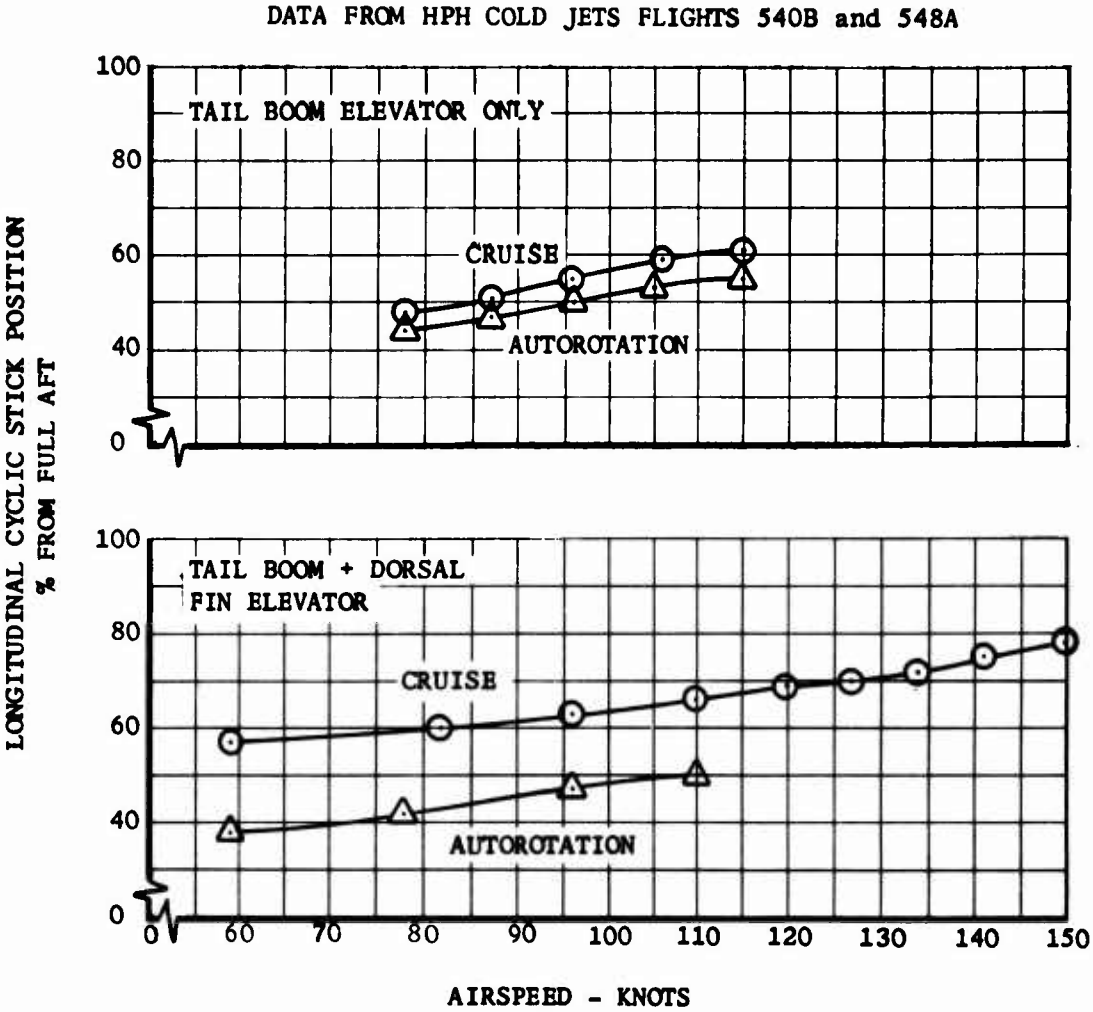

FIGURE 28. DORSAL-FIN ELEVATOR EFFECT ON LONGITUDINAL STICK PLOT.

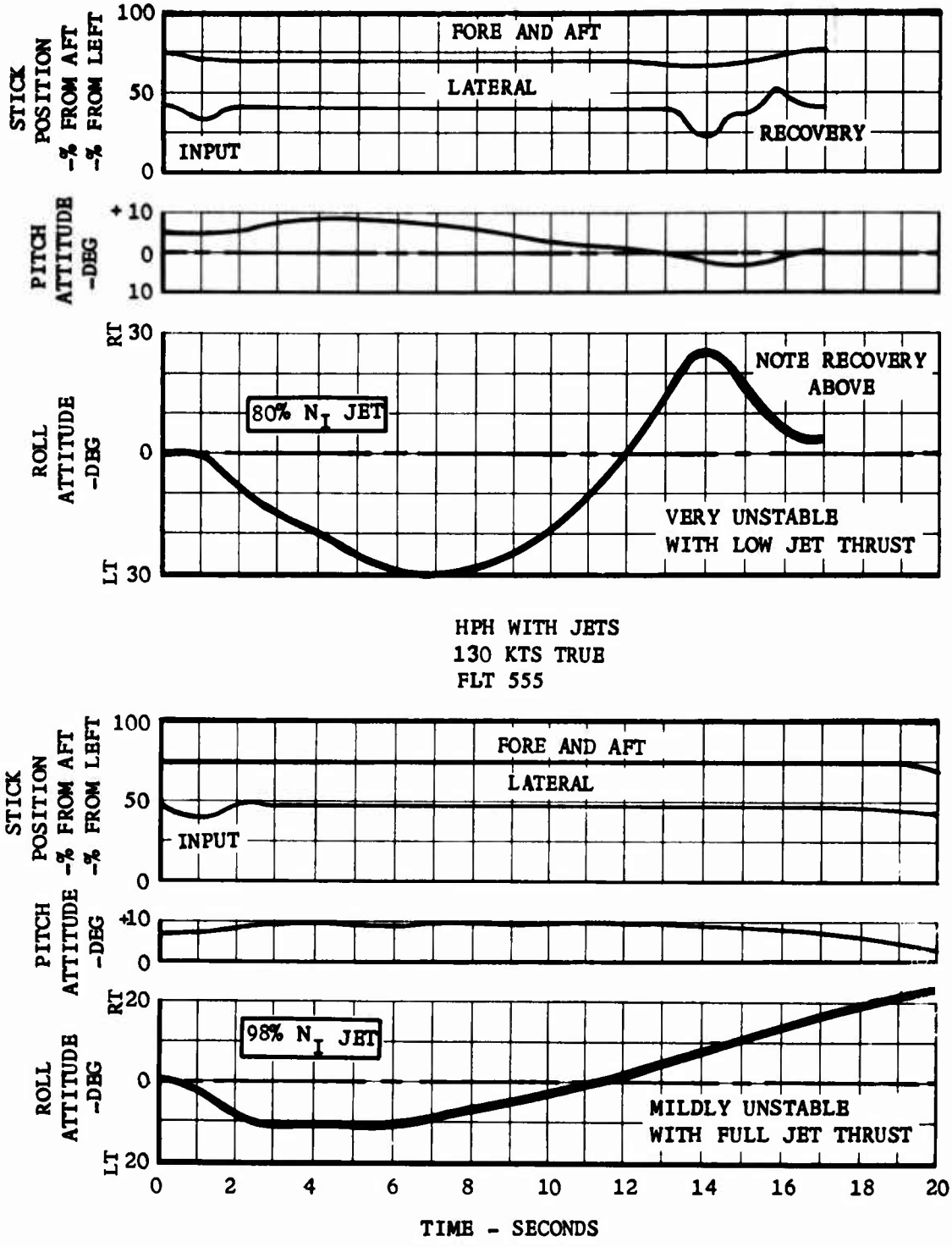

FIGURE 29. EFFECT OF JET THRUST ON ROLL STABILITY.

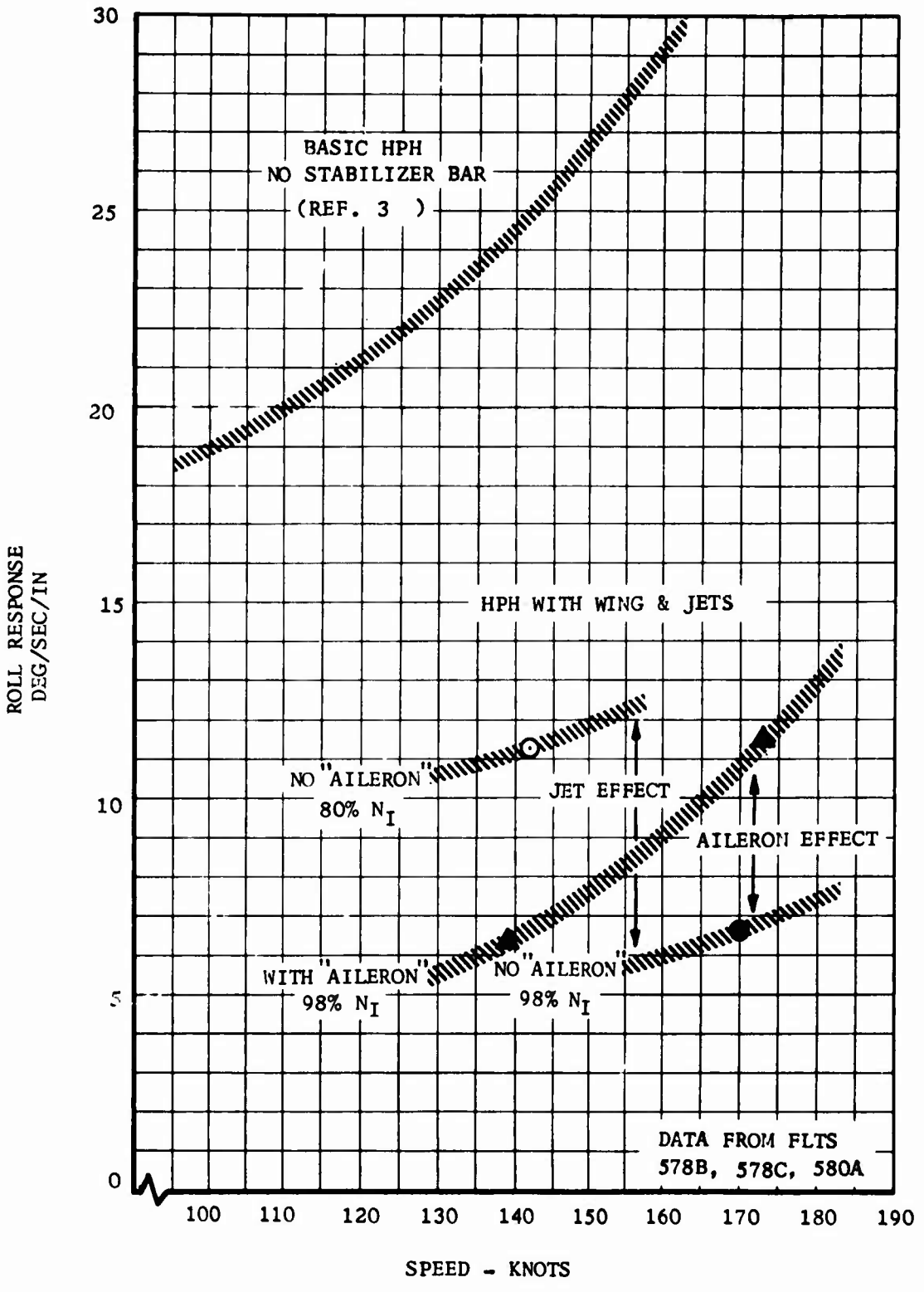

FIGURE 30. ROLL CONTROL RESPONSE -
AILERON, JET, AND SPEED EFFECTS.

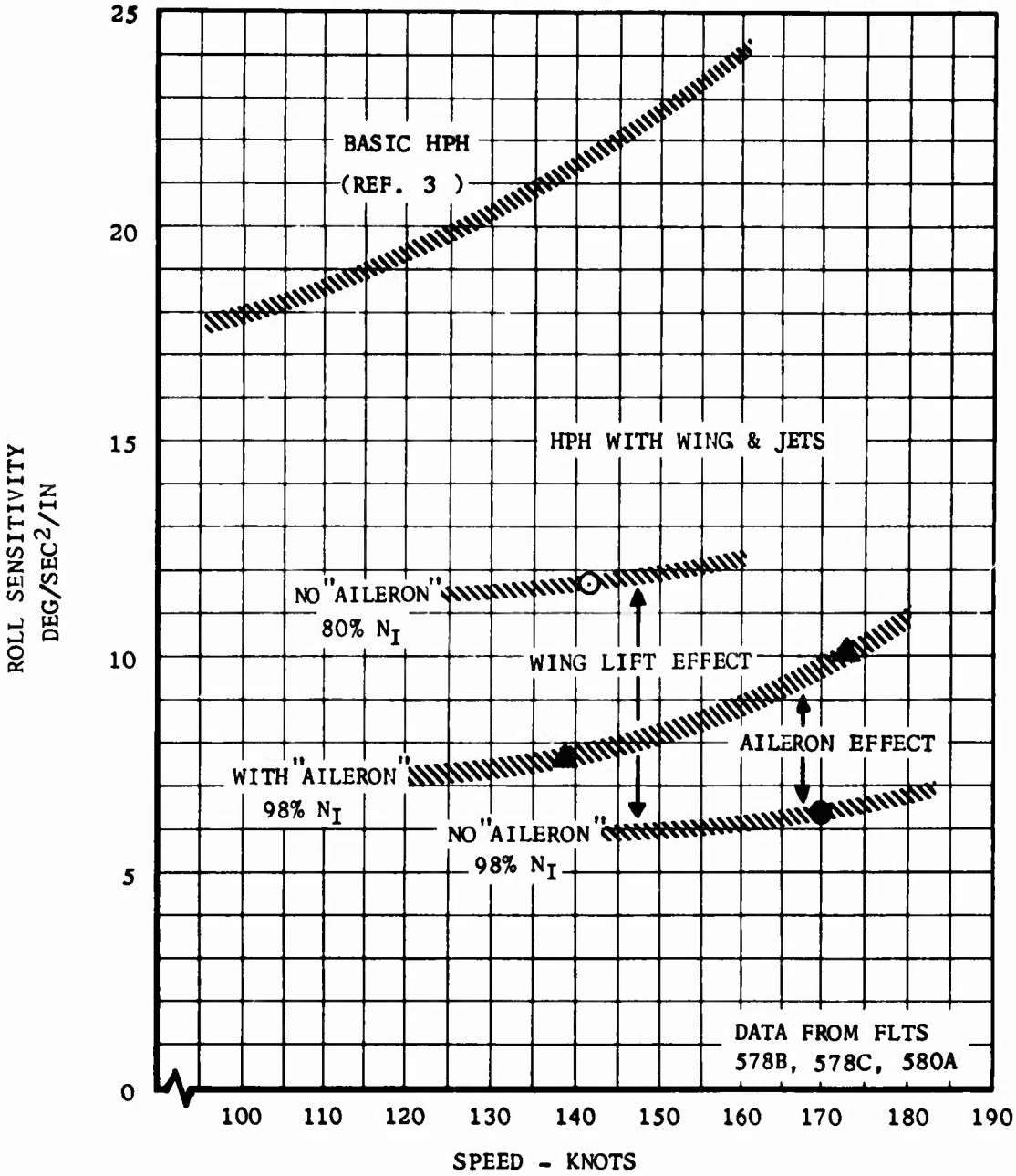

FIGURE 31. ROLL CONTROL SENSITIVITY -
AILERON, WING LIFT, AND SPEED EFFECTS.

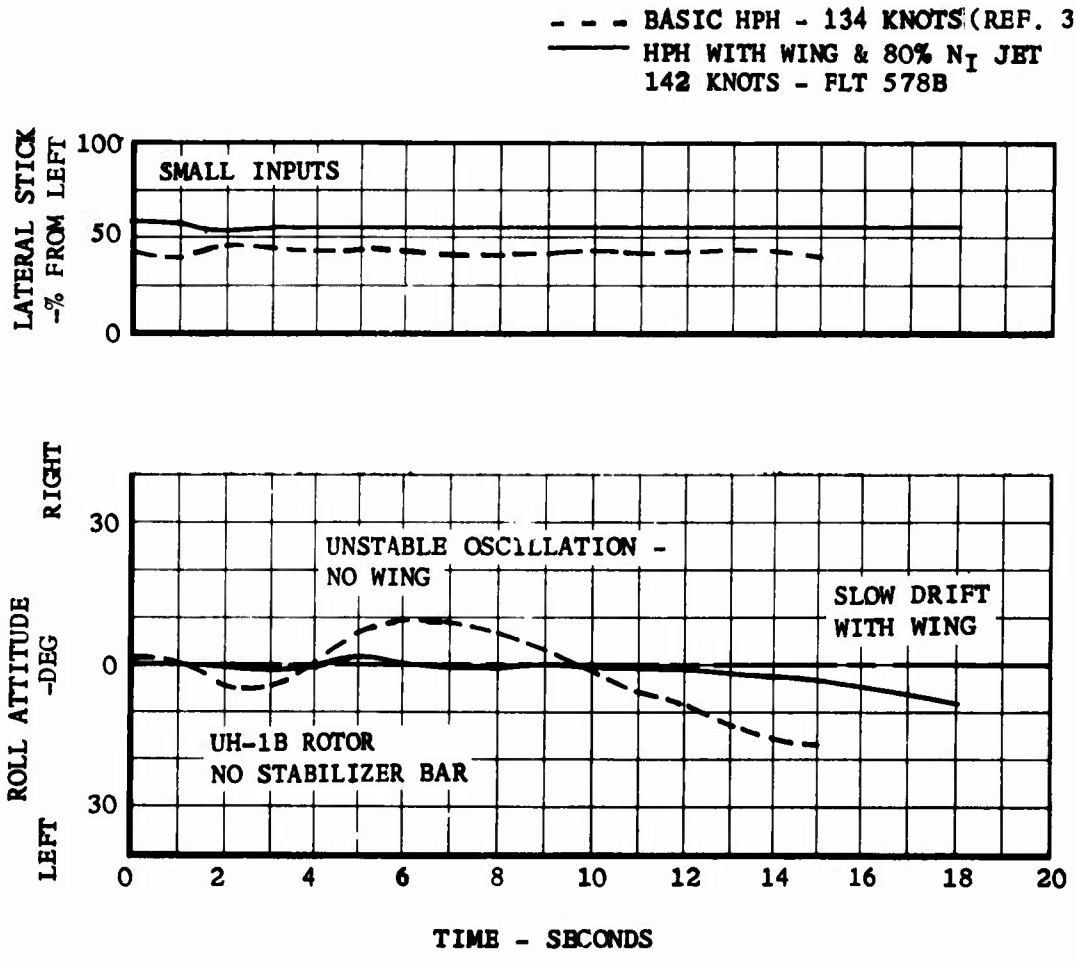

FIGURE 32. WING EFFECT ON ROLL STABILITY.

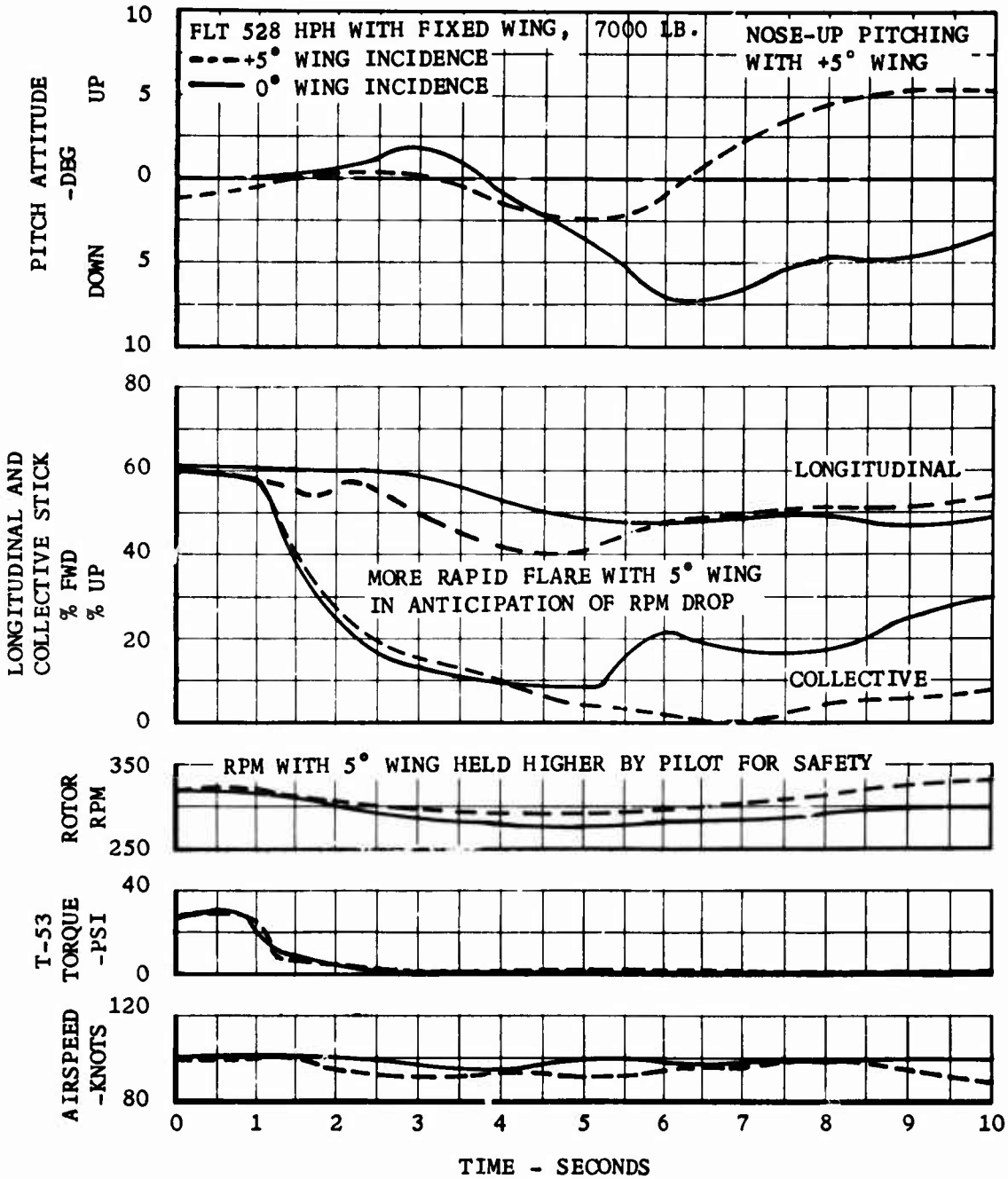

FIGURE 33. EFFECT OF WING INCIDENCE DURING AUTOROTATION ENTRY.

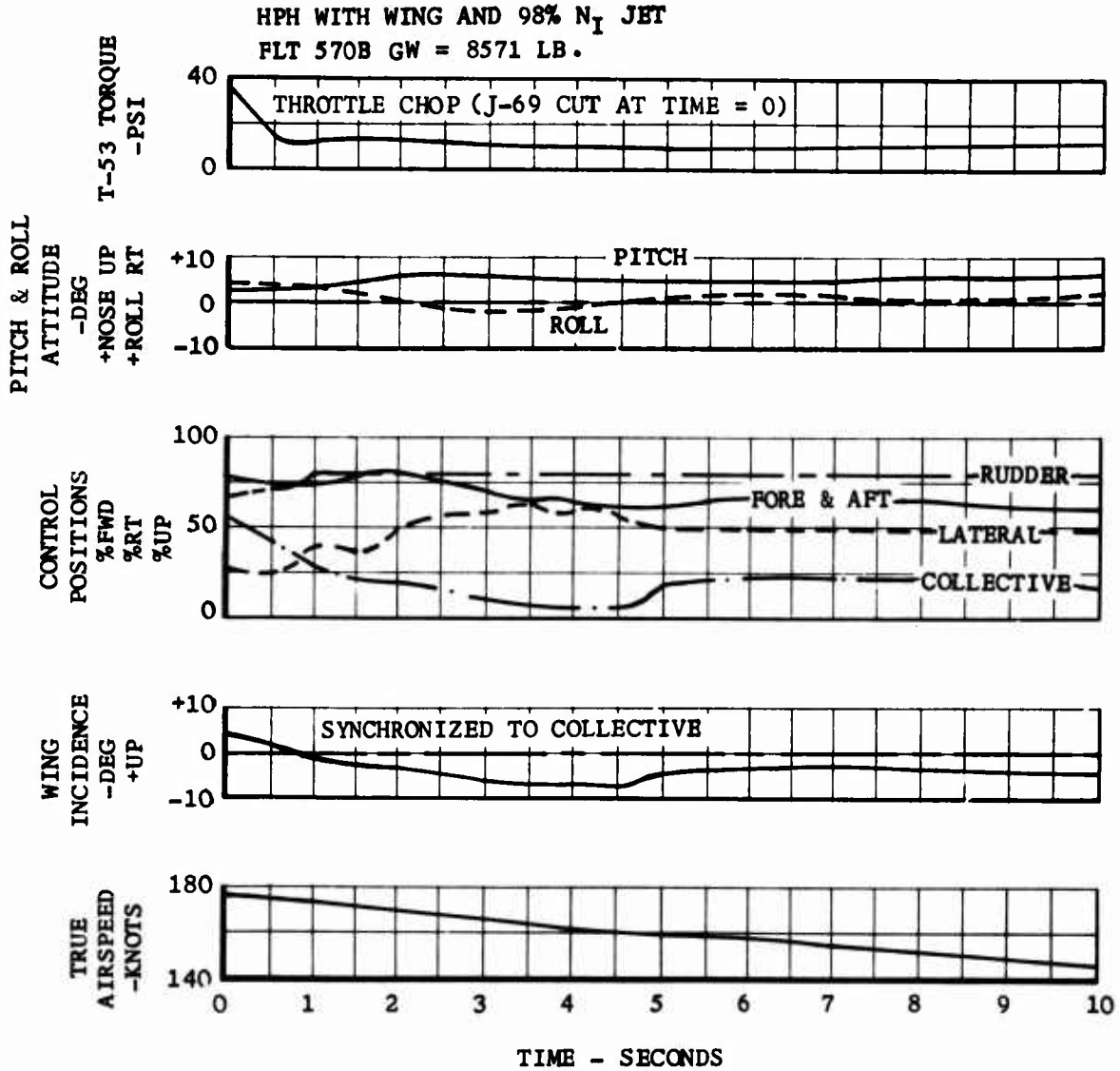

FIGURE 34. T-53 AND J-69 THROTTLE CHOP (ENTRY SPEED, 177 KNOTS).

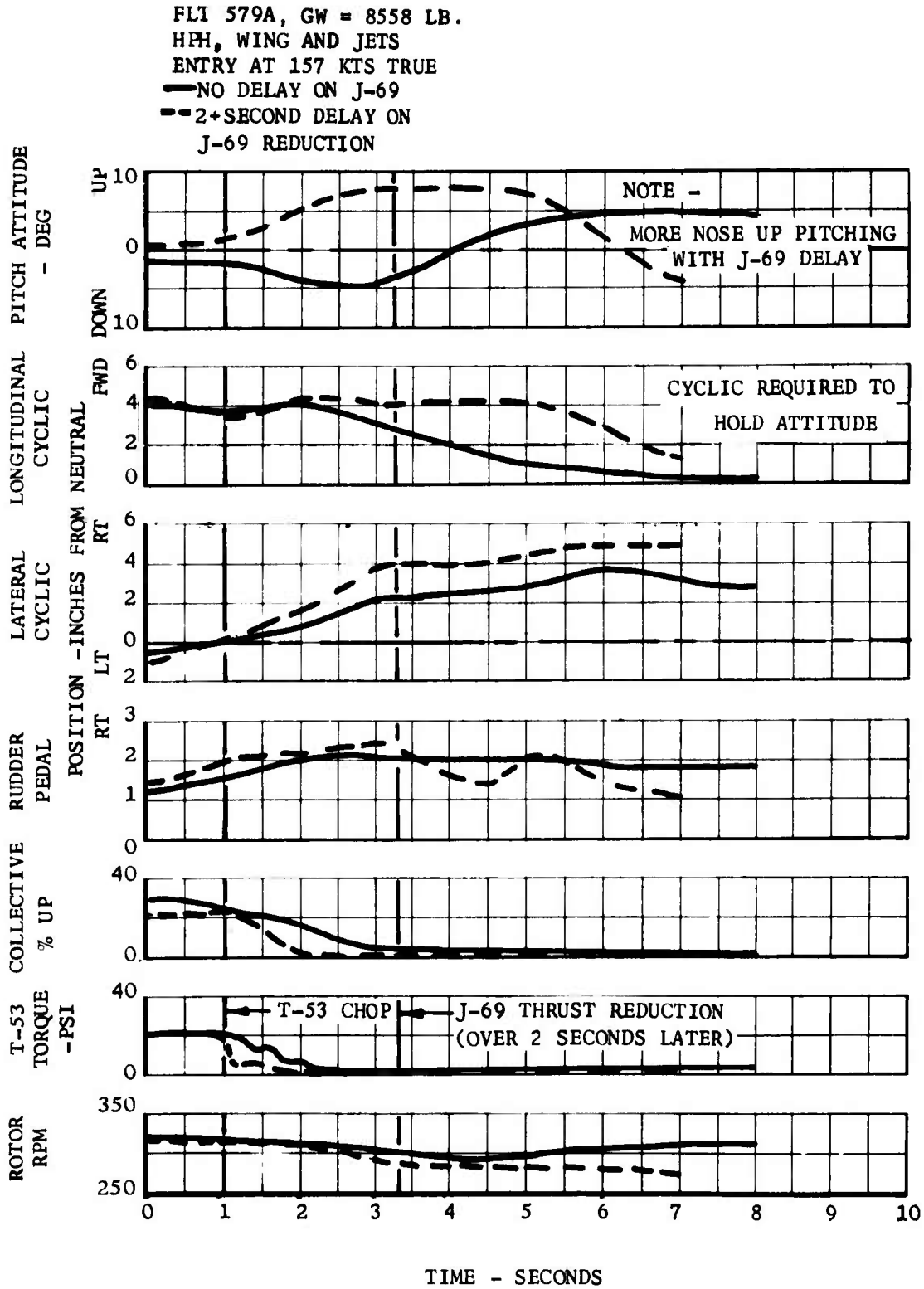

FIGURE 35. EFFECT OF DELAY IN J-69 POWER REDUCTION FOLLOWING SIMULATED T-53 FAILURE.

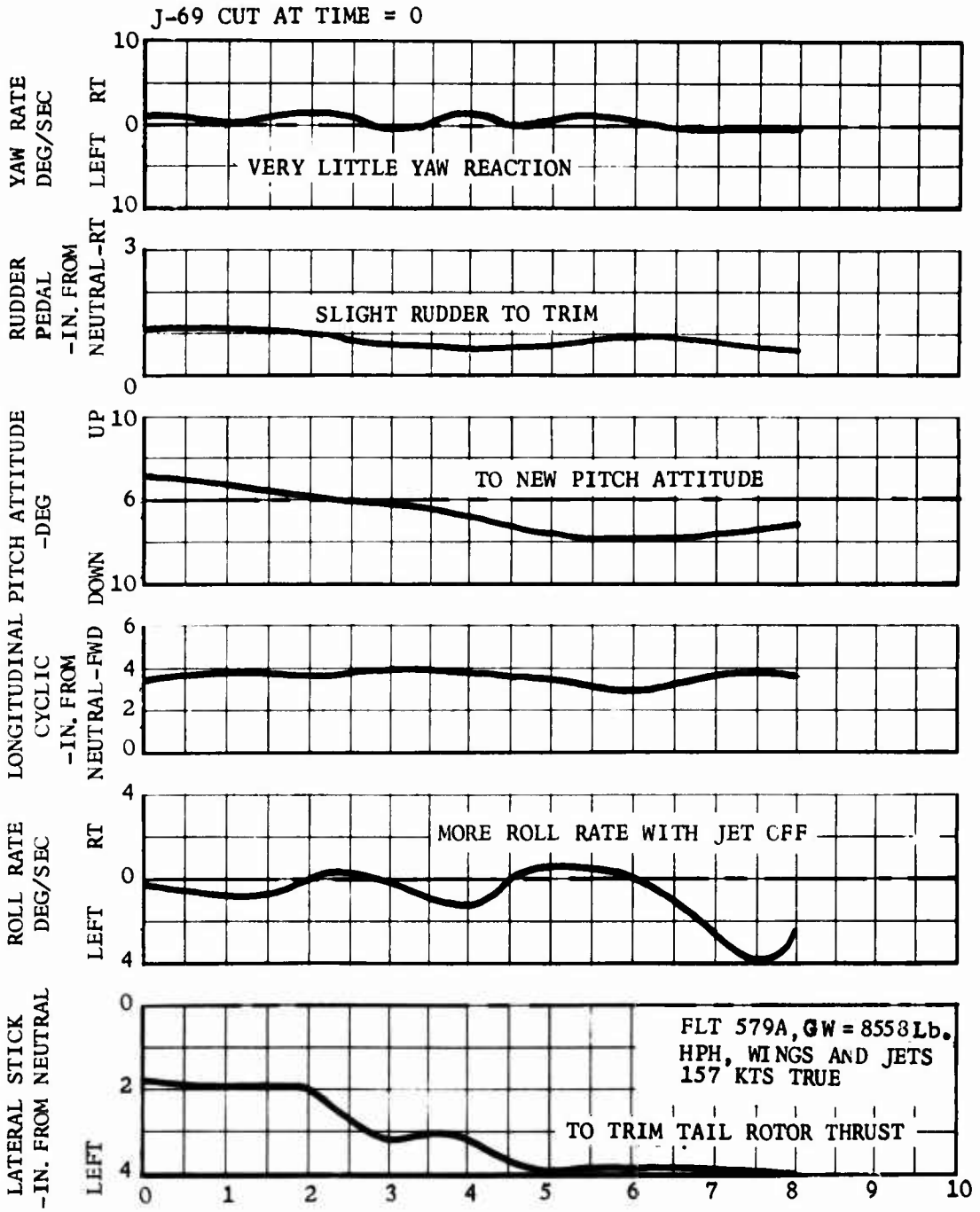

FIGURE 36. TIME HISTORY FOLLOWING SIMULATED RIGHT-HAND J-69 JET FAILURE

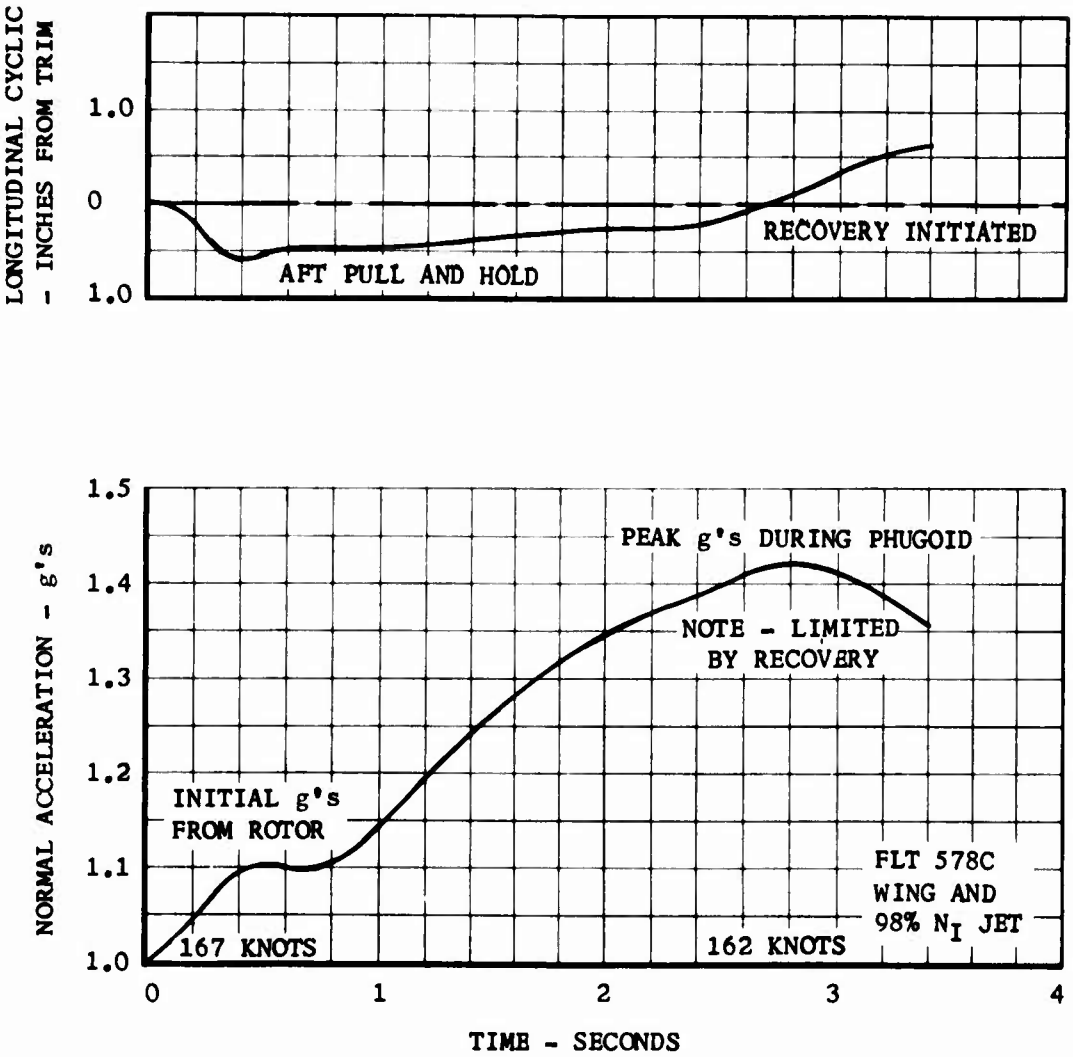

FIGURE 37. NORMAL ACCELERATION (g) RESPONSE TO A LONGITUDINAL CYCLIC PULL AND HOLD.

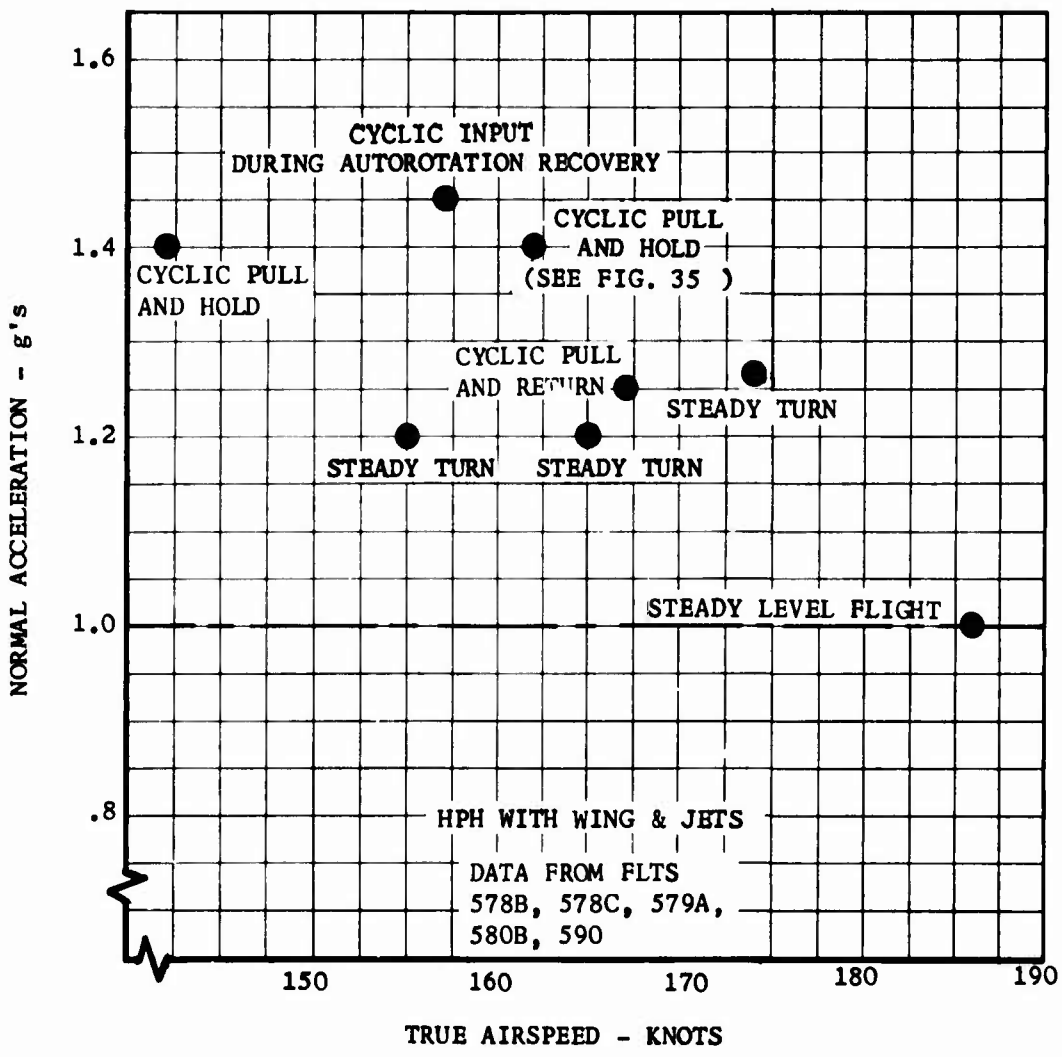

FIGURE 38. MANEUVER (g) LEVELS ATTAINED DURING HPH PHASE II FLIGHT TESTS.

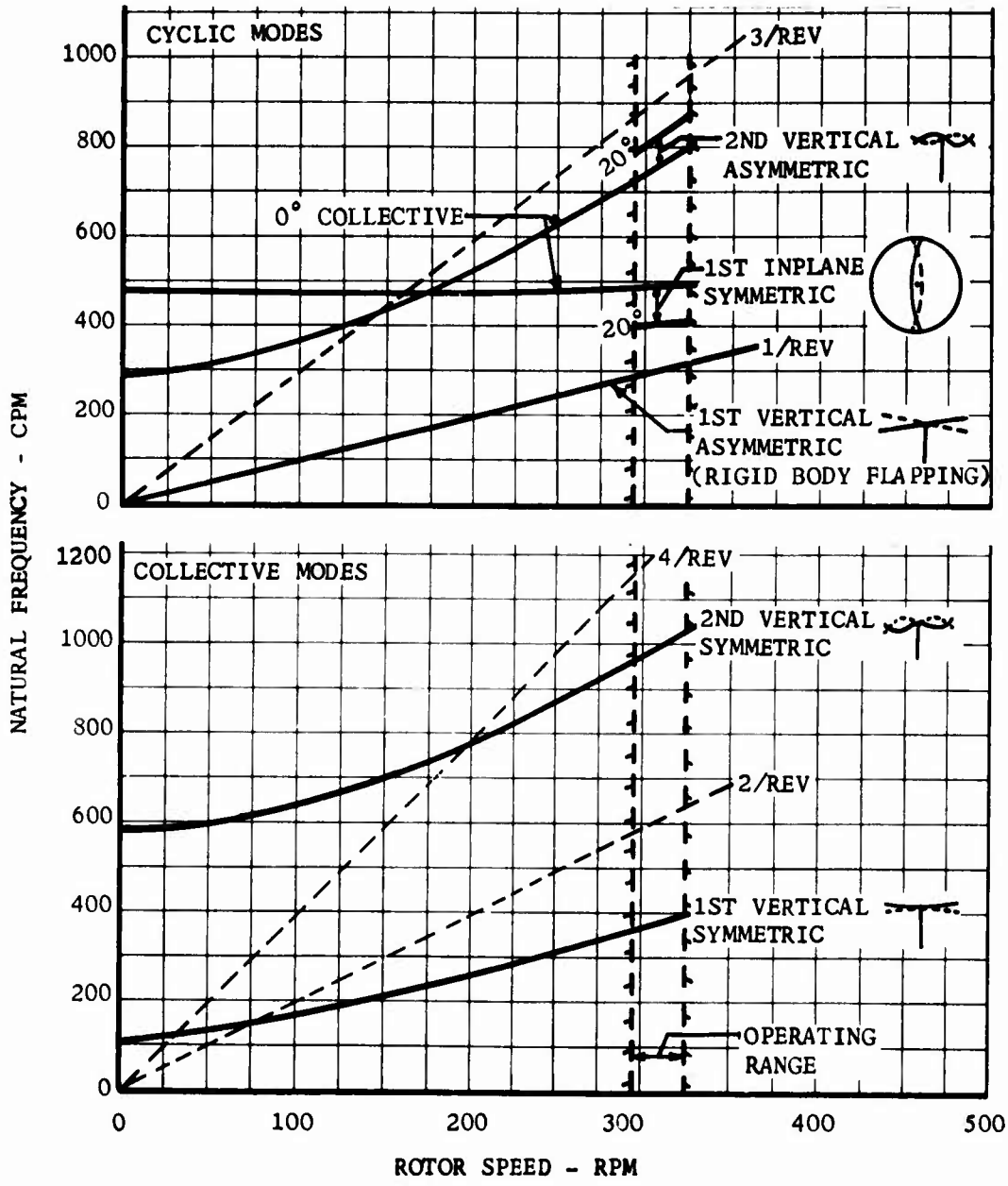

FIGURE 39. NATURAL FREQUENCIES OF THE STANDARD UH-1B/HPH MAIN ROTOR SYSTEM.

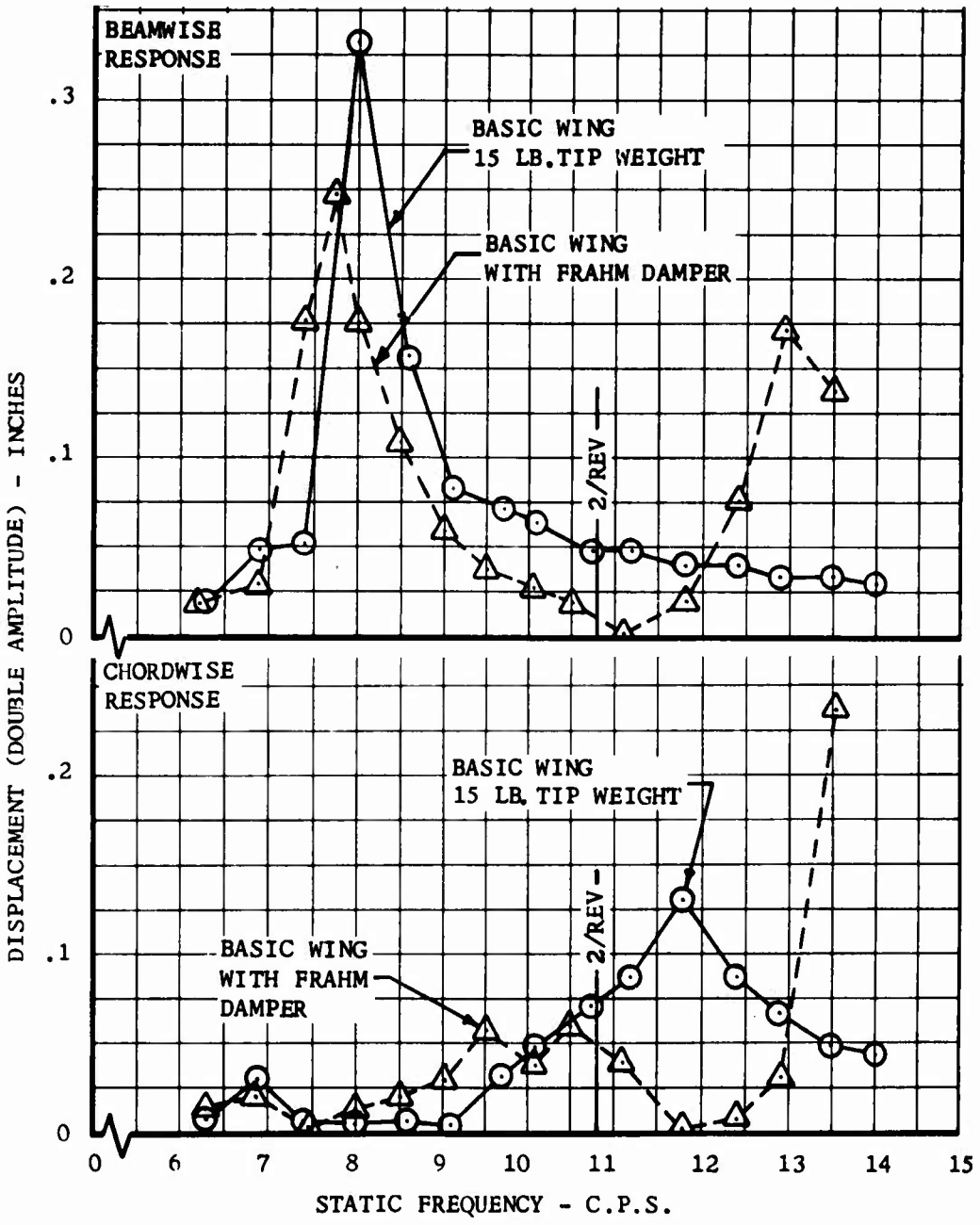

FIGURE 40. WING DYNAMIC RESPONSE WITH
FRAHM DAMPERS AND TIP WEIGHTS

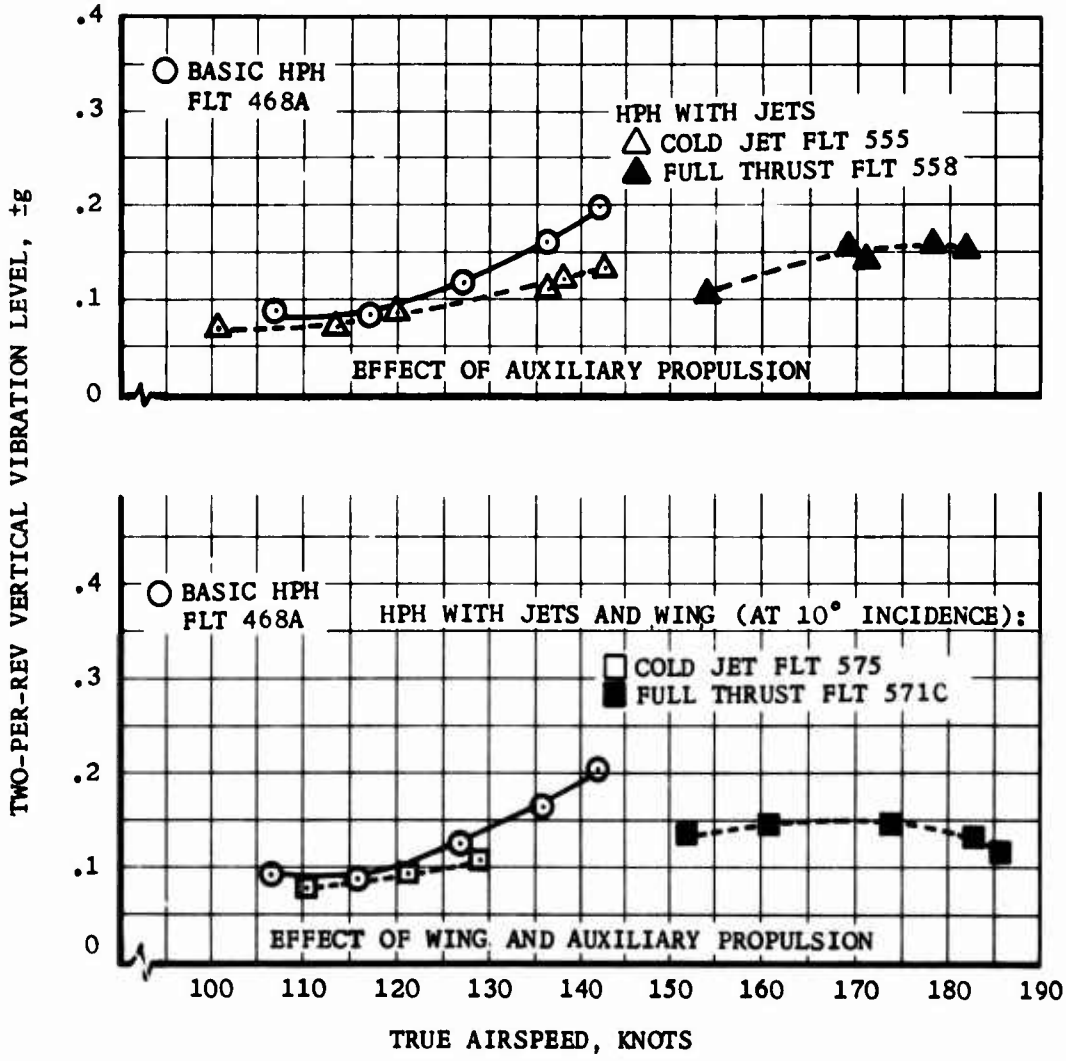

FIGURE 41. PILOT STATION VIBRATION LEVELS

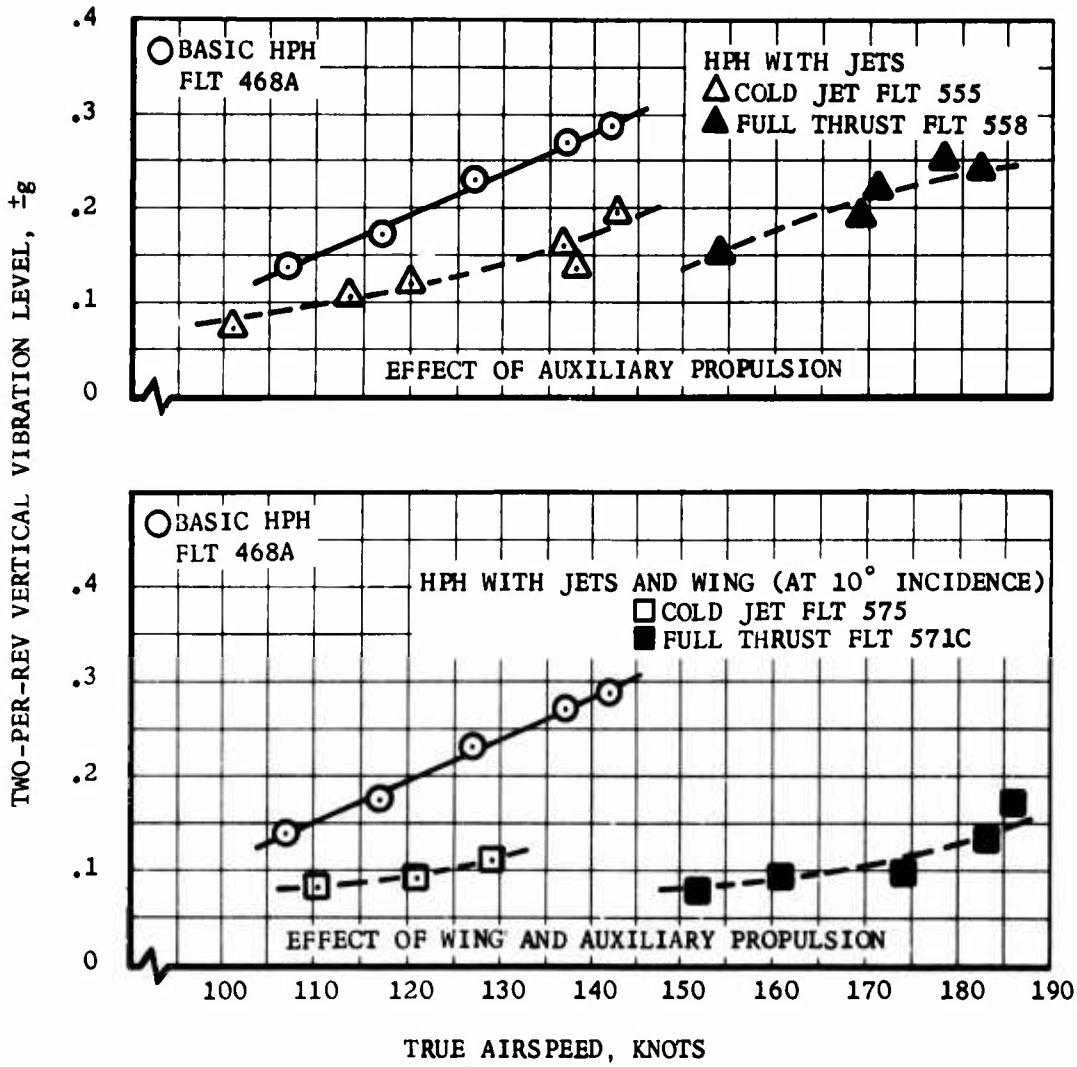

FIGURE 42. COPILOT STATION VIBRATION LEVELS

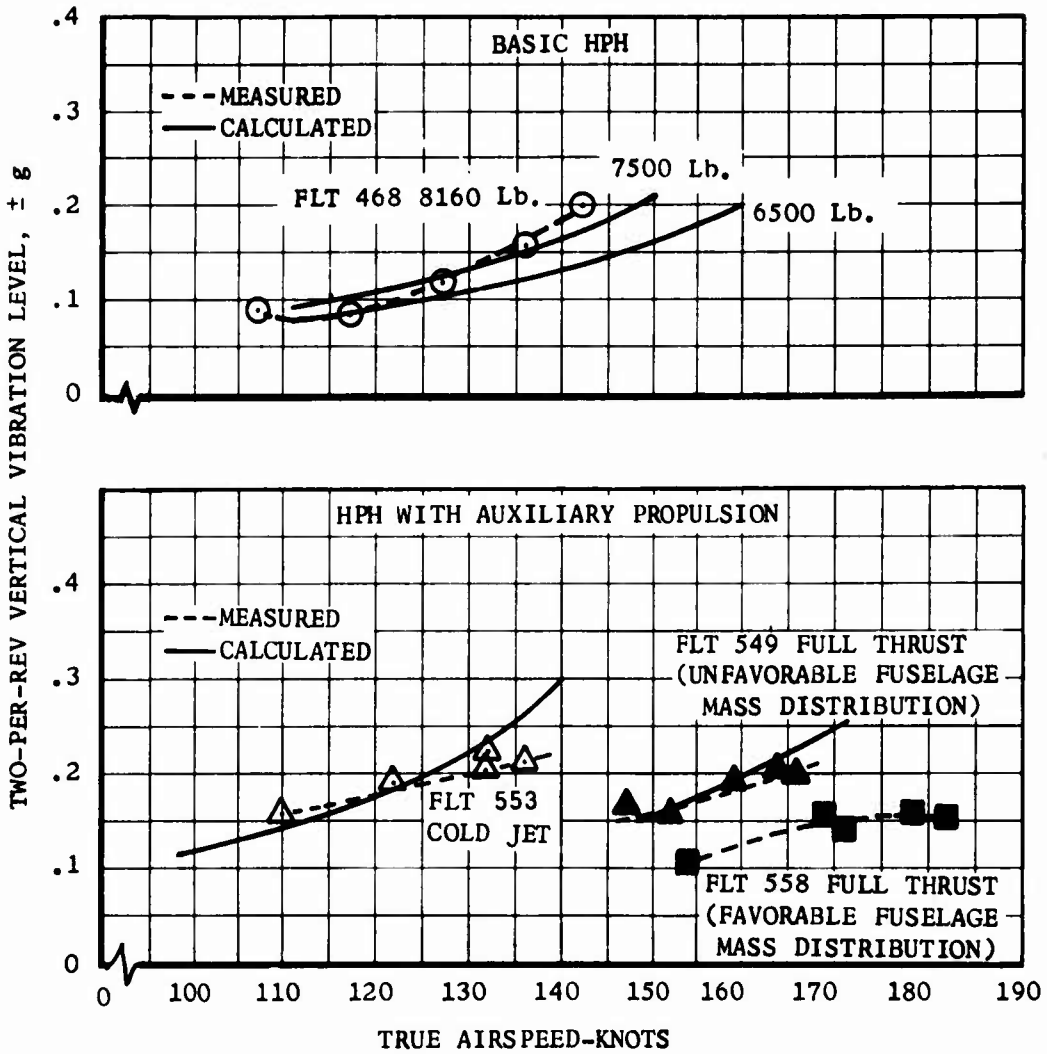

FIGURE 43. COMPARISON OF CALCULATED AND MEASURED PILOT STATION VIBRATION LEVELS

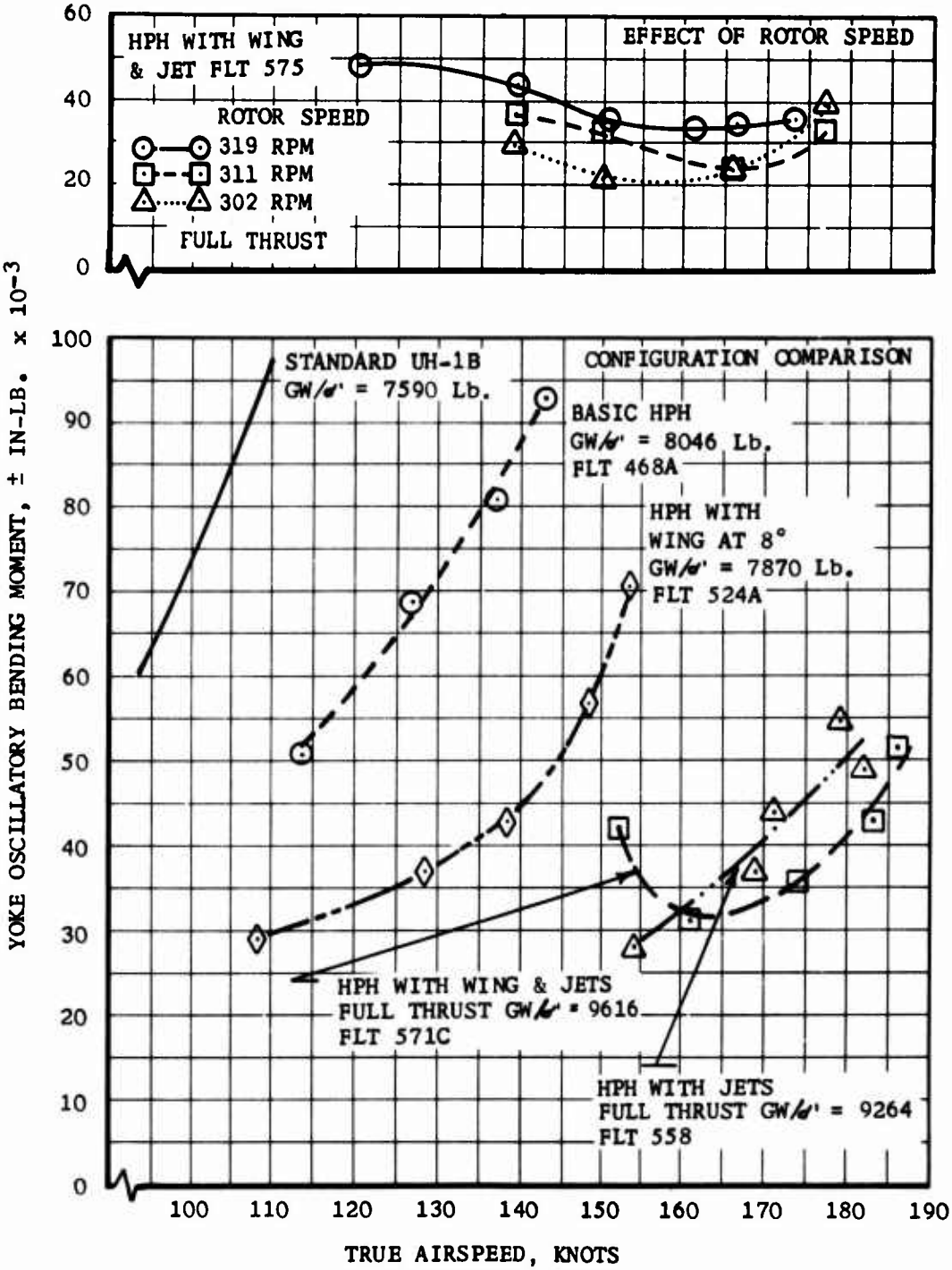

FIGURE 44 MAIN ROTOR CHORD LOADS

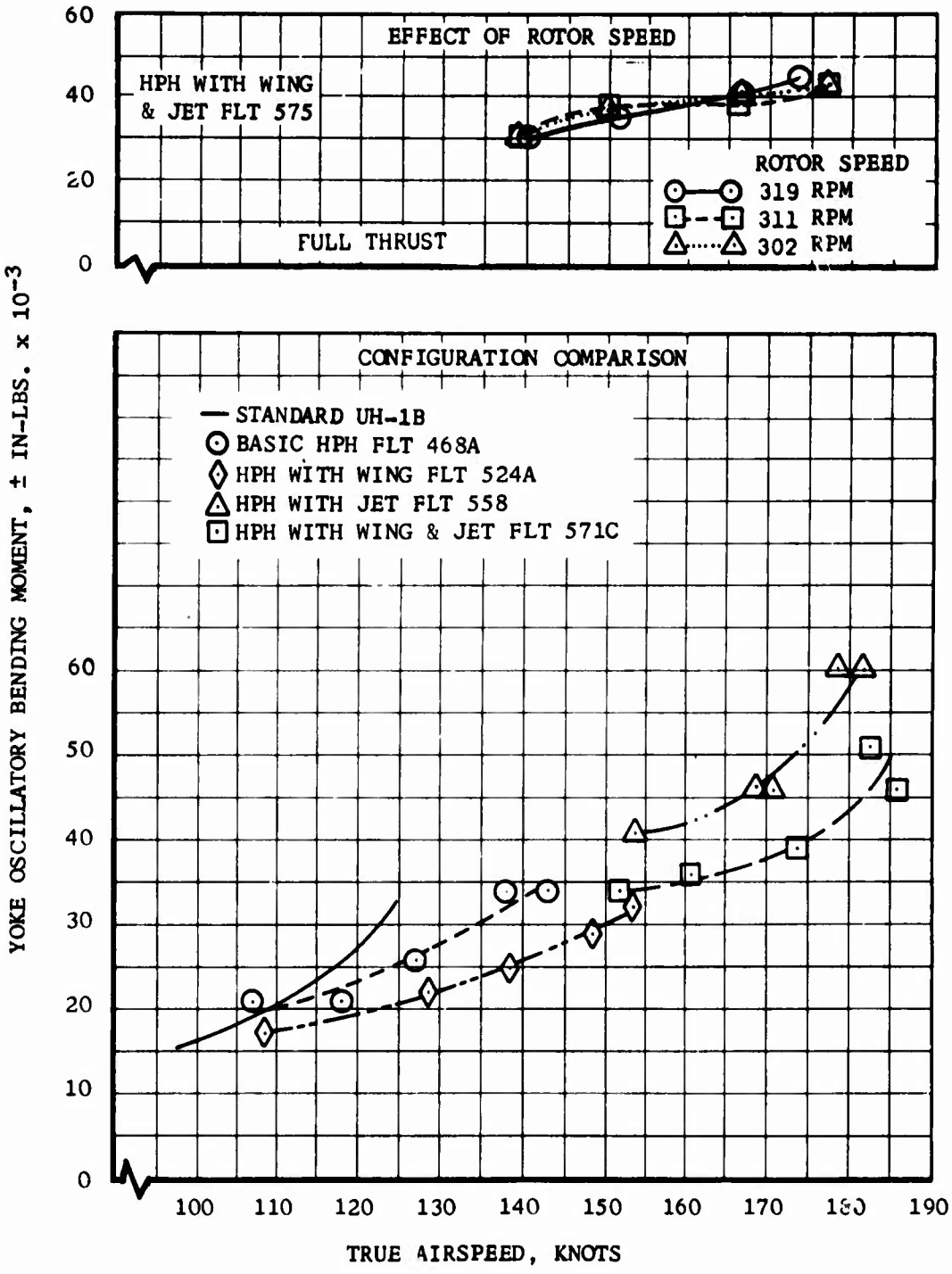

FIGURE 45 MAIN ROTOR BEAM LOADS

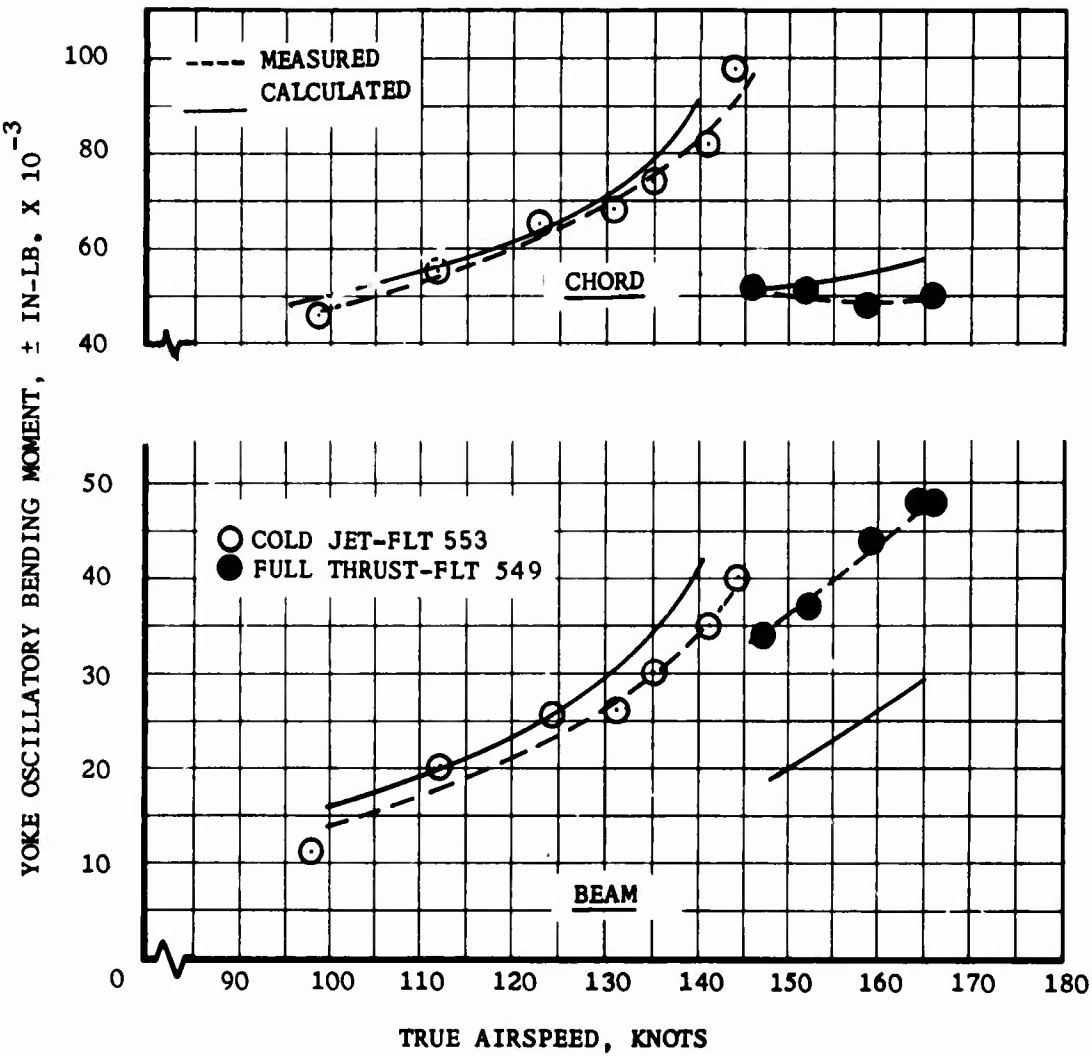

FIGURE 46 COMPARISON OF CALCUALTED AND MEASURED MAIN ROTOR LOADS FOR HPH WITH AUXILIARY PROPULSION

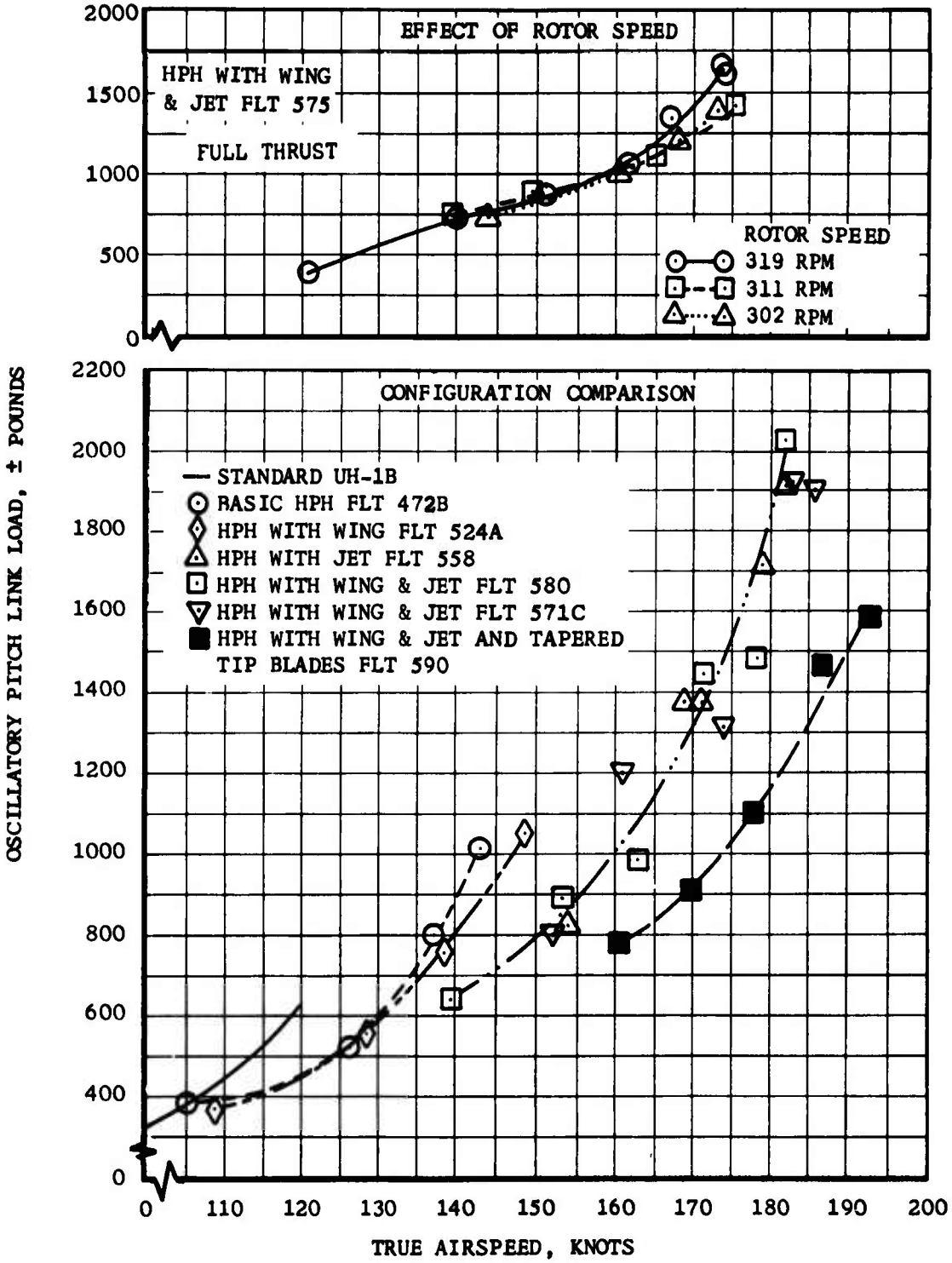

FIGURE 47 MAIN ROTOR CONTROL LOADS

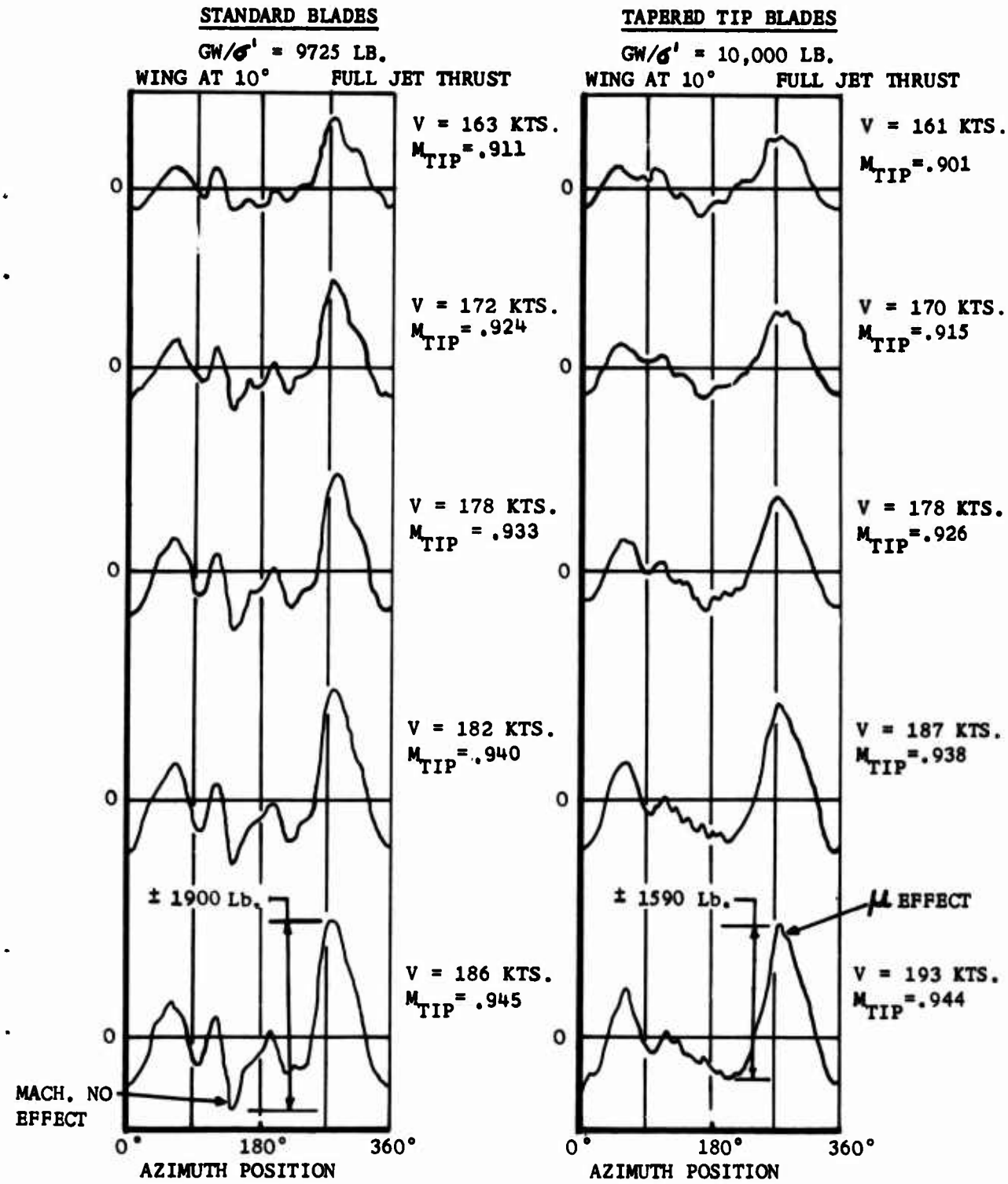

FIGURE 48. COMPARISON OF MAIN ROTOR PITCH LINK LOADS FOR STANDARD AND TAPERED TIP BLADES.

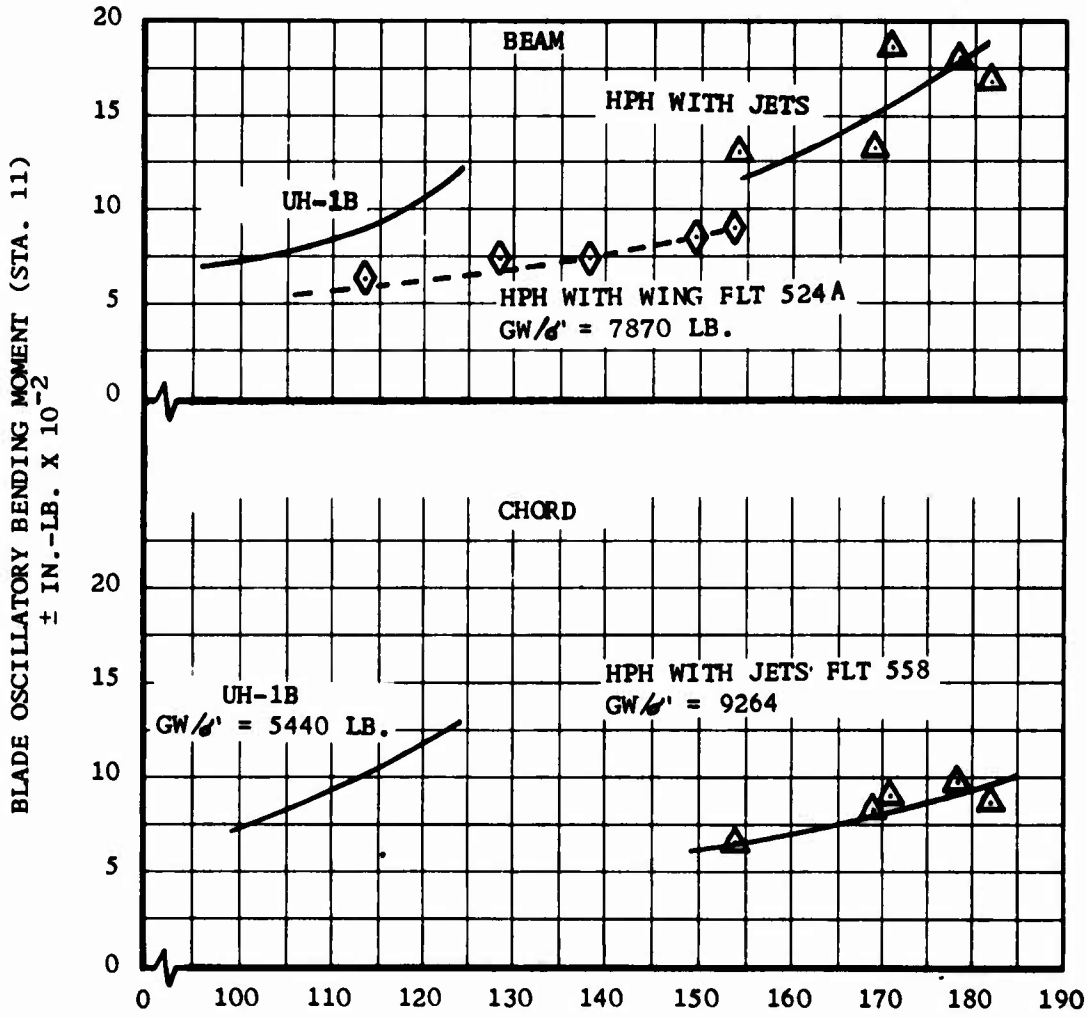

FIGURE 49 TAIL ROTOR LOADS

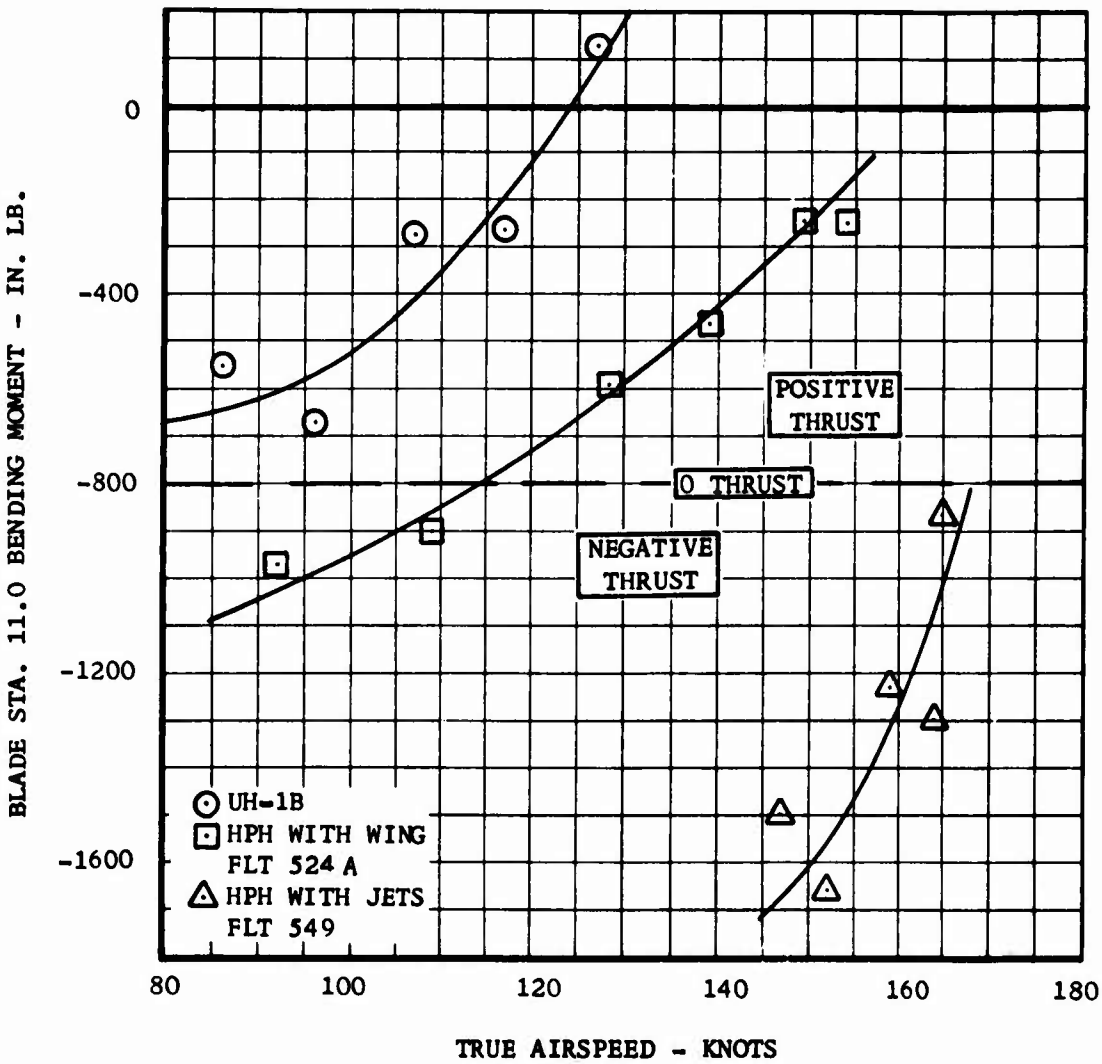

FIGURE 50 TAIL ROTOR STEADY BEAM BENDING MOMENT

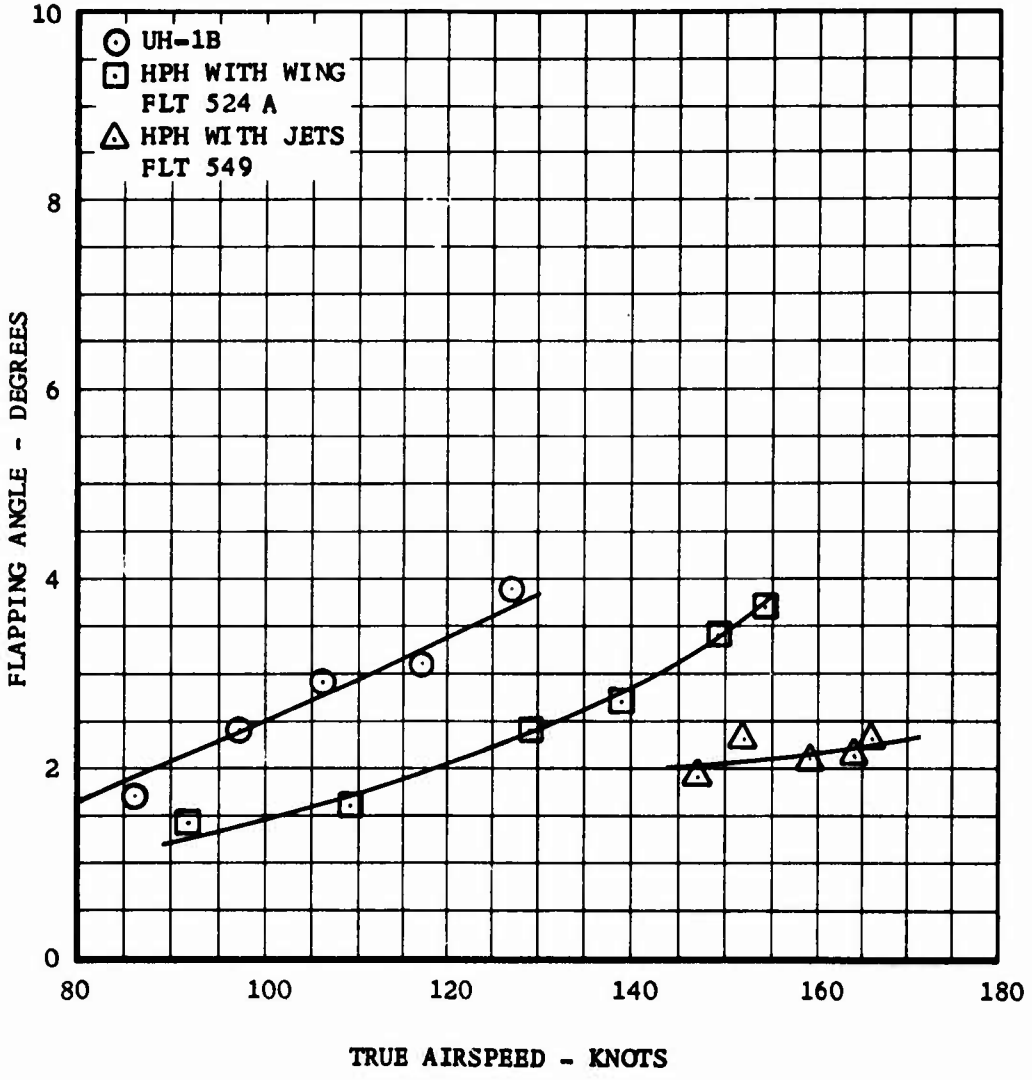

FIGURE 51 TAIL ROTOR FLAPPING ANGLE

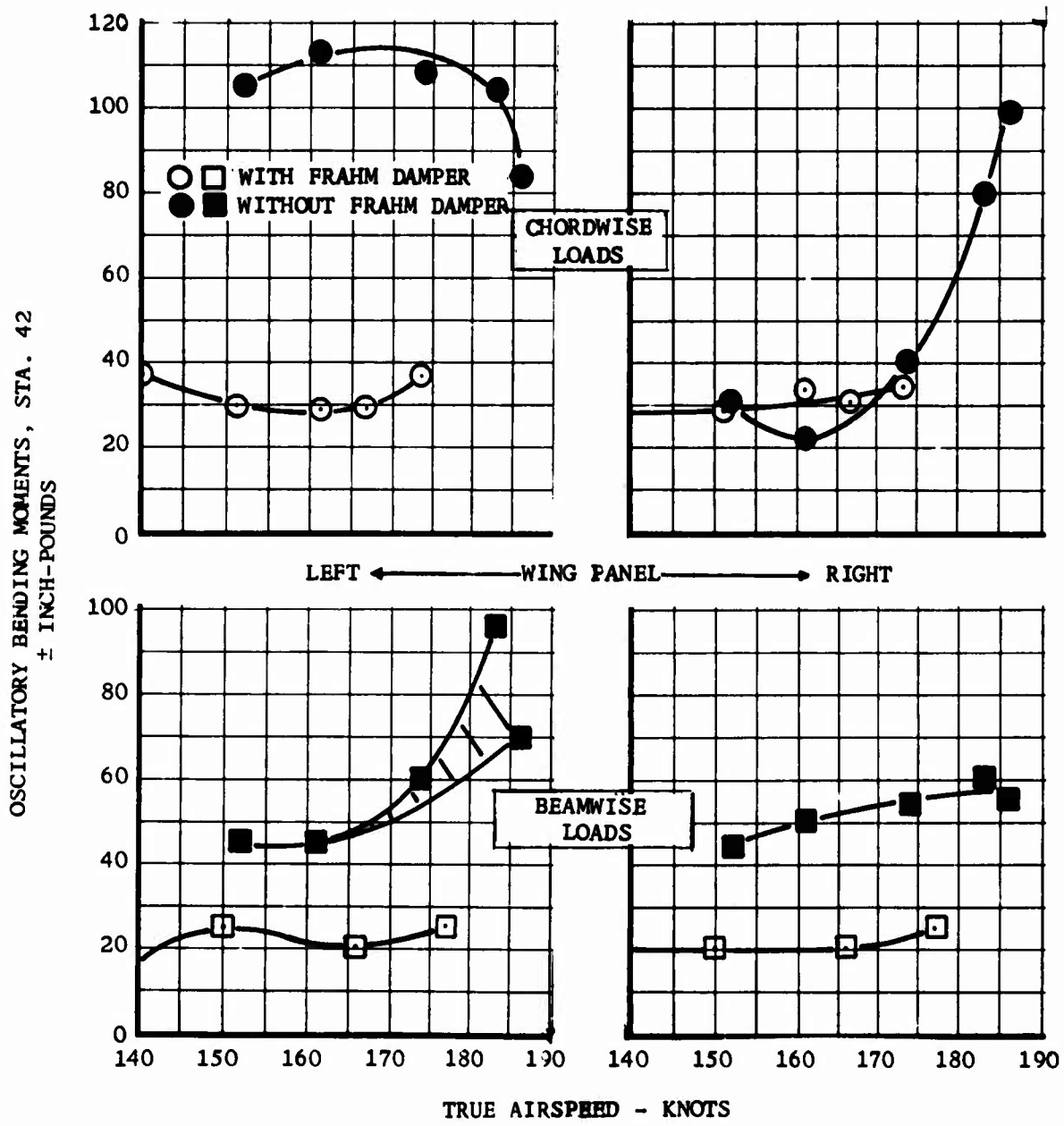

FIGURE 52 EFFECT OF FRAHM DAMPER ON WING LOADS

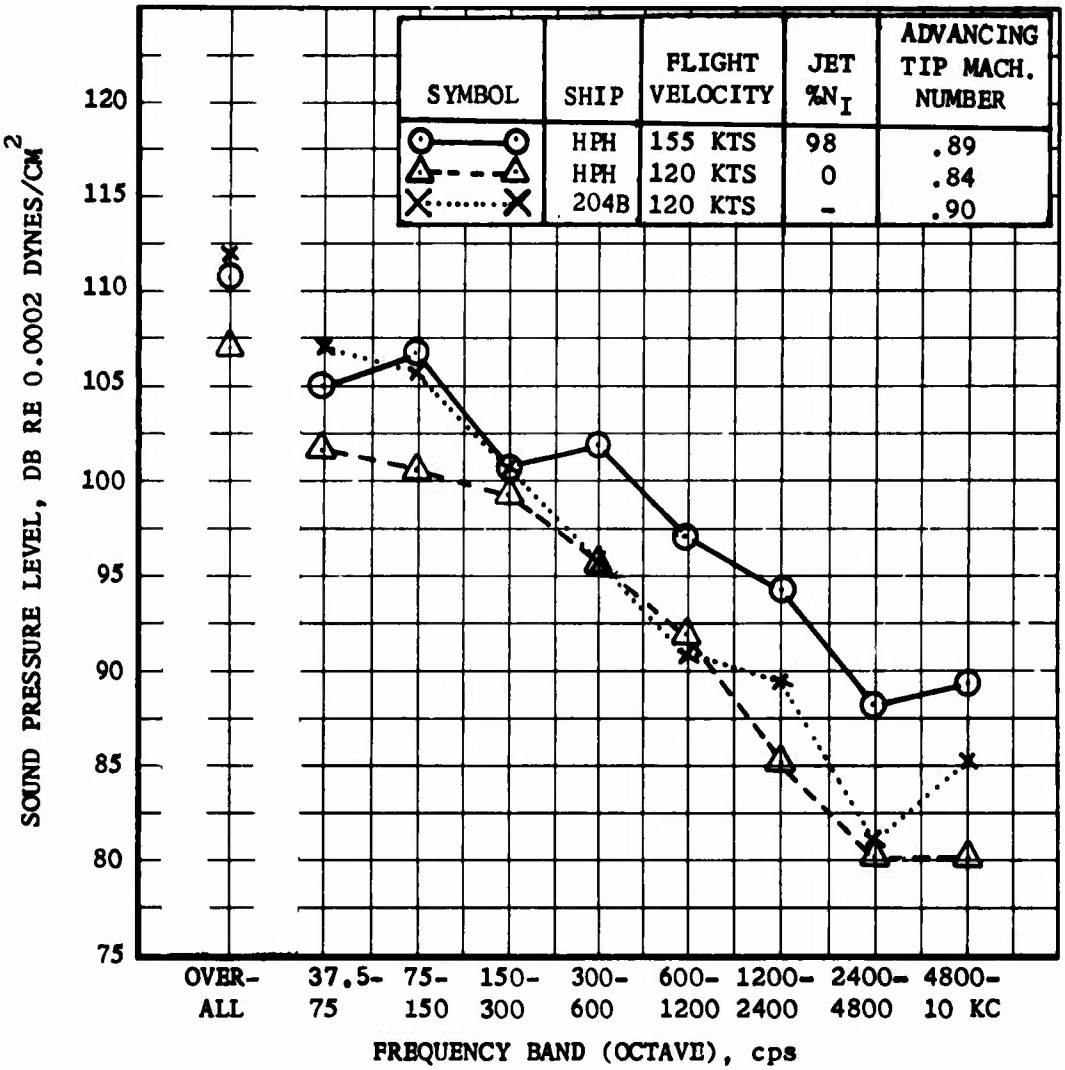

FIGURE 53 FLY-OVER NOISE OF THE FULL COMPOUND HPH AND COMPARISON WITH 204B

DISTRIBUTION

U. S. Army Materiel Command	14
U. S. Army Mobility Command	6
U. S. Army Aviation Materiel Command	2
U. S. Army Combat Developments Command Aviation Agency	5
U. S. Army Test and Evaluation Command	5
U. S. Army Aviation Test Board	5
U. S. Army Aviation School	1
U. S. Army Aviation Test Activity	5
Defense Research and Engineering, Office of Aeronautics	5
U. S. Army Combat Developments Command	5
U. S. Army Transportation Research Command	217
U. S. Army Research and Development Group (Europe)	3
U. S. Army Combat Developments Command Transportation Agency	1
U. S. Army Transportation School	4
U. S. Strike Command	3
U. S. Army Limited War Laboratory	3
U. S. Army War College	1
Canadian Liaison Officer, U. S. Army Transportation School	3
U. S. Army Standardization Group, Canada	1
British Army Staff, British Embassy	1
U. S. Army Standardization Group, U. K.	1
U. S. Army Electronics Research and Development Laboratory	3
Bureau of Naval Weapons	9
Naval Air Test Center	5
Ames Research Center,NASA	5
NASA-LRC, Langley Station	3
NASA Representative, Scientific and Technical Information Facility	2
U. S. Air Force Flight Test Center, Edwards AFB	4
Special Air Warfare Center, Eglin AFB	3
Air Proving Ground Center, Eglin AFB	1
Air University Library, Maxwell AFB	1
National Aviation Facilities Experimental Center	3
Defense Documentation Center	20
U. S. Government Printing Office	1
Chief of R&D, D/A	2

Bell Helicopter Company, Fort Worth, Texas, HIGH-PERFORMANCE HELICOPTER PROGRAM, Summary Report, Phase II - J. P. Van Wyckhouse and W. L. Cresap, et.al.

TRECOM Tech Rept 64-61, October 1964, 93 pp. (Contract DA44-177-TC-711) USATRECOM Proj. 9R38-13-014-01 Unclassified Report.

The results of a flight research program to investigate high-speed loaded and unloaded rotors are presented. The program is an extension of the high-performance UH-1B flight research program reported in TREC 63-42.

The compound flight research helicopter, instrumentation, and test program are described and the test results are discussed. Major modifications to the basic high-performance helicopter involved the addition of two continental J69-T9 jet engines, a controllable incidence wing and controls and elevator-horizontal stabilizer changes.

Level-flight true airspeeds of 154 knots (wing only), 182 knots (jets only), and 186 knots (wing and jets) were attained using the UH-1B rotor system. It is shown that the structural loads, vibration characteristics and stability and control of the vehicle were satisfactory for all conditions tested. With

(over)

Unclassified

1. Helicopters - Performance
2. Helicopter Rotors
3. VTOL/STOL Aircraft
I. Van Wyckhouse, J. P.
II. Cresap, W. L.
III. Contract DA44-177-TC-711

the exception of the pitch link loads, rotor system loads and vibrations were found to be lower than those of the UH-1B at its power limit speed. The pitch stability of the machine in its final configuration was excellent, and although the lateral stability was deficient, no difficulty was encountered by Bell and Army pilots who flew the machine.

During the program, the UH-1B rotor blades were replaced by an experimental set with a tapered thickness over the outboard 20 percent of the blades. With these blades, the full-compound machine was flown to a true airspeed of 193 knots at a gross weight of about 40 percent greater than the basic HPH. Control loads were found to be reduced with the tapered-tip blades.

It is concluded that higher speed and increased load capability can be achieved by compounding the helicopter. This can be accomplished with good stability and control, with no increase in vibration and structural loads, and without compromising the autorotation safety characteristics of the helicopter.

Bell Helicopter Company, Fort Worth, Texas, HIGH-PERFORMANCE HELICOPTER PROGRAM, Summary Report, Phase II - J. P. Van Wyckhouse and W. L. Cresap, et.al.

TRECOM Tech Rept 64-61, October 1964, 93 pp. (Contract DA44-177-TC-711) USATRECOM Proj. 9R38-13-014-01 Unclassified Report.

The results of a flight research program to investigate high-speed loaded and unloaded rotors are presented. The program is an extension of the high-performance UH-1B flight research program reported in TREC 63-42.

The compound flight research helicopter, instrumentation, and test program are described and the test results are discussed. Major modifications to the basic high-performance helicopter involved the addition of two continental J69-T9 jet engines, a controllable incidence wing and controls and elevator-horizontal stabilizer changes.

Level-flight true airspeeds of 154 knots (wing only), 182 knots (jets only), and 186 knots (wing and jets) were attained using the UH-1B rotor system. It is shown that the structural loads, vibration characteristics and stability and control of the vehicle were satisfactory for all conditions tested. With

(over)

Unclassified

1. Helicopters - Performance
2. Helicopter Rotors
3. VTOL/STOL Aircraft
I. Van Wyckhouse, J. P.
II. Cresap, W. L.
III. Contract DA44-177-TC-711

Bell Helicopter Company, Fort Worth, Texas, HIGH-PERFORMANCE HELICOPTER PROGRAM, Summary Report, Phase II - J. P. Van Wychhouse and W. L. Cresap, et.al.

TRECOM Tech Rept 64-61, October 1964, 93 pp. (Contract DA44-177-TC-711) USATRECOM Proj. 9R38-13-014-01 Unclassified Report.

The results of a flight research program to investigate high-speed loaded and unloaded rotors are presented. The program is an extension of the high-performance UH-1B flight research program reported in TREC 63-42.

The compound flight research helicopter, instrumentation, and test program are described and the test results are discussed. Major modifications to the basic high-performance helicopter involved the addition of two continental J69-T9 jet engines, a controllable incidence wing and controls and elevator-horizontal stabilizer changes.

Level-flight true airspeeds of 154 knots (wing only), 182 knots (jets only), and 186 knots (wing and jets) were attained using the UH-1B rotor system. It is shown that the structural loads, vibration characteristics and stability and control of the vehicle were satisfactory for all conditions tested. With

(over)

Unclassified

1. Helicopters - Performance
2. Helicopter Rotors
3. VTOL/STOL Aircraft
- I. Van Wychhouse, J. P.
- II. Cresap, W. L.
- III. Contract DA44-177-TC-711

the exception of the pitch link loads, rotor system loads and vibrations were found to be lower than those of the UH-1B at its power limit speed. The pitch stability of the machine in its final configuration was excellent, and although the lateral stability was deficient, no difficulty was encountered by Bell and Army pilots who flew the machine.

During the program, the UH-1B rotor blades were replaced by an experimental set with a tapered thickness over the outboard 20 percent of the blades. With these blades, the full-compound machine was flown to a true airspeed of 193 knots at a gross weight of about 40 percent greater than the basic HPM. Control loads were found to be reduced with the tapered-tip blades.

It is concluded that higher speed and increased load capability can be achieved by compounding the helicopter. This can be accomplished with good stability and control, with no increase in vibration and structural loads, and without compromising the autorotation safety characteristics of the helicopter.

the exception of the pitch link loads, rotor system loads and vibrations were found to be lower than those of the UH-1B at its power limit speed. The pitch stability of the machine in its final configuration was excellent, and although the lateral stability was deficient, no difficulty was encountered by Bell and Army pilots who flew the machine.

During the program, the UH-1B rotor blades were replaced by an experimental set with a tapered thickness over the outboard 20 percent of the blades. With these blades, the full-compound machine was flown to a true airspeed of 193 knots at a gross weight of about 40 percent greater than the basic HPM. Control loads were found to be reduced with the tapered-tip blades.

It is concluded that higher speed and increased load capability can be achieved by compounding the helicopter. This can be accomplished with good stability and control, with no increase in vibration and structural loads, and without compromising the autorotation safety characteristics of the helicopter.

Bell Helicopter Company, Fort Worth, Texas, HIGH-PERFORMANCE HELICOPTER PROGRAM, Summary Report, Phase II - J. P. Van Wychhouse and W. L. Cresap, et.al.

TRECOM Tech Rept 64-61, October 1964, 93 pp. (Contract DA44-177-TC-711) USATRECOM Proj. 9R38-13-014-01 Unclassified Report.

The results of a flight research program to investigate high-speed loaded and unloaded rotors are presented. The program is an extension of the high-performance UH-1B flight research program reported in TREC 63-42.

The compound flight research helicopter, instrumentation, and test program are described and the test results are discussed. Major modifications to the basic high-performance helicopter involved the addition of two continental J69-T9 jet engines, a controllable incidence wing and controls and elevator-horizontal stabilizer changes.

Level-flight true airspeeds of 154 knots (wing only), 182 knots (jets only), and 186 knots (wing and jets) were attained using the UH-1B rotor system. It is shown that the structural loads, vibration characteristics and stability and control of the vehicle were satisfactory for all conditions tested. With

(over)

Unclassified

1. Helicopters - Performance
2. Helicopter Rotors
3. VTOL/STOL Aircraft
- I. Van Wychhouse, J. P.
- II. Cresap, W. L.
- III. Contract DA44-177-TC-711